Robotic Strategies to Characterize and Promote Postural Responses in Standing, Squatting and Sit-to-Stand

Tatiana Dinora Luna

Submitted in partial fulfillment of the
requirements for the degree of
Doctor of Philosophy
under the Executive Committee
of the Graduate School of Arts and Sciences

COLUMBIA UNIVERSITY

2022

Abstract

Robotic Strategies to Characterize and Promote Postural Responses

in Standing, Squatting and Sit-to-Stand

Tatiana Dinora Luna

In people with neuromotor deficits of trunk and lower extremities, maintaining and regaining balance is a difficult task. Many undergo rehabilitation to improve their movement capabilities, health, and overall interactions with their environment. Rehabilitation consists of a set of interventions designed to improve the individual's mobility and independence. These strategies can be passive, active or task-specific and are dependent on the type of injury, how the individual progresses, and the intensity of the activity. Some of the common rehabilitation interventions to strengthen muscles and improve coordination are accomplished either by the manual assistance of a physical therapist, bodyweight suspension systems or through robotic-assisted training.

There are several types of rehabilitation robotic systems and robotic control strategies. However, there are few robotic studies that compare their robotic device's control strategy to common rehabilitation interventions. This dissertation introduces robotic strategies centered around rehabilitation ones and characterizes human motion in response to the robotic forces. Two cable-driven robotic systems are utilized to implement the robotic controllers for different tasks. Further details of the two cable-driven systems are discussed in Chapter 1. The validation and evaluation of these robotic strategies for standing rehabilitation is discussed in Chapter 2. A case study of a robotic training paradigm for individuals with spinal cord injury is presented in Chapter 3. Chapter 4 introduces a method to redistribute individuals' weight using pelvic lateral forces. Chapter 5 and 6 characterizes how young and older groups respond to external perturbations during their sit-to-stand motion.

This dissertation presents robotic strategies that can be implemented as rehabilitation interventions. It also presents how individuals' biomechanics and muscle responses may change depending on the force control paradigm. These robotic strategies can be utilized by training individuals to improve their reactive and active balance control and thus reduce their risk of falling.

Table of Contents

List of Figures x

List of Tables xi

Acknowledgments xii

Dedication xiv

Introduction 1

Chapter 1: Cable-Driven Robotic Systems 3

1.1 Robotic Upright Stand Trainer (RobUST) 3

1.2 Tethered Pelvic Assist Device (TPAD) 3

1.3 Control System 4

1.4 Tension Distribution Problem 6

1.4.1 RobUST 7

1.4.2 TPAD 8

1.4.3 Logic-Based Tension Planner 9

1.4.3.1 System Performance 10

1.5 Assist-as-Needed Force Controllers 12

1.5.1 Irregular Force Field 12

1.5.2 Trajectory Based Control and Experiment Example 13

Chapter 2: Comparing Traditional Rehabilitation Method to RobUST 16

2.1 Introduction 16

2.1.1 Motivation 16

2.1.2 Research Questions 17

2.2 System Description 18

2.3 Experiment Design 19

2.3.1 Procedure 19

2.3.2 Participants 21

2.3.3 Data Processing 21

2.3.4 Statistical Analysis 22

2.4 Results 23

2.4.1 Postural Stability 23

2.4.2 Postural Control Mechanisms: Surface EMGs 25

2.4.3 Force Output Responses 29

2.5 Discussion 30

2.5.1 The Stability Effects of Pelvic Support from RobUST 30

2.5.2 The Additive Support Effect of HPS 33

2.5.3 Study Limitations 34

2.6 Conclusion 34

Chapter 3: Feasibility and Tolerance of a Robotic Postural Training in a Person with Ambulatory Spinal Cord Injury 36

3.1 Introduction 36
3.2 Experimental Setup and Procedure 36
3.2.1 Study Design 36
3.2.2 RobUST Setup and Training 37
3.3 Data Analysis 38
3.4 Results 40
3.5 Discussion 42
3.6 Conclusion 43

Chapter 4: Redistributing Ground Reaction Forces During Squatting 44
4.1 Introduction 44
4.1.1 Research Aims 45
4.2 System Description 46
4.3 Experiment Design 47
4.3.1 Study Design 47
4.3.2 Data Acquisition 47
4.3.3 Data Analysis 49
4.3.4 Statistical Analysis 50
4.4 Results 52
4.4.1 Baseline Squat Results 52
4.4.2 Lateral Force Results 52
4.4.3 Timed Results 53
4.5 Discussion 56

4.5.1 Baseline Squat Comparisons . . . 56
4.5.2 Lateral Force Squat Condition . . . 57
4.5.3 Study Limitations . . . 58
4.6 Conclusion . . . 59

Chapter 5: Characterizing Reactive Control in Sit-to-Stand . . . 60
5.1 Introduction . . . 60
5.1.1 Research Aims . . . 61
5.2 System Description . . . 62
5.3 Experiment Design . . . 62
5.3.1 Study Design . . . 62
5.3.2 Data Acquisition . . . 65
5.3.3 Data Analysis . . . 65
5.3.4 Statistical Analysis . . . 68
5.4 Results . . . 69
5.4.1 Perturbation Threshold Results . . . 69
5.4.2 Muscle Activity Results . . . 69
5.4.3 Kinematic Results . . . 74
5.4.4 Ground Reaction Results . . . 77
5.5 Discussion . . . 77
5.5.1 Perturbation Direction . . . 77
5.5.2 Perturbation Type . . . 78
5.5.3 Perturbation Intensity . . . 79

5.5.4 Sit-to-Stand Perturbations . . . 79
5.5.5 Study Limitations . . . 80
5.6 Conclusion . . . 81

Chapter 6: Characterizing Sit-to-Stand Reactive Responses in Young and Older Adults . . . 82
6.1 Introduction . . . 82
6.2 Experiment Design . . . 84
6.2.1 Participant Information . . . 84
6.2.2 Study Design . . . 84
6.2.3 Data Analysis . . . 85
6.2.3.1 Kinematic Variables . . . 87
6.2.3.2 Ground Reaction Force Variables . . . 88
6.2.3.3 Muscle Variables . . . 88
6.2.4 Statistical Analysis . . . 91
6.3 Results . . . 91
6.3.1 Margin of Stability Results . . . 91
6.3.1.1 Low Perturbation Intensity . . . 91
6.3.1.2 Threshold Perturbation Intensity . . . 92
6.3.1.3 Fail Perturbation Intensity . . . 92
6.3.2 Muscle Activity Results . . . 96
6.3.2.1 Low Perturbation Intensity . . . 96
6.3.2.2 Threshold Perturbation Intensity . . . 96
6.3.2.3 Fail Perturbation Intensity . . . 98

6.3.3 Joint Total Excursion Results 98
6.3.3.1 Low Perturbation Intensity 98
6.3.3.2 Threshold Perturbation Intensity 105
6.3.3.3 Fail Perturbation Intensity 107
6.3.4 Primary Joint Movement 107
6.4 Discussion 113
6.4.1 Young versus Older Group Reactions 113
6.4.2 Perturbation Direction Effects 114
6.4.3 Perturbation Type 114
6.4.4 Study Limitations 115
Conclusion 116
References 118

List of Figures

Figure 1.1: RobUST Setup with Participant Standing 4

Figure 1.2: The TPAD System 5

Figure 1.3: Control System 6

Figure 1.4: An example of how the logic-based tension planner case structure functions. 11

Figure 1.5: A visual layout of how the irregular force field functions 13

Figure 1.6: A visual layout of how the trajectory force assistance functions 15

Figure 2.1: Representation of the Pelvic Force Field and Trunk Perturbations 19

Figure 2.2: Trunk Perturbation Force Profile 20

Figure 2.3: Group Averages of Normalized COP Amplitude in the A-P Direction . . . 24

Figure 2.4: Group Averages of Trunk and Pelvis Amplitude During A-P Perturbations . 26

Figure 2.5: Group Averages of Trunk and Pelvis Amplitude During M-L Perturbations 27

Figure 2.6: Normalized iEMG Results 28

Figure 2.7: Handrail Force Results 29

Figure 3.1: The SCI Summary Training Timeline 37

Figure 3.2: RobUST Setup for SCI Training 39

Figure 3.3: The SCI Postural Star Standing Outcomes 40

Figure 3.4: The SCI Perturbation Outcomes 41

Figure 3.5: The SCI iEMG Results 42

Figure 4.1: A Participant Squatting with RobUST 46

Figure 4.2: RobUST Output Lateral Squat Force 48

Figure 4.3: Representation of Body Markers and Joint Axis Coordinates 51

Figure 4.4: Right and Left Normalized Ground Reaction Forces 54

Figure 4.5: Group Averages and Standard Deviations of the CV 55

Figure 5.1: A Participant Seated within the TPAD System 63

Figure 5.2: The Sit-to-stand Perturbation Experiment Design 66

Figure 5.3: Representative Reactions to Sit-to-Stand Perturbations 67

Figure 5.4: Means and SD of Participants' MG iEMG Results 70

Figure 5.5: Means and SD of Participants' RF iEMG Results 71

Figure 5.6: Means and SD of Participants' BF iEMG Results 72

Figure 5.7: Means and SD of Participants' ES iEMG Results 73

Figure 5.8: Means and SD of Participants' Trunk TE Flexion 75

Figure 5.9: Means and SD of Participants' Trunk TE Rotation 76

Figure 6.1: Participant Seated in the TPAD System 83

Figure 6.2: The Perturbation Experiment Design for Sit-to-Stand 86

Figure 6.3: Margin of Stability and Base of Support Diagram 89

Figure 6.4: Representative Location of the Muscles Used for EMG Collection 90

Figure 6.5: AP MoS at Low Perturbation Intensity 92

Figure 6.6: AP MoS at Threshold Perturbation Intensity 93

Figure 6.7: ML MoS at Threshold Perturbation Intensity 94

Figure 6.8: Perturbation Direction Affects AP MoS at Fail Perturbation Intensity . . . 94

Figure 6.9: Perturbation Type Affects AP MoS at Fail Perturbation Intensity 95

Figure 6.10: Groups respond with different AP MoS at Fail Perturbation Intensity 95

Figure 6.11: Perturbation Direction Affects ML MoS at Fail Perturbation Intensity . . . 96

Figure 6.12: Biceps Femoris at Low Perturbation Intensity 97

Figure 6.13: Medial Gastrocnemius at Low Perturbation Intensity 98

Figure 6.14: Medial Gastrocnemius at Threshold Perturbation Intensity 99

Figure 6.15: ES iEMG at Threshold Perturbation Intensity 100

Figure 6.16: RF iEMG at Threshold Perturbation Intensity 100

Figure 6.17: BF iEMG at Threshold Perturbation Intensity 101

Figure 6.18: TA iEMG at Threshold Perturbation Intensity 101

Figure 6.19: ES iEMG at Fail Perturbation Intensity 102

Figure 6.20: RF iEMG at Fail Perturbation Intensity 102

Figure 6.21: Medial Gastrocnemius at Fail Perturbation Intensity 103

Figure 6.22: TA iEMG at Fail Perturbation Intensity 103

Figure 6.23: BF iEMG Responses at Fail Perturbation Intensity Averaged by Perturbation Direction 104

Figure 6.24: BF iEMG Responses at Fail Perturbation Intensity Averaged by Perturbation Type 104

Figure 6.25: BF iEMG Responses at Fail Perturbation Intensity Averaged by Age Group 105

Figure 6.26: The trunk TE flexion was significantly effected by Age Group 106

Figure 6.27: The trunk TE flexion was significantly effected by Perturbation Type 106

Figure 6.28: The left ankle TE had significant interaction effects between the perturbation type and direction. 106

Figure 6.29: The right knee TE flexion was significantly effected by Age Group 107

Figure 6.30: The right knee TE flexion was significantly effected by Perturbation Type . 107

Figure 6.31: The trunk TE flexion had significant interaction effects between the perturbation type and direction. 108

Figure 6.32: The trunk TE flexion had significant interaction effects between the perturbation direction and age group. 108

Figure 6.33: The right ankle TE flexion had significant interaction effects between the perturbation type and age group. 109

Figure 6.34: The left ankle TE flexion had significant interaction effects between the perturbation type and direction. 109

Figure 6.35: The right knee TE flexion had significant interaction effects between the perturbation direction and age group. 110

Figure 6.36: The left knee TE flexion had significant interaction effects between the perturbation direction and age group. 110

Figure 6.37: The right hip TE flexion had significant interaction effects between the perturbation direction and age group. 111

Figure 6.38: The trunk TE flexion at Fail Perturbation Intensity. 111

Figure 6.39: The left ankle TE flexion was significantly effected by Age Group 112

Figure 6.40: The left ankle TE flexion was significantly effected by Perturbation Direction 112

Figure 6.41: The right knee TE flexion at Fail Perturbation Intensity. 112

Figure 6.42: The left knee TE flexion was significantly effected by Age Group 113

Figure 6.43: The left knee TE flexion was significantly effected by Perturbation Direction 113

List of Tables

2.1 COP and GRF Results for Each Test Condition 23

4.1 Variable Means, (SD) and Statistical Results for SI, COP and Joint Angle Flexion . 53

5.1 Perturbation Thresholds Pearson's Correlation Coefficients 69

6.1 Demographic Information for Sit-to-Stand Study Participants 84

Acknowledgements

My PhD. journey has been like a roller coaster. Thrilling and exciting at first, new research projects, new lab, new friends, New York. And then the fun ride intensified, nose-diving, then going through upside-down loops and rolls. Going into unknown research depths, where no one is in sight. I was being hurled from side to side in my seat, but I was not about to let go, even with COVID. But as the journey got harder, the end got closer. As I got into a groove, the ride's speed significantly increased to an exciting state. The ride was approaching the end, and all of a sudden the tracks disappeared, throwing me forward. Forward into a new explorable space.

I am truly grateful for the support I have been given during my PhD. studies. I would like to first thank my research advisor Dr. Sunil K. Agrawal for always encouraging new ideas and challenging me to be my best. I thank Dr. Nicolas W. Chbat for his time and valuable inputs in my research proposal and dissertation. I thank Dr. Joel Stein, Dr. Jeffrey W. Kysar, and Dr. Michael J. Massimino for reviewing my work and giving me constructive feedback. I also thank and express my gratitude to everyone who participated in my studies; this research wouldn't be possible without you.

I want to express my thanks to my family. Even though they were far away, their encouragement was always felt near by. Les doy gracias a mis padres for always saying good morning, reminding me to call them, sending me words of encouragement and packages of surprises. Thank you Carlos for always offering advice, tech gadgets and lunches. Thank you to my cousins, aunts and uncles for encouraging us to travel together on family trips.

I thank my roommates Dr. Nicole Lee and Dr. Danielle Stramel. Without the two of you my PhD. journey would have been a lot bumpier of a roller coaster. I can't even express the appreciation I have for the two of you. I have been fortunate to have two great roommates as best

friends, thank you for all of the laughs and support throughout my PhD. journey.

I also want to thank Dr. Antonio Prado and Mariana Basilio for their extensive support and the fun times we've had in New York and while traveling together. Thank you Dr. Biing-Chwen Chang for your encouragement and all the cakes you've made. Thank you Dr. Haohan Zhang for all of the advice and fun lab distractions. Thank you Dr. Victor Santamaria for all of the research collaborations we've had together. Thank you for always offering to test the new robotic changes I've made and thank you for making me a better researcher. Thank you Dr. Moiz Khan for always encouraging and mentoring me. Thank you to my labmates for always promoting a friendly work environment, for our daily 12 pm lunches, for acknowledging the "are you in or are you out?" ear, for the shenanigans, and of course, for the support. Thank you to the friends I've made during my PhD. and to the friends who have always supported me.

Now it's time for a new journey. Thank you to those who made this one possible.

Dedication

I dedicate this thesis to my family and friends who have supported me throughout this Ph.D. journey.

Introduction

The presented work describes two cable-driven systems and how they were adapted and modified for rehabilitating standing, squatting, and sit-to-stand movements.

In people with severe neuromotor deficits of trunk and lower extremities, regaining balance in standing is often performed in rehabilitation with manual assistance, rigid body supports or by the use of handrails [1]. Previously, we developed a Robotic Upright Stand Trainer (RobUST), but only characterized the technical features of the robotic system [2]. In this dissertation, RobUST's controller was modified to investigate and further expand postural control training in standing. Postural control encompasses the active control of the body to obtain a posture and the reactive control of the body to obtain a balanced stance from internal or external imbalances, also known as perturbations [3].

Two standing studies are presented in this dissertation. The first study [4], delivered trunk perturbations while simultaneously providing postural assistive forces on the pelvis in 10 able-bodied adults. Posture control responses with 'pelvic support' was then compared to 'no support' and 'hand supported' standing, with and without assistance from RobUST. Postural imbalance was characterized with kinematic displacements and center of pressure (COP) outcomes, such as amplitude and root mean square of the excursions of COP. Surface electromyography (sEMG) was also applied to investigate muscle control. Additionally, we investigated ground reaction and handrail forces during standing to analyze how postural strategies and muscle mechanisms with 'pelvic support' via RobUST would differ from standing with 'no support' and with the 'handrail support'. In the second standing study with RobUST [5], we investigated the feasibility of a robotic standing training paradigm for an individual with spinal cord injury.

Another rehabilitation robotic method incorporated and presented in this dissertation was to

apply forces that redistribute an individual's weight bearing distribution. Squatting is a dynamic task that is often done for strengthening and improving balance [6]. Most squat training systems partially support body weight. However, one of the benefits of a squat exercise is efficiently distributing the body weight among the feet while maintaining stability. Several studies have shown how redistributing body weight among the feet can improve balance [7, 8]. Therefore, in the present dissertation, a squat study is presented with the aims of (i) to show a robotic device that is transparent for studying human behavior during the squatting task, (ii) to investigate how ground reaction forces can be altered among the feet by applying a pelvic force during squatting.

In addition, this dissertation presents a method to characterize and train reactive postural control during sit-to-stand motion. Previously, the Tethered Pelvic Assist Device (TPAD) has been shown to alter individuals gait patterns by applying external forces to the pelvis [9, 10, 11]. Therefore, to characterize sit-to-stand motion, this dissertation presents how the TPAD software and hardware were modified.

Moving from a seated position to a standing position is essential for performing daily functions. However, a sit-to-stand task may lead to falls in people with neuromotor disorders [12]. Previous studies have shown that perturbation-based training can improve individuals' reactive control and reduce the risk of falls, [13]. However, few studies have investigated individuals' reactive control while transitioning from sit-to-stand. The present dissertation aims to understand how young and older adults react to physical perturbations when transitioning from sitting to standing. Two types of perturbations were delivered to the participants. In one condition, a cable-driven robotic system displaces the user's pelvis. In the second condition, a treadmill displaces the participants' support surface. A set of perturbations were delivered until participants failed to maintain balance. The type of perturbation delivered, i.e., force applied on the pelvis or displacement of the support surface, was randomized within each set. In addition, the direction of the perturbation, i.e., anterior or posterior, was also randomized within each set. Joint angles, ground reaction forces, and muscle activity using surface electromyography were measured to characterize their balance control strategies.

Chapter 1

Cable-Driven Robotic Systems

1.1 Robotic Upright Stand Trainer (RobUST)

RobUST is a cable-driven robotic system that can actuate belts placed on a participant's trunk and pelvis, as shown in Fig. 1.1. RobUST contains 14 motors (Maxon Motor, Switzerland) each instrumented with an encoder and a load-cell (LSB302 Futek, California) in series with the motor. In Fig. 1.1, four motors are used to actuate the four cables attached to each of the two belts. The cables can be rerouted via pulleys to accommodate the participant's height and the task. A motion capture system (Vicon Vero 2.2, Denver) provides real-time information on the position and orientation of the two belts to the robotic controller, programmed in LabVIEW (National Instrument v2017). The system contains two force plates that participants stand on, (Bertec Force Plate V1, Ohio) and a height adjustable handrail (Bertec, Ohio) that measures forces applied onto the bar.

1.2 Tethered Pelvic Assist Device (TPAD)

TPAD actuates eight cables attached around a pelvic belt. Four of the cables are routed up from the pelvic belt and four are routed down from the pelvic belt. All cables are routed to load cells (mlp200, Transducer Techniques, California), then passed to AC motors with gearboxes (Kollmorgen, Pennsylvania). The motors are all mounted on an aluminum frame (80/20 Inc., Indiana). The TPAD system has an instrumented force plate treadmill (Bertec, Ohio), two handrails along the sides, and a visual dome, Fig.1.2. For the sit-to-stand studies, a bar was secured across the center

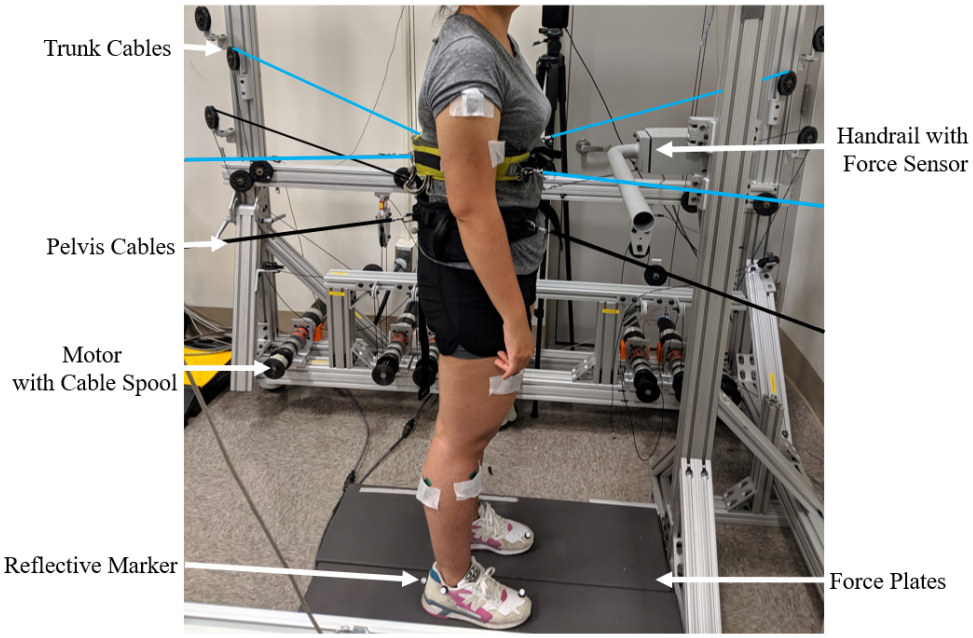

Figure 1.1: A participant inside the RobUST system with labeled parts of the device. The trunk and pelvis cables are attached to the respective belts on the user.

of the treadmill and mounted on the aluminum frame. A rowing seat cushion (Kohree Rowing Seat, Amazon Store) was attached to the bar. The height of the top of the bar from the treadmill was set to 46.5cm, and the height of the seat cushion was 7cm. Ten motion capture cameras detected markers placed around the pelvic belt and on the participant's joints to get real-time position data (Bonita-10 series from Vicon, Colorado).

1.3 Control System

The control system for both cable driven devices consists of a low-level and a high-level controller, Fig. 1.3. For the work covered in this dissertation, the main modifications to the systems were in the tension planner, Sect. 1.4, and the force controller, Sect. 1.5. The low-level controller uses a closed loop PID control law to achieve the desired tensions. The high-level controller uses the position of the pelvic belt to determine the desired forces, F_d, and uses a tension planner to calculate the cable force distribution. Motion capture cameras are used to determine the location of the pelvic belt. Load cell, tension sensors, are used to determine the current tension of the cables

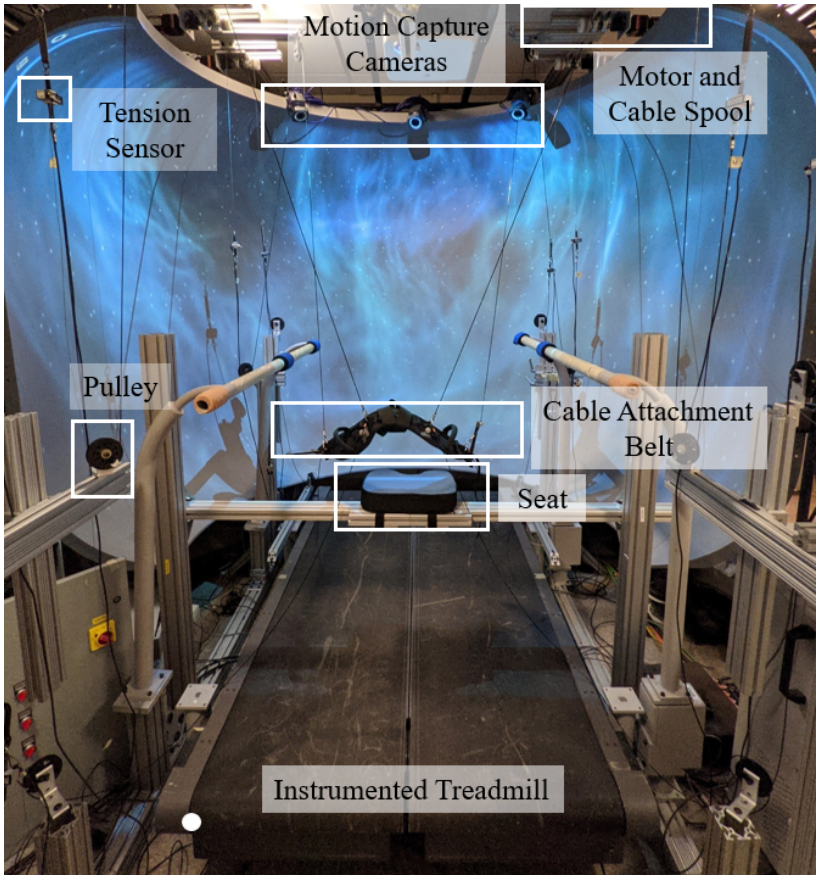

Figure 1.2: The TPAD System. A pelvic cable attachment belt has 8 cables attached, routed through pulleys to tension sensors. The cable is then routed to a cable spool on a rotating motor shaft. Motion capture cameras surround the TPAD system to track in real-time the position of the belt and body markers. A visual is displayed on the dome to the user when conducting experiments.

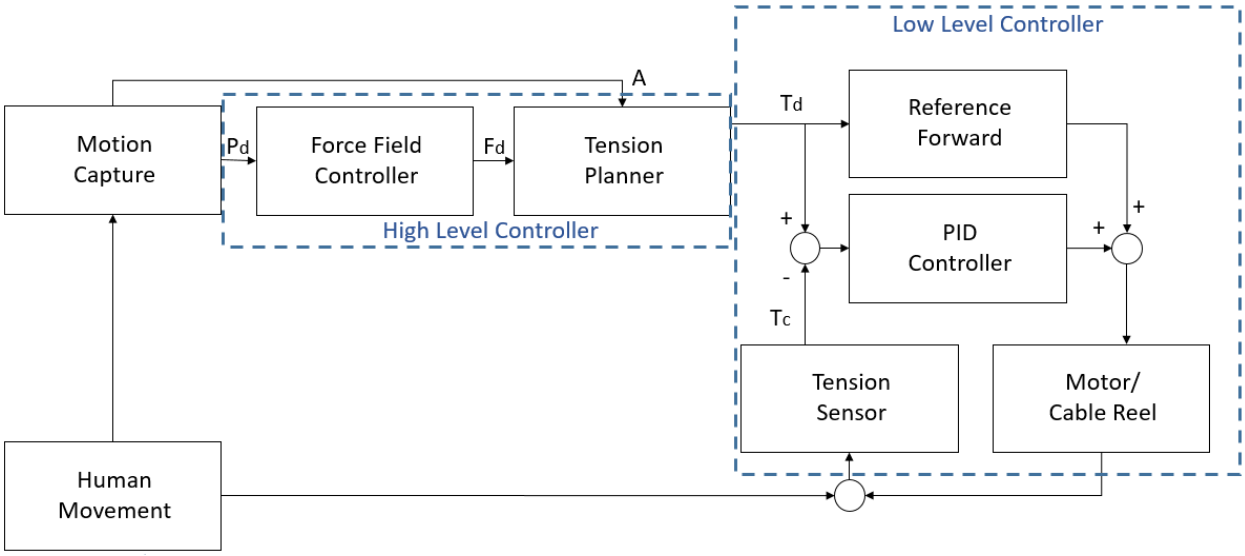

Figure 1.3: The control system for both RobUST and TPAD. The main variations between the two systems are within the high level controller. The high level controller consists of the force field controller and the tension planner. The low level controller relates the desired and current tension information to motor input signals via a PID controller and reference forward.

that are attached to a belt the user wears. Both systems are controlled using a custom Labview script.

1.4 Tension Distribution Problem

The RobUST and TPAD cable-driven systems apply a force to a belt the user wears. To achieve a desired force $\vec{F}$, the desired cable tensions $\vec{T}$ are related to desired forces F by a matrix A which represents the geometry of the cabled system:

$$\vec{F} = A\vec{T} \tag{1.1}$$

where

$$\vec{F} = \begin{bmatrix} F_x \\ F_y \\ F_z \\ M_x \\ M_y \\ M_z \end{bmatrix}, A = \begin{bmatrix} \hat{I}_i \\ \hat{r}_i \times \hat{I}_i \end{bmatrix}_{6\times n}, \vec{T} = \begin{bmatrix} T_1 \\ . \\ . \\ . \\ T_n \end{bmatrix} \tag{1.2}$$

Here A is 6xn, representing the six degrees of freedom of the end-effector belt and the n actuated cables of the robotic systems. $\hat{I}_i$ is the cable unit vector away from the pelvis attachment point on the belt towards the corresponding routing pulley exit point. $\hat{r}_i$ is the unit vector from the center of the pelvic belt towards the i^{th} cable attachment point on the pelvic belt. How to solve for the tensions, is the tension distribution problem, Eq. 1.1.

1.4.1 RobUST

RobUST has high-level and a low-level controllers. The low-level controller uses a closed loop PID control law to achieve the desired tensions [2]. The high-level controller and the tension distribution problem was modified for the studies in this dissertation.

For cable driven systems, they require at least n-degrees-of-freedom (DoF) + 1 cables with positive tension to fully constrain it mathematically [14]. The system is therefore redundantly restrained because of the n+1 actuated cables. Infinitely many tension solutions are possible for redundantly restrained cabled systems. Therefore, to solve for an optimal tension solution to the distribution problem (Eq.1.1), quadratic programming was used.

For RobUST, the objective of the quadratice programming was to to solve for the cable tension distribution problem (Eq.1.1) by finding the minimum tension that achieves a feasible solution

using:

$$\begin{gathered} min f \\ f = \frac{1}{2}(T - T_p)^T (T - T_p) \\ s.t.\ F = AT\ and\ T_{i,min} \leq T_i \leq T_{i,max} \end{gathered} \tag{1.3}$$

where T_p is the set of solved tension values of the previous iteration. The cable tension algebraic inequality range was set to 12N minimum, the minimum tension value to avoid cables becoming slack, and a maximum of 80N, a maximum tension value the cables are safely rated for. This method is used to accomplish a continuous tension profile per cable.

1.4.2 TPAD

TPAD has a high-level and a low-level controller Fig.1.3. The low-level controller uses a closed loop PID control law to achieve the desired tensions [15]. The high-level controller and the tension distribution problem was modified for the studies in this dissertation. The high-level controller uses the position of the pelvic belt to determine the desired forces, F_d, and uses a tension planner to calculate the cable force distribution. The cable tensions T are related to forces F by a matrix A related to the geometry of the system Eq. 1.1.

Here A is a 6x8 matrix, representing the six degrees-of-freedom of the end-effector and the 8 actuated cables of TPAD. $\hat{I}_i$ is the cable unit vector away from the pelvis attachment point on the belt towards the corresponding routing pulley exit point. $\hat{r_i}$ is the unit vector from the center of the pelvic belt towards the i^{th} cable attachment point on the pelvic belt.

Similar to RobUST, TPAD is also a redundantly restrained system. Therefore, quadratic programming is used to solve for the cable tension distribution problem by finding the minimum

tension that achieves a feasible solution using:

$$\begin{aligned} &min f \\ &f = F_e^T F_e + \mu T^T T \\ &s.t.\ T_{i,min} \leq T_i \leq T_{i,max}, \\ &F_e = AT - F_d \end{aligned} \tag{1.4}$$

where the objective function tries to minimize the tension value solution, with a weighting factor μ, an algebraic equality constraint of the desired force error, F_e, in case there is no solution to Eq.(1.1), and an inequality algebraic constraint of the positive cable tension range. The cable tension range was set to 15N minimum, to avoid cables becoming slack, and a maximum of 75N, the safety rating of the TPAD cables. This method results in a solution across the sit-to-stand motion.

1.4.3 Logic-Based Tension Planner

Quadratic optimizers for tension distribution can be slower in real-time applications when compared to a Barycentric or closed-form approach [16]. Another limitation of using a quadratic optimizer is the likelihood of no solution being found using the set of applied constraints [17]. To overcome these obstacles, a logic-based tension planner is defined and presented in this work.

Unlike numerical solvers, like quadratic solvers, this logic case planner takes virtually no computation time: it selects which cables to distribute the force to based on the desired resultant force direction, $\vec{F}$. An example of the case structure selection is illustrated in Fig.1.4.

To accommodate for 3D motion of the pelvis such as during a squat movement or sit-to-stand, eight cables are used to actuate the pelvis. Four cables are routed from the top of the frame to the pelvic belt and four from the bottom of the frame to the pelvic belt Fig.1.4. The desired cable tensions $\vec{T}$ are related to desired forces $\vec{F}$ by a matrix A related to the geometry of the system, Eq. 1.1.

The 8 cables utilized are symmetrically routed around the frame to simplify the force distri-

bution, an example of how the cables are routed are shown in Fig.1.4. The logic-based tension planner defined in this work goes through a case structure that depends on the direction of the desired resultant pelvic force components $F_{des} = [F_x, F_y, F_z]$. The logic-based tension planner iterates through the three force components and selects the case associated with the sign of the component's direction (+/-). Within each case structure, there is a preset selection of motors that correlates with the cables that are in that force component F_j direction (+/-). The force component F_j is then distributed equally to the respective cables unit direction $\hat{I}_i$, using the following:

$For\ i = 1 : n$

$$T_i = k_j \vec{F}_{des} \begin{bmatrix} 0 \\ j \\ 0 \end{bmatrix} \cdot \hat{I}_i \tag{1.5}$$

end

where n is the number of cables, $j = 1$ and it's location is relative to the force component ($F_x, F_y, or F_z$), and k_j is a constant gain component found via physical tuning of the cabled system. For this work, $k_j(x, y, z) = (0.625, 0.875, 0.5)$. The desired tension values T_j are then summed to get the combined desired tension for cable i, as in

$$\begin{bmatrix} T_i \\ . \\ . \\ T_n \end{bmatrix} = T_{min} + \sum_{j=1}^{3} \begin{bmatrix} T_i \\ . \\ . \\ T_n \end{bmatrix}_j \tag{1.6}$$

The cables which were not used in the force distribution had a minimum tension value.

1.4.3.1 System Performance

To evaluate the system performance utilizing the logic-based tension planner, the absolute error in forces, (desired force minus actual force), was calculated given squat pelvic trajectory motion from six participants.

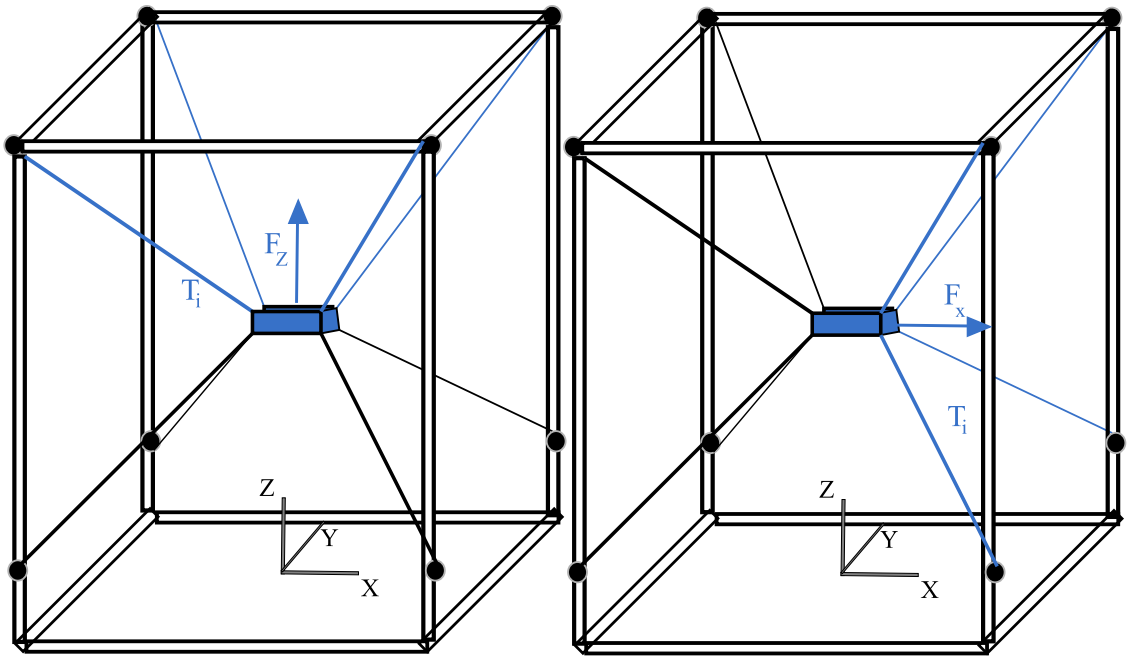

Figure 1.4: An example of how the logic-based tension planner case structure functions. For a desired force component F_j, the case structure checks the direction of the component and then selects the highlighted cables associated with that direction. The force is then distributed amongst the four.

The actual forces are calculated based on the actual tension values and the structure matrix A, Eq (1). The force error in squat motion was averaged over the six participants and are reported based on the average participants body weight (BW). Error in the lateral direction was $F_x error = 10.25N(1.44\%BW)$. Error in the anterior-posterior direction, $F_y error = 10.89N(1.52\%BW)$, and in the vertical direction, $F_z error = 21.75N(3.05\%BW)$.

A disadvantage of using the logic-based tension planner instead of the quadratic solvers, is that the resultant moment on the pelvis cannot be controlled. On average the moment components were $M_x = 1.57, M_y = 1.02, M_z = 1.29$ N·m. The logic-based planner required tuning of the gains to achieve the desired forces.

For one component desired forces, $(F_x, F_y, or F_z)$, and faster real-time applications, the logic-based tension planner is suitable for symmetric cabled systems. However, for force and moment control, a quadratic optimizer is better suited. Therefore, quadratic solvers are implemented for the studies in this dissertation, as described in Eq. 1.3 and Eq. 1.4.

1.5 Assist-as-Needed Force Controllers

An assist-as-needed force controller is a method to determine the desired force to apply to the belt worn by the user. Assist-as-needed indicates the system will only apply forces to the user when they need it, as determined by the controller and the user's needs. The force controller parameters can be altered with a custom user interface during testing. To achieve a transparent force mode, the desired force on the pelvis can be set to zero. This would command the tensions to remain at a minimum tension value throughout the user's motion. The researcher can also specify a direction and %BW magnitude of the desired force. The force controller uses the locations of the pelvic markers to determine the current position of the pelvis, then determines a desired force accordingly. Examples of implemented assist-as-needed force controllers are described in the following sections.

1.5.1 Irregular Force Field

In this dissertation, an assist-as-needed force controller has been implemented in both systems. Assist-as-needed controllers applies the user a set force once the user goes beyond their stability limits. The set force is customized to the individual. The force is in the direction of the user's neutral trunk center, either while seated or standing. Previously, this boundary was a predetermined circle of a set radius [18]. This assumed the participants had a symmetric seated postural control limit. In individuals with spinal cord injury or individuals with asymmetrical stabilities, there is a need for a force field boundary that is both individualized and designed around their irregular and asymmetric postural control limits [19]. A new force field controller was implemented that was obtained through a customized test, the postural star test. This test measures the participants maximal trunk excursion in eight directions while they are seated or standing. Infrared motion capture cameras are used to obtain the displacement of the participant's trunk. The participants were asked to move as far as they could and return to their center seated position while maintaining control and without any assistance from the hands. The maximum area of excursion, their range of

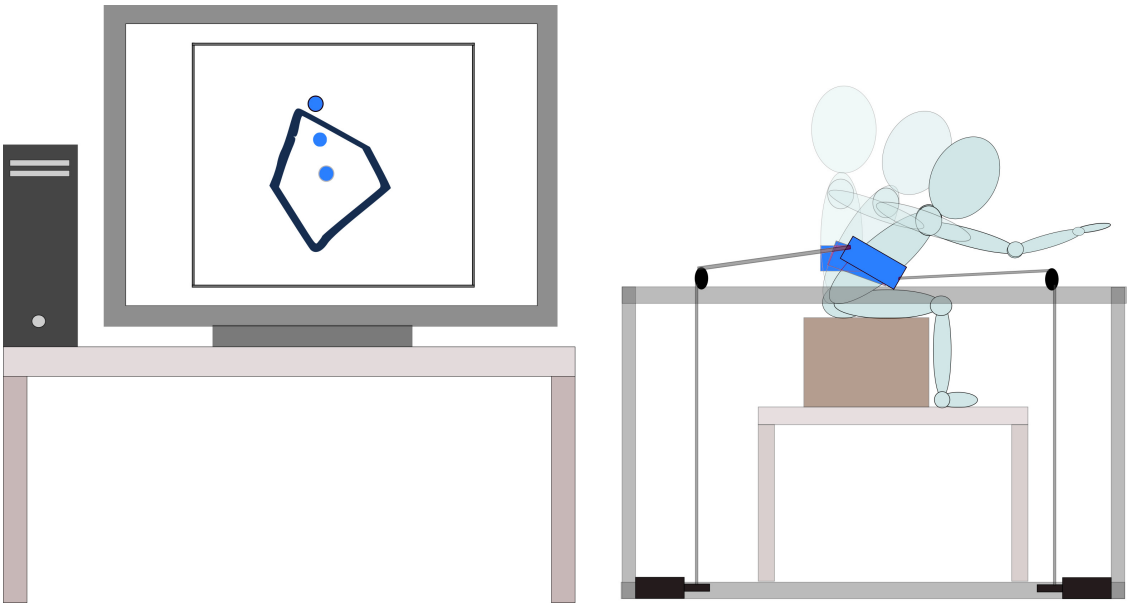

Figure 1.5: A visual layout of how the irregular force field functions. The assistive force is applied towards the center once the individual goes beyond the stability boundary.

motion, was used as the 'irregular' force field boundary. The participants performed the postural star test without any assistive forces of either device. An example of the irregular force field during seated trunk movement is shown in Fig. 1.5.

1.5.2 Trajectory Based Control and Experiment Example

In rehabilitation, repetitive practice in certain motions are encouraged to improve joint coordination and strength. Therefore, an assist-as-needed trajectory based force controller was developed and implemented in RobUST. A visual schematic is shown in Fig.1.6. A trajectory based force controller tracks the position of the user and can apply an assistive force to the user depending on how far away they are from the trajectory path. This trajectory path is considered the target trajectory.

Every individual behaves and moves within a certain way, in order to adapt and customize how individuals move, the assist-as-needed trajectory can be customized. The target trajectory can be predetermined by the researcher or can be custom to the user by recording in real-time a set trajectory. For these experiments, the researcher asked participants to squat in RobUST's transparent mode while recording the pelvic trajectory during these squats. The average squat

profile is then calculated and stored in the controller as the target trajectory. Two waypoints, positions used as reference, are used to determine the direction the participant is moving. The first waypoint is the neutral standing position of the participant. This first position is saved at the beginning, before the participant begins to squat. If the participant needs to adjust their neutral standing position, the researcher can update the waypoint at any point. The second waypoint is the minimum Z target trajectory point.

The trajectory force controller continuously checks if the participant's current position is within a set distance of the target trajectory. This set distance can be declared in the front panel of the interface, for these experiments a 2cm distance was used.

To determine if the participant is descending or ascending, the trajectory based controller uses an indicator value, 0 = $descending$ and 1 = $ascending$. In the beginning, it is initially set to zero, therefore the controller will know that the participant will begin to descend. Once the participant is within 2cm range of the second waypoint, the controller switches to 1 = $ascending$. Depending on this, the controller will search if the participant's current position is within range of the target ascending trajectory points or the descending trajectory points.

If the participant is within a magnitude distance threshold, 2cm, from either waypoint or from any of the trajectory points, the desired force is set to zero. Once the participant is outside the threshold range, an assisting force guides the participant towards a position along the pelvic target trajectory 10% ahead of their current position. The assistive force's magnitude is set by the researcher and is a percentage of the participant's BW. The force direction is calculated by finding the closest point along the trajectory, then the corresponding position which is 10% ahead. The unit vector from the current position to the desired position is then calculated.

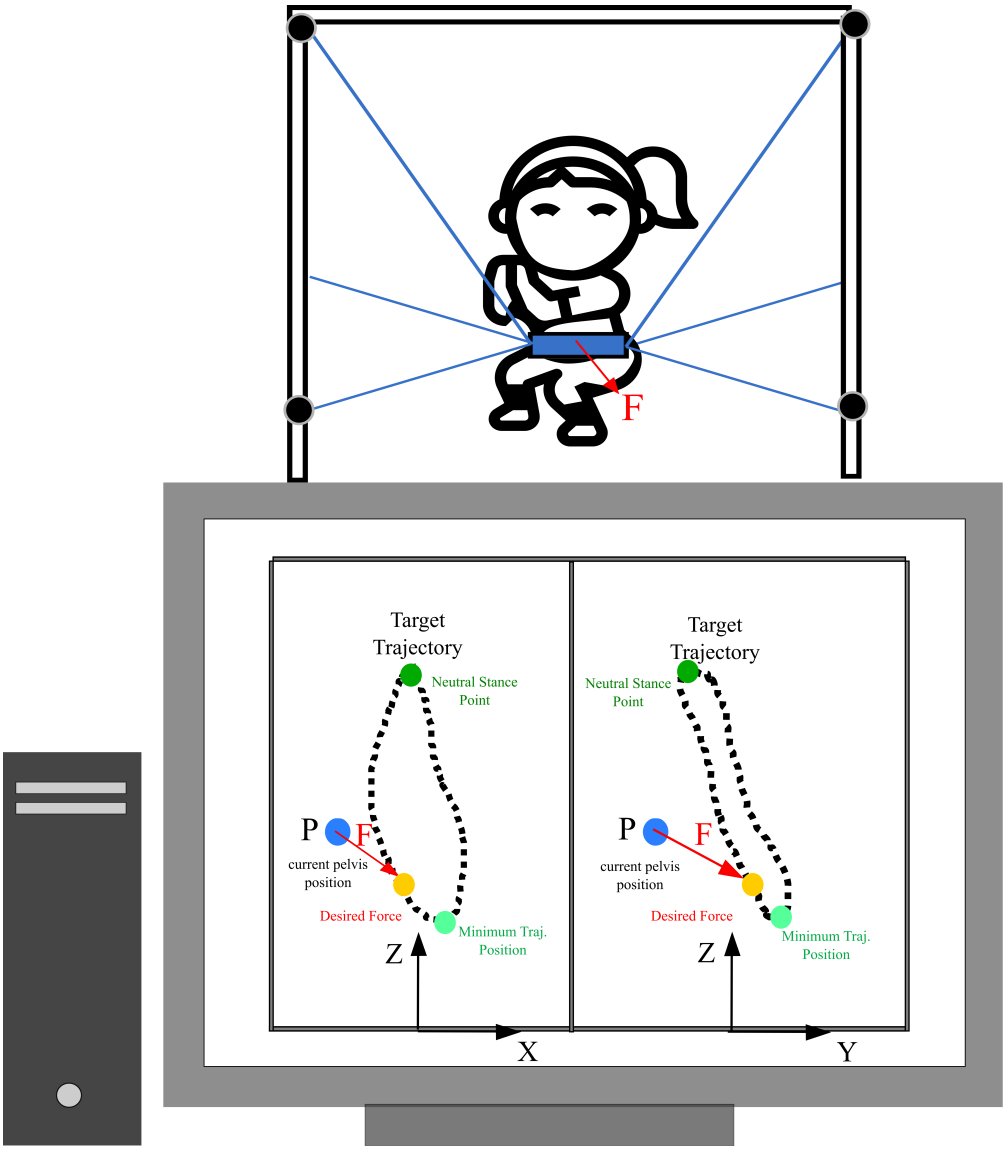

Figure 1.6: A visual layout of how the trajectory force assistance functions. The assistive force is applied towards the desired target trajectory point. The two waypoints are the green points. The blue point P, is the current pelvis position. The yellow point is the desired position. If the current point is further than a threshold distance to the trajectory, a force is then applied from the current point toward the desired point.

Chapter 2

Comparing Traditional Rehabilitation Method to RobUST

2.1 Introduction

Postural responses are task and environment dependent, and hence require different neuromuscular control strategies appropriate to the task [20, 21]. Posture is central to effectively and efficiently perform activities of daily life [22]. External perturbations are frequent during daily life, from sudden bus stops to accidental crowd pushing. Unexpected perturbations disrupt the person's equilibrium and elicit muscle responses to restore balance in standing position. These are called *in-place* postural strategies [23]. When muscle responses cannot overcome the postural imbalance, a person needs to perform compensatory actions such as taking a step or reaching for an external support to avoid falling. These are termed as *change-in-support* postural strategies [22, 24]. This situation is frequent in individuals with neuromotor disorders who continuously step or reach for support to recover balance even under small perturbations [25]. The goal of postural rehabilitation in neuromotor disorders is to practice and relearn *in-place* and *change-in-support* postural strategies to adapt postural control to diverse perturbations present in everyday surroundings.

2.1.1 Motivation

We have developed a novel cable-driven system, Robotic Upright Stand Trainer (RobUST), that can apply forces on the trunk and the pelvis [2]. Previously, we focused on the technical features of RobUST. However in this study, we investigate and compare postural control strategies that able-bodied participants use in standing with RobUST versus a traditional rehabilitation method,

such as the use of a handrail.

In rehab settings, grasping a handrail is a recurrent *change-in-support* postural strategy adopted by individuals with impaired trunk and lower extremity control to prevent falls during unexpected perturbations [22, 24, 26]. The main functional goal of RobUST is to promote independent postural standing while encouraging users to elicit *in-place* postural strategies via assistive forces. The rationale is that RobUST would allow users to fully experience sensorimotor cues during trunk perturbations and balance recovery. In addition, RobUST can potentially train critical control strategies to maintain postural balance without the need to step or use an external support, such as a handrail. In this study, we predict that our cumulative experimental findings with RobUST will have a major impact on improving current training approaches in postural standing.

In our previous study with RobUST [2], we analyzed upper body displacements when perturbations were applied at the trunk and pelvis, with and without assistive forces. We observed that trunk perturbations were accompanied by large-amplitude postural imbalances, as opposed to perturbations when applied on the pelvis [2]. This previous study, however, did not consider i) a two level assistive force, ii) the neuromuscular mechanisms by which users control postural stability, iii) how the postural responses differed when using RobUST compared to traditional balance training methods, and iv) the potential additive assistance effects when combining assistive forces with a static support such as handrails. These scenarios are particularly interesting for individuals with profound lack of control of trunk and lower extremities.

2.1.2 Research Questions

For this study, RobUST provides randomized perturbations at the level of the trunk. We characterize postural stability with output variables from two force plates and body translation from motion capture cameras. Muscle control mechanisms are characterized with surface electromyography (sEMG). Specifically, we aim at answering the following questions: I. How does RobUST's assistive force field on the pelvis improve postural control and modulate muscle activity (sEMG) during direction-specific trunk perturbations? II. Can the RobUST's pelvic assistive force field im-

prove postural stability to the same level as when participants support themselves with a handrail? III. Do we observe an additive effect in postural control when people stand holding a handrail while receiving pelvic assistive forces via RobUST?

We hypothesize that the use of RobUST will provide significant stabilizing effects, such as reducing postural excursions and variability. This increase in postural stabilization would be associated with higher muscle sEMG activity with RobUST compared to the traditional use of a handrail.

2.2 System Description

A closed-loop PID controller modulates the tension to achieve the desired force. Further details on the PID controller are described in [2]. The force assistance in this study was configured differently from our previous research [2, 27]. However, the framework of how the tension planner distributes the force among the cables remains the same. The architecture of the assistive force controller resembles a virtual donut-shaped ring, Fig. 2.1, around the pelvis. In this study, the force controller has two main boundaries, the first is an inner radius of 5 cm and the second has an outer radius of 10 cm. Within the first boundary, the force controller creates a 'transparent' mode, i.e., nearly zero external forces are applied during motion. There is a force applied to keep the cables in tension. This transparent mode allows participants to move freely within their standing workspace. The motion capture system detects the Cartesian coordinates of the center of the belt and is used to determine whether the user is within the inner or outer boundary. Once the subject is outside the first boundary, an assistive force of 5% of body weight (BW) is applied. In this study, when the subject reaches the outer boundary, an assistive force of 20% BW is applied to keep the center of pelvis from going further. This 20%BW force was selected to ensure that participants would be safe and not fall. These forces can be adjusted to personalize RobUST to the motor and postural characteristics of the individual. The direction of the assistive force is towards the center, i.e., the neutral position of the subject when standing upright. This center position can be redefined through the graphical user interface of the RobUST system during the experiment,

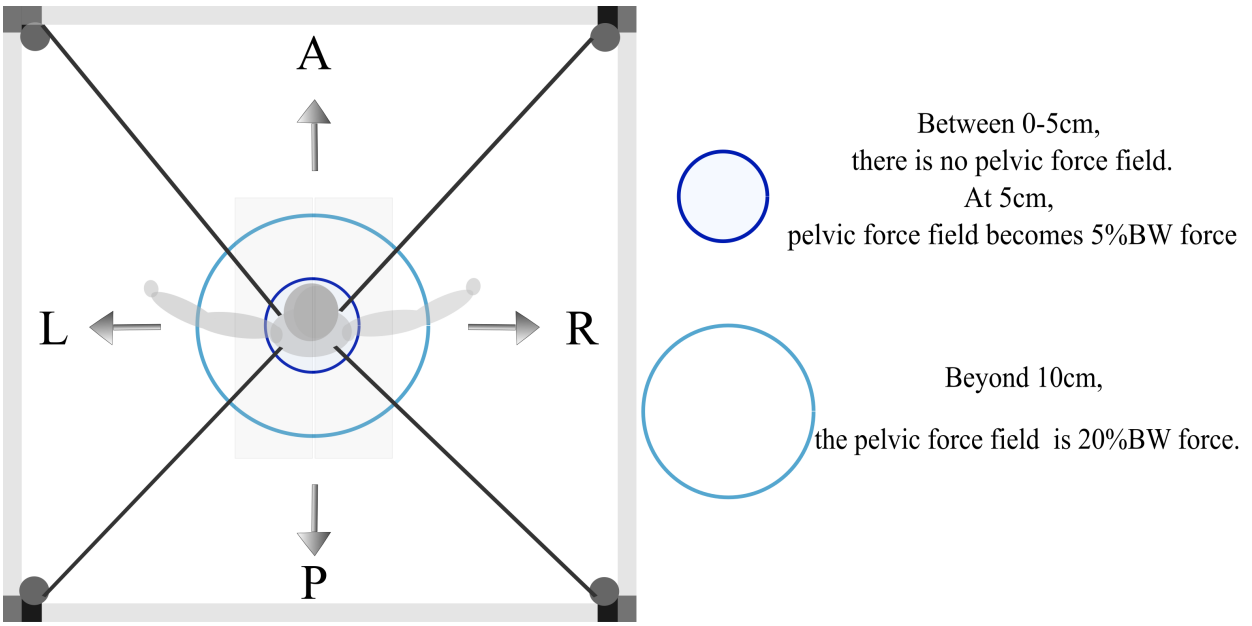

Figure 2.1: Representation of the force field and trunk perturbations: Anterior (A), Right (R), Posterior (P), and Left (L).

allowing re-centering of the geometrical center of the belt within force field boundaries if a new standing position is acquired. The RobUST force field had an average absolute error of 4.1N between the desired and actual forces in the x-direction and 4.0N in the y-direction.

2.3 Experiment Design

2.3.1 Procedure

The protocol had four experimental conditions and in each condition, RobUST delivered 8 randomized trunk perturbations. Two perturbations along each of the four directions were examined: anterior (A), posterior (P), Left (L), and Right (R). The trunk perturbation force was set to 20% of the participant's body weight. The force profile was trapezoid with 0.5 seconds of ramp up, 0.5 seconds of constant force equal to 20% body weight, and 0.5 seconds of ramp down to minimum tension, Fig. 2.2. The force magnitude and duration were chosen based on a previous study that showed kinematic displacements were adequate at these settings to study the response [2]. Participants were instructed to stand upright and recover balance without taking any step when RobUST

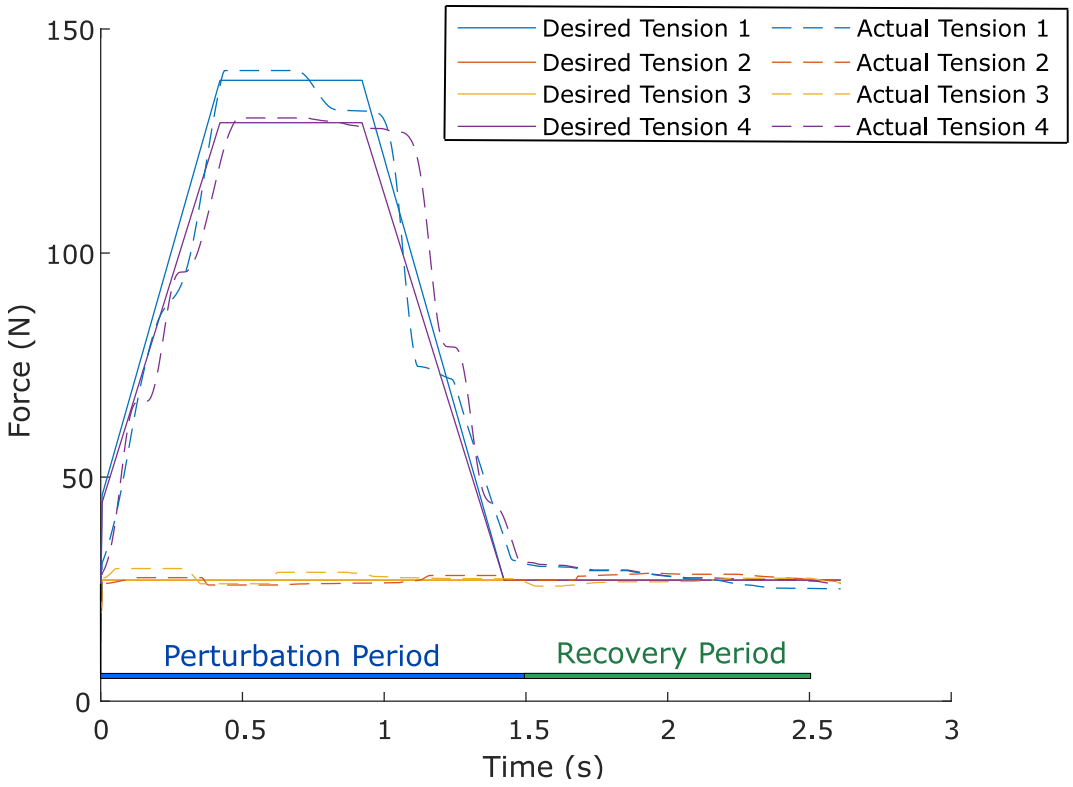

Figure 2.2: A trunk perturbation force profile for a representative participant in the anterior direction. The perturbation duration is 1.5s followed by a recovery period of 1s.

delivered the trunk perturbation. However, the participants were advised to reach for the handlerail before taking a step, only if it was necessary. The position of the trunk belt was consistent across participants, placed on the lower ribs, Fig. 1.1. The four experimental conditions were as follows: No Support (NS), Handrail Support (HS), Pelvic Support (PS) from RobUST, and Handrail support along with Pelvic support from RobUST (HPS). In the NS, participants received trunk perturbations without handrail contact and without cables attached to the pelvic belt. In the HS condition, participants held onto a firm handrail placed at elbow's height but did not have cables attached to the pelvic belt. For the PS condition, RobUST provided assistive forces on the pelvis. In the HPS, participants held onto a handrail and received pelvic support from RobUST.

Kinematic position data of trunk, pelvis and feet were collected using nine Vicon cameras. Participants stood on two six-axis Bertec force plates, each foot on a different plate. Surface electromyography (sEMG) muscle activity was recorded by a 14 channel Delsys Trigno Wireless

System (Delsys Incorporated, Massachusetts). Bilateral sEMG signals were registered from deltoids (DT), trapezius (TP), biceps (BC), erector spinae (ES), rectus femoris (RF), gastrocnemius (LG), and tibialis anterior (TA) and were recorded making up 14 channels. The abdominal muscles were not measured due to the trunk and pelvic belt locations.

2.3.2 Participants

Ten adults, 5 females and 5 males, with no musculoskeletal or neurological conditions participated in the experiment. The participants' characteristics were: height 170 ± 12.3cm, weight 70.7 ± 18kg, and age 26.8 ± 4yrs. Participants were informed about the research procedures and signed a written consent approved by the Institutional Review Board of Columbia University before participating.

2.3.3 Data Processing

Data was processed offline using MATLAB (Mathworks Inc.). Statistical analyses were carried with SPSS (version 27, IBM, 2020). Data recordings were synchronized with the perturbation onset; which was determined once cable tension increased above 5% from the desired onset. Data was segmented into two periods, Fig. 2.2, perturbation period, from onset to the end of the perturbation (1.5s), and the recovery period, which corresponded to a duration of 1s after the end of the perturbation.

Kinematic data was sampled at 100Hz. Reflective body markers were placed, three around each trunk and pelvic belt, one at each shoulder, (near the acromion), and three per foot (positioned about the toe, heel and ankle). Marker data was passed through a 4th order low-pass filter at 6Hz cut off frequency. The mean and amplitude (maximum-minimum) of the pelvis and upper trunk position was determined for each perturbation and recovery period. Local coordinate frames were calculated for each foot, pelvis and trunk based on the International Society of Biomechanics (ISB) recommendations [28]. The feet and pelvic angles were calculated in reference to the initial ground frame at the start of perturbation, and the trunk angles are in reference to the local pelvic frame.

The force plate and handrail force data was recorded at 1000Hz and passed through a 4th order low-pass filter at 6Hz cut off frequency. We analyzed the root mean square (RMS) position of the ground COP, as defined in [29, 30], and the amplitude COP (maximum-minimum), as defined in [31]. The ground COP in the anterior-posterior (AP) and medio-lateral (ML) directions were exported from Vicon Nexus software (Vicon Vero 2.2). Center of pressure variables were normalized based on the participants BOS, ML COP by the width of BOS, and AP COP by the length of the BOS, similarly to Maki et al. [32]. Mean handrail forces and mean ground reaction forces were normalized by participant's weight. For the ML directions, the data was processed based on participants dominant and non-dominant hemibody side.

The average EMG value was removed from the entire signal. Then the EMG signal was band-pass filtered (60-500Hz), rectified, and low-pass filtered at 100Hz. The integrated EMG (iEMG) data was calculated and normalized by the integrated EMG activity obtained while participants stood still without postural disturbance (baseline EMG) [33]:

$$iEMG_{norm} = \frac{\int_0^t EMG - \int_0^t EMG_{baseline}}{\int_0^t EMG_{baseline}} \tag{2.1}$$

where t is dependent on the period, 1.5s for perturbation and 1s for recovery. For each participant, the baseline iEMG of each muscle group was registered during steady standing. The iEMG data was added for postural muscles (ES, RF, LG and TA) during anterior-posterior perturbations. Dominant and non-dominant muscles were examined during lateral perturbations.

2.3.4 Statistical Analysis

A total of 320 trials were examined. Data did not follow a normal distribution (Shapiro-Wilk test = p <0.05) and was highly variable across trials, participants, and perturbation directions. We found that postural and muscle responses across conditions depended on both perturbation directions and experimental conditions. Generalized Estimating Equations (GEEs) account for within-subject correlation responses of many different distributions when data are clustered within

Table 2.1: COP and GRF Variable Means and Standard Error for Each Test Condition during Trunk Perturbation Periods ($*p < 0.05$ in Exp. Condition Compared to NS, $*p < 0.05$ in Exp. Condition Compared to HS, $*p < 0.05$ in Exp. Condition Compared to PS, $*p < 0.05$ in Exp. Condition Compared to HPS)

Experimental Conditions	Variables	Anterior mean ± SE	Posterior mean ± SE	Dominant mean ± SE	Non-Dominant mean ± SE
No Support*	RMS COP	0.25 ± 0.02	0.12 ± 0.02	0.37 ± 0.08	0.28 ± 0.07
	COP Amplitude	0.46 ± 0.05	0.31 ± 0.03	0.70 ± 0.09	0.66 ± 0.07
	GRF (%bw)	1.02 ± 0.01	1.03 ± 0.01	1.03 ± 0.01	1.02 ± 0.01
Handrail Support*	RMS COP	0.13* ± 0.03	0.07** ± 0.018	0.34 ± 0.09	0.25 ± 0.09
	COP Amplitude	0.27* ± 0.06	0.17* ± 0.04	0.65* ± 0.10	0.66 ± 0.11
	GRF (%bw)	0.98**± 0.01	1.02 ± 0.01	1.00**± 0.01	1.00**± 0.01
Pelvic Support*	RMS COP	0.14** ± 0.03	0.07** ± 0.022	0.25* ± 0.08	0.20 ± 0.08
	COP Amplitude	0.26**± 0.05	0.22* ± 0.04	0.53* ± 0.07	0.52 ± 0.08
	GRF (%bw)	1.02** ± 0.01	1.03 ± 0.01	1.03** ± 0.01	1.02** ± 0.01
Handrail+Pelvic Support*	RMS COP	0.08** ± 0.02	0.01**** ± 0.009	0.19* ± 0.07	0.18 ± 0.06
	COP Amplitude	0.15** ± 0.03	0.08* ± 0.01	0.48 ± 0.06	0.48 ± 0.07
	GRF (%bw)	0.99**± 0.01	1.01 ± 0.01	1.00**± 0.01	0.99**± 0.01

subgroups [34]. Thus, GEEs were used to analyze events-in-trials following a repeated-measures procedure. In the analysis, participants and perturbation trials were used as clusters and experimental conditions and perturbation directions as within-subject variables. A linear model was selected. An exchangeable covariance structure was specified as correlation matrix based on the quasi-likelihood under independence criterion (QIC) goodness of fit coefficient, and because certain level of correlation between trails and within participants is expected. *Post-Hoc* testing with sequential Holm-Bonferroni method to correct multiple comparisons was applied if the statistical model was significant.

2.4 Results

2.4.1 Postural Stability

In the three external support conditions, the AP COP amplitude was significantly reduced in both anterior (Wald $\chi2 = 44.79$, $p<0.001$), and posterior perturbations (Wald $\chi2 = 40.38$, $p<0.001$), Fig. 2.3. The ML COP amplitude was also significantly different in the lateral directions, toward the dominant (Wald $\chi2 = 15.357$, $p<0.05$) and non-dominant hemibody (Wald $\chi2 = 10.533$, $p<0.05$). Table 2.1 summarizes means and standard errors for each support condition.

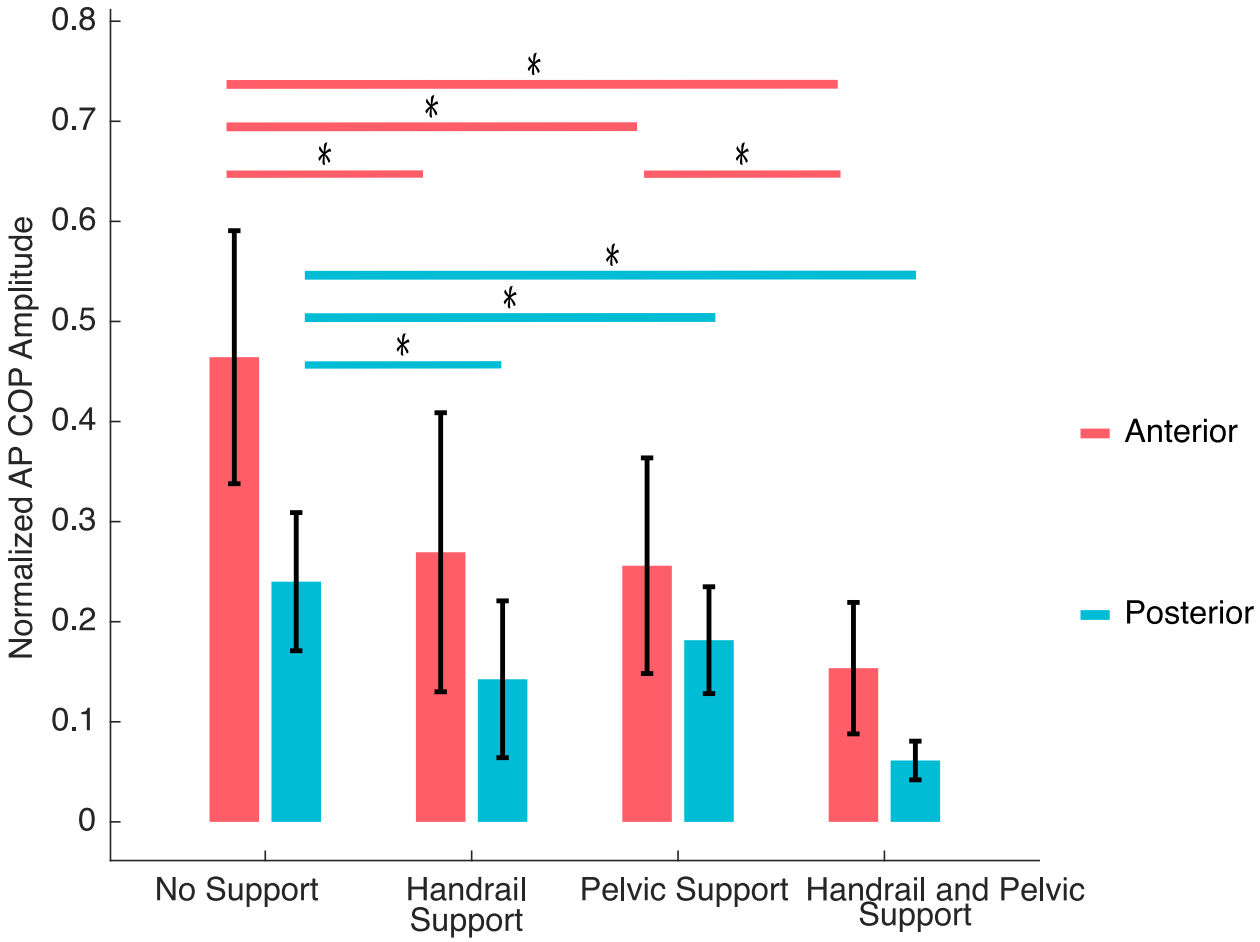

Figure 2.3: Group averages of normalized COP amplitude in the AP direction across experimental conditions during anterior-posterior perturbations are shown. HPS offered the most stable postural control during anterior-posterior perturbations. $*p$ <0.05

The use of a handrail, RobUST's PS, and the combination of both in HPS, assisted postural recovery by significantly decreasing the normalized RMS COP, Table 2.1, during anterior (Wald $\chi 2$ = 61.11, p<0.001) and posterior perturbations (Wald $\chi 2$ = 31.42, p<0.001). In the ML directions, there was a significant effect towards the dominant hemibody (Wald $\chi 2$ = 16.533, p<0.001) but not towards the non-dominant hemibody (Wald $\chi 2$ = 6.87, $p > 0.05$).

The pelvis amplitude displacement was significantly reduced in only the pelvic support conditions, PS and HPS, during anterior (Wald $\chi 2$ = 12.63, $p < 0.01$) and posterior perturbations (Wald $\chi 2$ = 46.62, $p < 0.001$), Fig. 2.4. When perturbations were towards the dominant hemibody (Wald $\chi 2$ = $p < 0.001$), ML pelvis amplitude decreased in PS and HPS, Fig. 2.5, and towards the

non-dominant hemibody (Wald $\chi 2$ = 16.53, $p < 0.001$). The AP trunk amplitude displacement significantly decreased in the pelvic support conditions, PS and HPS, during anterior (Wald $\chi 2$ = 30.27, $p < 0.001$), and posterior perturbations (Wald $\chi 2$ = 14.08, $p < 0.005$). The ML trunk amplitude displacement significantly decreased in the PS condition, Fig. 2.5, during perturbations towards the dominant hemibody (Wald $\chi 2$ = 17.82, $p < 0.001$), and towards non-dominant hemibody (Wald $\chi 2$ = 16.32, $p < 0.001$).

2.4.2 Postural Control Mechanisms: Surface EMGs

The sEMG data of dominant postural muscles, trunk and lower extremities, show that participants executed specific-direction muscle responses during perturbations: anterior (ES: Wald $\chi 2$ = 19.39, p <0.001; LG: Wald $\chi 2$ = 34.93, p <0.001, RF: Wald $\chi 2$ = 14.29, p <0.005, TA: Wald $\chi 2$ = 10.28, p <0.05) and posterior (TA: Wald $\chi 2$ = 29.63, p <0.001, RF: Wald $\chi 2$ = 18.03, p <0.001). When RobUST delivered anterior perturbations, Fig. 2.6, participants showed significantly greater iEMG of ES muscles in NS (Mean = 2.04 ± 0.84) than in HPS (Mean = 0.15 ± 0.17, p = 0.047), HS (Mean =-0.05 ± 0.14, p = 0.014). Participants also showed greater iEMG of ES muscles in PS(Mean =0.94 ± 0.35) than in HS (p = 0.001) and than in HPS (p = 0.001).

Similarly, the iEMG activity of LG was higher in NS (Mean = 6.29 ± 1.72) than in HS (Mean = 1.76 ± 1.04, p <0.001), PS (Mean = 3.1 ± 1.58, p <0.001) or HPS (Mean = 0.41 ± 0.28, p = 0.001).

During posterior perturbations, the activation of TA had a significant role for participants to recover postural stability. Compared to NS (Mean = 19.5 ± 4.47), the TA activity was significantly reduced when participants received PS (Mean = 9.2 ± 2.03, p <0.005) and HPS (Mean = 0.91 ± 0.67, p <0.001). The use of HS did not significantly reduce the muscle activity of TA compared to NS (Mean = 6.42 ± 4.4, p = 0.121).

The EMG analysis of arm muscles showed high level of variability and did not reveal statistical differences among conditions in perturbation or recovery periods.

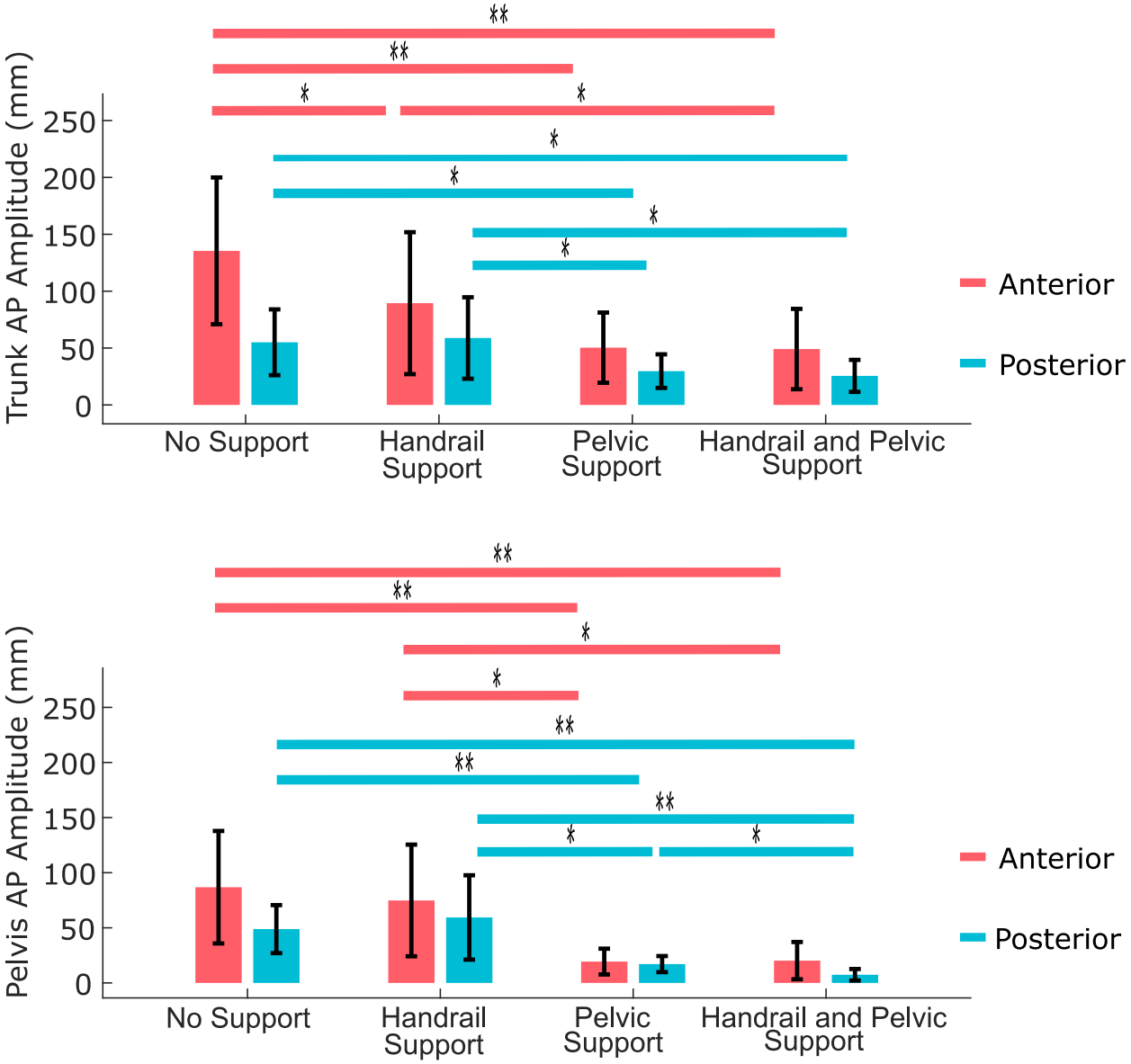

Figure 2.4: Group averages of trunk and pelvis amplitude during anterior-posterior perturbations across the experimental conditions. PS and HPS provided the most decrease in amplitude. $*p < 0.05, **p < 0.005$

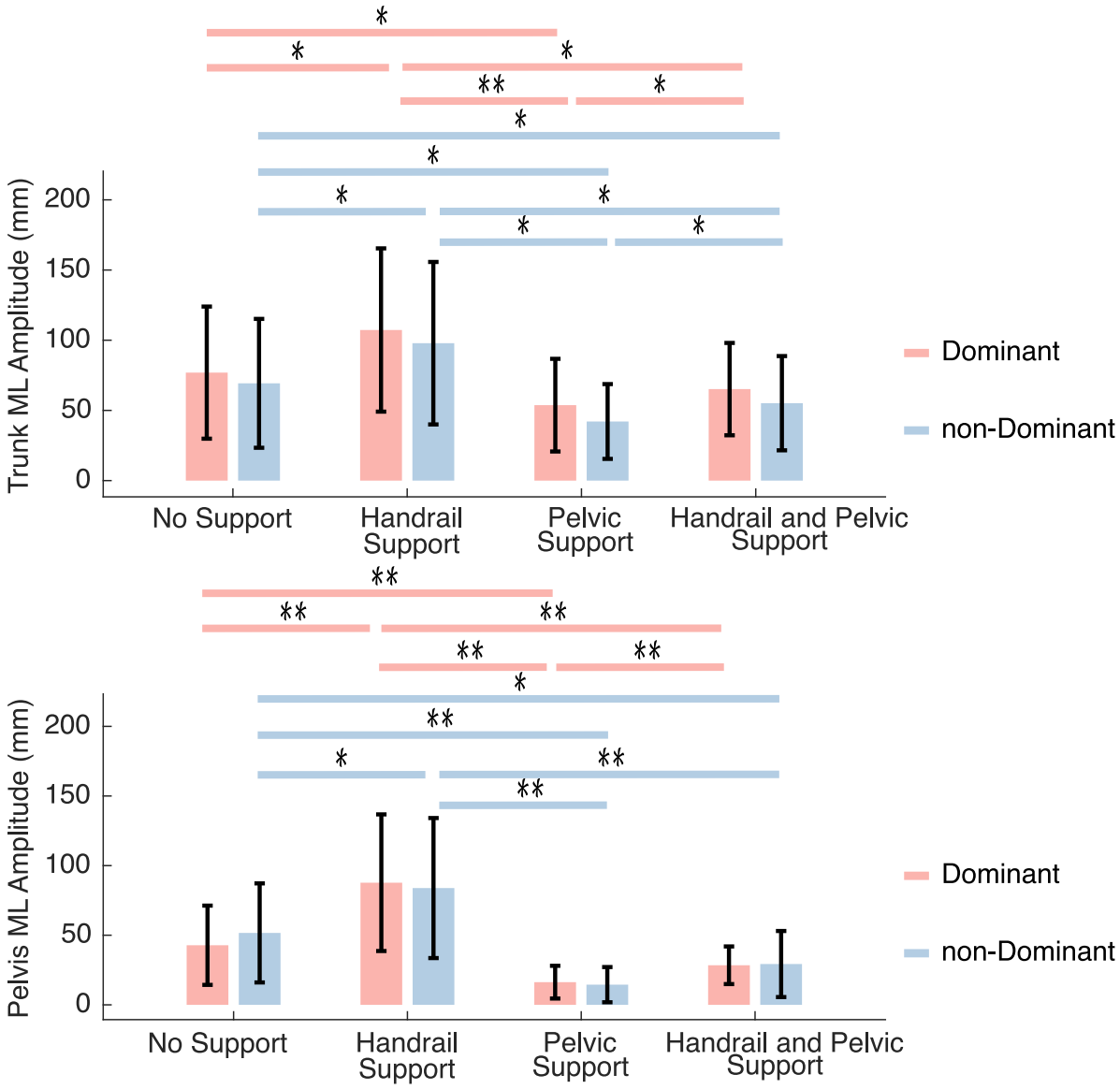

Figure 2.5: Group averages of trunk and pelvis amplitude during medio-lateral perturbations across the experimental conditions. PS provided the most decrease in amplitude. HS significantly increased ML amplitude. $*p < 0.05, **p < 0.005$

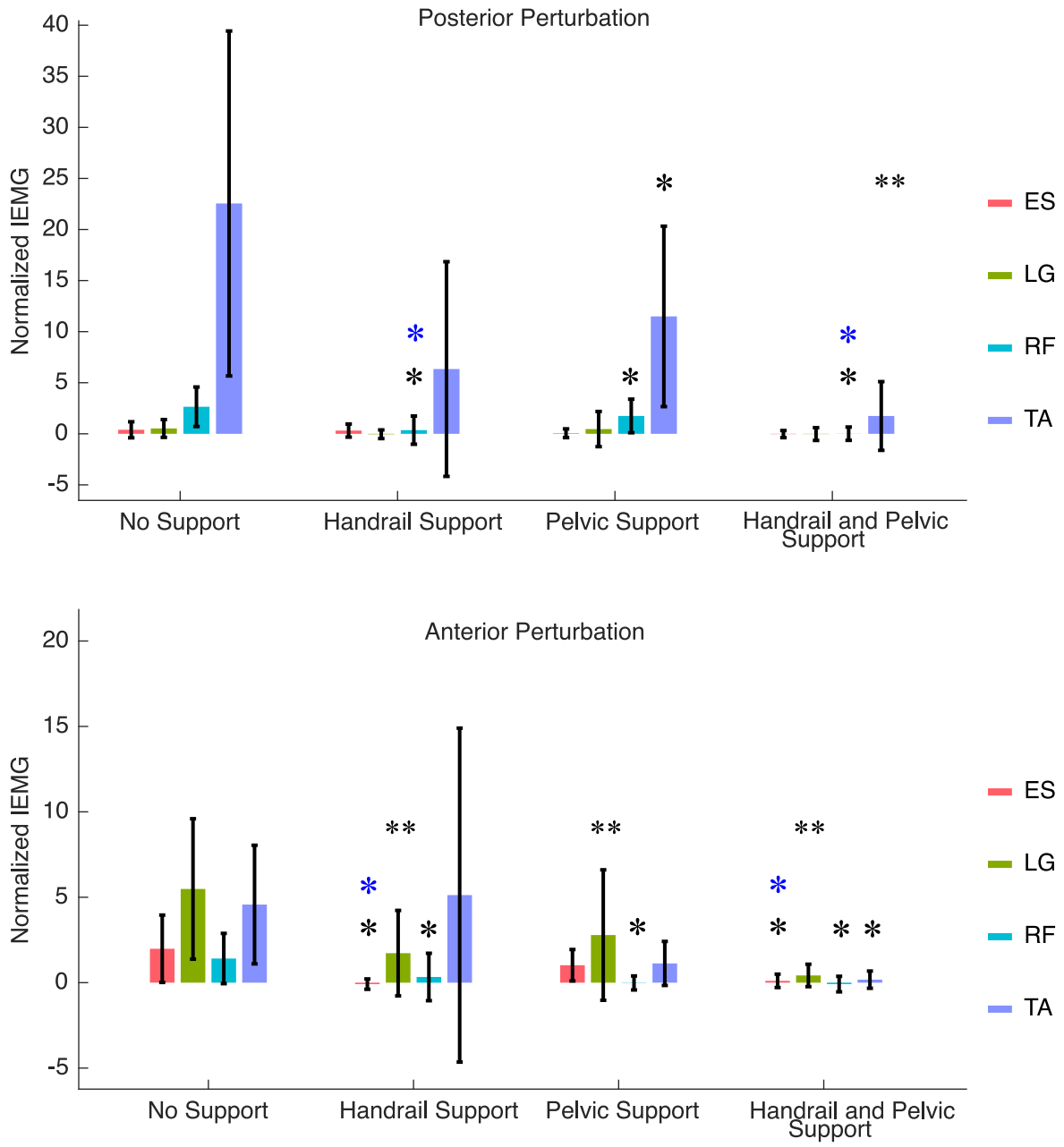

Figure 2.6: The normalized iEMG averages across experimental conditions. ($*p < 0.05$, $** = p$ <0.001, in Exp. Condition Compared to NS, and $*p < 0.05$ in Exp. Condition Compared to PS). During posterior perturbations, the HS and HSP conditions significantly reduced RF compared to NS and PS. During anterior perturbations the HS and HPS significantly reduced ES compared to NS and PS. In PS the ES and TA were not significantly altered during the anterior perturbation.

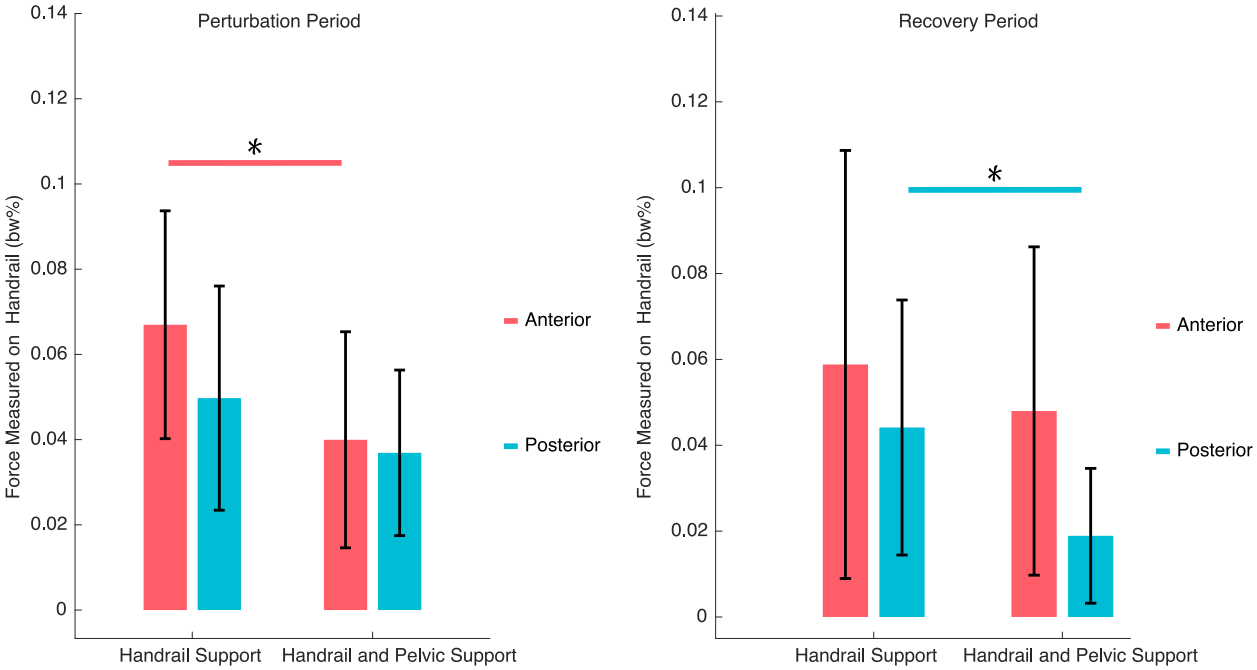

Figure 2.7: Group averages of handrail force magnitude across perturbation and recovery period for anterior-posterior perturbations are shown. $*p$ <0.05.

2.4.3 Force Output Responses

Mean ground reaction forces (GRF) were dependent on perturbation direction: anterior (Wald $\chi 2 = 95.84$, p <0.001), posterior (TA: Wald $\chi 2 = 7.64$, p >0.05), non-dominant (Wald $\chi 2 = 33.83$, p <0.001) and dominant (Wald $\chi 2 = 56.17$, p <0.001). Both handrail conditions, HS and HPS, significantly reduced the GRF in all directions except posterior perturbation, Table 2.1.

Mean handrail force magnitude was also dependent on perturbation direction, only during an anterior perturbation significance was found (Wald $\chi 2 = 42.57$, p <0.001). The force magnitude in HPS was significantly less than HS Fig. 2.7. An interesting effect was identified in the recovery period from a posterior perturbation, the force magnitude in HPS was significantly less than HS, Fig. 2.7.

2.5 Discussion

In this study, we tested the dual action of RobUST to generate postural imbalance, via controlled perturbative forces on the trunk and stabilizing postural strategies through assistive forces on the pelvis. Then, we investigated how postural recovery with RobUST differed from standing with handrail support, which is a common postural paradigm and first step in rehab settings. Futhermore, we examined the potential combinatory effect of pelvic assistance from RobUST and handrail support to improve upright postural balance.

The data analysis revealed that 1) the use of pelvic assistive force field via RobUST substantially improved postural stability in standing during trunk perturbations, mainly in the AP direction and towards the dominant hemibody; 2) RobUST provided similar level of COP postural stabilization as when participants supported their posture with the handrail; but interestingly, participants experienced less body displacements with pelvic assistive force support compared to postural support offered by a handrail 3) with pelvic support from RobUST, EMG activity of postural muscles resembled the muscles active during standing with no support 4) the combination of assistive force field and handrail support resulted in the greatest level of postural stability at the expense of substantial decrease in weight bearing forces between the feet and the ground.

2.5.1 The Stability Effects of Pelvic Support from RobUST

During postural imbalance, participants improved their stability in standing position while receiving assistive forces with RobUST compared to standing with no support. They experienced less degree of postural variability and decreased postural excursions with the assistive pelvic forces. Interestingly, participants showed similar COP stability outcomes while receiving pelvic support from RobUST as compared to when participants used a handrail for support. The use of the handrail decreased participant's natural weight bearing load, (i.e., ground reaction forces); whereas this effect was not observed with pelvic support mediated by RobUST. In standing, ground reaction forces have a relevant effect on postural control strategies. For instance, in slow low-amplitude

horizontal ground displacements, healthy adults exert torques against the floor at the level of the ankles (i.e., ankle strategies) to recover sway [35]. From a rehabilitation standpoint, Olivetti et al. [36] has shown that weight bearing forces increase hip extensor strength in older people. Ground reaction forces also play an important role in some ankle orthotics to enhance lower limb alignment in the crouch position that children with cerbral palsy manifest [37]. Therefore, in future interventions, the pelvic assistive forces from RobUST would be beneficial in encouraging a natural ground reaction force profile for training standing postural control strategies in those with neuromotor disorders.

The postural muscles active with assistive forces at the pelvis were similar to the EMG of muscles active during standing without any support during anterior perturbations. However, this finding was not present for the other two handrail conditions, HS and HPS. The use of the handrail demanded other postural control adjustments that differed from *in-place* postural control strategies at the level of the ankle, knee, hip or a combination of these [38]. Hall et al. [39] showed the flexibility of the postural control system able bodied individuals have to adjust to different external rigid supports and body configurations. We observed direction specific postural adjustments, TA and RF in posterior perturbations, and a combination of LG, ES and TA in anterior perturbations. During pelvic support from RobUST these muscles were still active, but with reduced EMG activity. This data may justify the potential applicability of RobUST to train postural balance via systematic perturbations in individuals with standing control impairments without the need of adopting a *change-in-support* postural strategy. RobUST may be used in future training paradigms to encourage *in-place* postural strategies while performing reaching or hand-arm related tasks. While stepping or reaching for support are essential to maintain balance and prevent falls, the postural strategy and neuromuscular demands to recover balance are different from those required for *in-place* postural strategies, which are highly impaired in individuals with neuromotor disorders [25].

Researchers have previously shown in individuals, with and without nervous system lesions, direction-specific postural adjustments during reactive postural control in standing via moving plat-

forms [35, 40, 41]. In our study, the perturbative forces acting on the torso were associated with direction-specific muscle activity of trunk and lower limb muscles so that participants could be displaying a combination of hip and ankle muscle strategies [42]. This reactive postural muscle strategy is different from studies using surface perturbations. A study [43], demonstrated the presence of complex postural responses that combined muscle responses from the typical ankle strategy (disto-proximal recruitment of distal leg muscles) and hip strategy (proximo-distal recruitment of trunk and thigh muscles). Therefore, the origin of the perturbation, how the perturbation is delivered and the perturbative force profile, has an impact on the type of postural control responses. Although different perturbations can induce different muscle control responses, they could have similar secondary outcomes. Mansfield et al. [26], describe there is some postural transfer effect in platform perturbation training to cable perturbations about the center of mass, this effect was a decrease in handrail contact time. Further research is needed to determine other outcomes that can be transferred from body based perturbations to ground based perturbation training.

When pelvic support from RobUST was provided, body translations were reduced in the ML directions. Meanwhile, COP stability outcomes were dependent on the perturbation direction, and only significantly reduced when directed towards the dominant hemibody direction. A possible explanation may be the greater mediolateral BOS and that individuals have a higher force threshold to lateral perturbations than to anterior-posterior [44]. In our study, the force magnitude was set to 20%BW of the participant in each of the four directions. This force intensity may have not been strong enough to induce a significant level of instability in the ML directions. This interpretation is also supported by our EMG results. Dominant or non-dominant ES were not significantly reduced or augmented with the use of force field or handrail during lateral perturbations. This may also be partly explained because hip abductors, i.e. gluteus medius, are the primary muscles to control body COM within the frontal plane and EMG of such muscles were not registered in our study [45].

The effects in the different stability supports, between pelvic and handrail, are depicted by the responses in body translations as well. Assistive forces at the pelvis significantly reduced

participant's trunk and pelvic displacements during the perturbations in all directions. However, in the handrail support, trunk and pelvis did not show a decrease in body translations in the ML perturbation directions. These results may indicate that trunk perturbation forces were high enough to displace the pelvic and trunk segments but low to cause destabilizing effect associated with a significant modulation of sEMG responses.

2.5.2 The Additive Support Effect of HPS

The application of a handrail and pelvic support reduced postural instability, i.e., COP and pelvic and trunk excursions. It also reduced the level of postural muscle activity required to control balance during anterior-posterior perturbations. Compared to standing without support, participants substantially reduced postural excursions and demonstrated a highly stable postural stance during perturbations.

Our data showed that handrail conditions, with or without the pelvic assistive support, were accompanied by a decrease in muscle activity and ground reaction forces. In other words, the excess of external fixed support can improve postural sway in standing at the expense of suppressing the active role of the neuromuscular system and weight bearing force distribution to control posture. While this strategy may not be the most efficient therapeutic strategy to retrain postural control in individuals with mild-to-moderate balance control disorders; the additional use of an external handrail in RobUST sheds light on its potential use to promote postural standing in individuals with severe loss of neuromotor postural control, such as in spinal cord injuries (SCI). However, as we observed in our analysis, the application of assistive pelvic support from RobUST may help modulate the amount of force exerted by the hands in postural training with external handrail assistance. We found that the combination of hand and pelvic support via RobUST significantly reduced the handrail force magnitude exerted by participants during anterior perturbations and during the recovery stage from posterior perturbations, Fig. 2.7. Patients with ambulatory SCI may acquire standing, however, they suffer from static and dynamic postural deficits that increase their risk to fall or transition from sitting to standing [46]. Hence, they would need to overcom-

pensate with their arms and hands because of the severe lack of postural loss. The combination of the two support systems can alleviate the hand and weight bearing force distributions required to obtain stability to trunk perturbations. This provides a method to structure a postural rehabilitation paradigm based on the individual's assistance needs.

2.5.3 Study Limitations

A methodological limitation was the inability to register EMG activity of abdominal muscles due to the location of the belts and cables around the area. The data from these muscles could have expanded our understanding of trunk control during posterior perturbations. We must also acknowledge the possibility that RobUST in transparent mode may have provided a certain level of postural stability in stance to the able bodied participants. This effect would come from the minimum tensions required to prevent the cables from slacking. Similar to how light touch improves balance [47], the presence of the low tensioned cables may be enough to provide some stability.

Another study limitation was the application of 20%BW across all participants in the AP and ML directions. Other researchers like Komisar et al. [48] determine an individual's perturbation threshold per direction by delivering forces until the individual steps or falls. Performing the study at the threshold magnitude could have provided more insight into participant's reaction to trunk perturbation, especially in the ML directions.

2.6 Conclusion

Pelvic assistive forces from RobUST allowed participants to have similar postural COP outcomes as holding a handrail, but without inhibiting as significantly the EMG activity of the postural muscles nor decreasing the ground reaction force distribution. The pelvic support via RobUST also decreased postural excursions for all perturbation directions. Additionally, the combination of the handrail and pelvic support provided the most postural stability and reduced the force magnitude exerted by the hands during anterior and posterior perturbations. RobUST could be systematically used in the training of individuals with neuromotor disorders to progressively build complex

automatic postural reactions [49] in upright standing.

The findings of the present study show the promise of RobUST for future training paradigms that target specific muscle strategies for *in-place* and *change-in-support* postural strategies. RobUST may provide a new evaluation and training paradigm for postural balance training of neurologically impaired individuals who require external assistance and aids during postural stance.

Chapter 3

Feasibility and Tolerance of a Robotic Postural Training in a Person with Ambulatory Spinal Cord Injury

3.1 Introduction

Spinal Cord Injury (SCI) is a multi-systemic condition accompanied by muscle tone dysregulation and paralysis that secondarily limits mobility, self-care, and participation. SCI frequently results from a trauma and is an unexpected life-changing event that requires costly, complex, and long-term rehabilitation procedures.

One ambulatory elder with SCI participated in six training sessions that tested the feasibility of an activity based postural training with the cable driven Robotic Upright Stand Trainer, RobUST. The training targeted reactive perturbation balance responses. The cable driven robot delivered trunk perturbations and pelvic assistive forces. Based off the American Spinal Injury (ASI) Association functional impairment scale, the individual had an SCI AIS grade C.

We hypothesized that RobUST-intervention could improve steady-state, proactive-active, and reactive postural control. Also, a substantial increase or severe fluctuations in heartrate (HR) or blood pressure (BP) were interpreted as inability to tolerate RobuST-Intervention.

3.2 Experimental Setup and Procedure

3.2.1 Study Design

Approval for this study was obtained by the IRB for Human Research at Columbia University (Protocol AAAR6780). The participant was informed about the study requirements and then con-

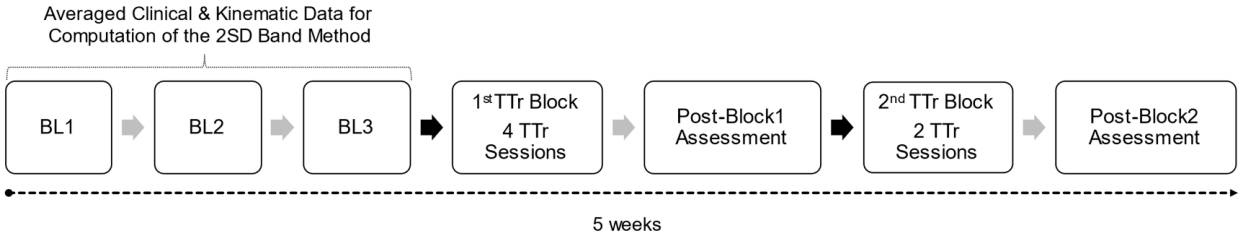

Figure 3.1: The training schedule followed was steady-state/proactive-active and then reactive. BL1,2, or 3 = Baseline 1, 2, or 3. 1stTTr Block = 1stTraining Block. TTr = Training. Post-Block1 Assessment = 1week after 1sttraining block. 2ndTTr Block = 2nd training block. Post-Block2 Assessment = 1 week after 2ndtraining block. 2SD = 2 Standard Deviations.

sented. Figure 3.1 outlines the multiphase single-subject-research-design study. The study had a total of 11 sessions and was completed in 5 weeks. In the first week, three baseline assessments were collected, scheduled one day apart. A 2SD bandwidth method was used to interpret postural outcomes as substantial improvements, detriments, or unchanged with respect to baseline. The participant only underwent RobUST-intervention during the study to avoid potential interferences from other therapies.

3.2.2 RobUST Setup and Training

The pelvic force assistance was modified in this study to accommodate for customizable boundaries and for the SCI participant's balance progression. In this feasibility study, the boundary was determined by a standing star test, where the participant moved their trunk and pelvis as far as possible without taking a step in eight directions. The maximum area of excursion, their range of motion, was used as the pelvic force field boundary. This test was repeated before and after each training session. During the activity based training, the pelvic boundary used was the result from the pre-training star test. Meanwhile, the training also consisted of perturbations to the trunk in eight directions. The SCI participant would perform reaching tasks while receiving randomized trunk perturbations and pelvic assistive forces when outside their pelvic range of motion. The objective was to train reactive responses to unexpected disturbed forces and only provided

pelvic assistive forces when the SCI participant was beyond their stability limits. The pelvic forces provided minimal tension when inside the boundary, Fig. 3.2.

The participant practiced i) pointing tasks with buzzers, ii) reaching for balls of different sizes and small checkers, iii) bimanual catching and throwing, iv) boxing, and v) tablet games that involved pointing and attention-to-task such as crosswords, puzzles or hangman. In each one of the six 90 min-training sessions, a 10-15min break was included. RobuST (Fig. 3.2) provides real-time visual feedback on the participant's trunk and pelvic position relative to the stability boundaries so that the clinician can objectively target postural strategies within and beyond stability limits. The training follows the same star-shaped scheme applied in the postural-star standing test. Within each proactive-active and reactive postural activity, a total of 20-30 repetitions X direction, within and beyond postural stability limits (40-60 trials), were performed in the first two sessions. However, in the remaining sessions, we increased the training intensity—longer time and greater number of repetitions—in the more-impaired directions: right-anterior, right, and right-posterior.

3.3 Data Analysis

MATLAB (R2017b, Mathworks, 2017) was used offline to filter and process data. Kinematics (100Hz) were smoothed with a zero time-lag 4th order Butterworth filter at 4Hz-cutoff. Rotations were computed as inter-segmental angles, following the right-hand convention and Euler sequence X-Y'-Z": sagittal, frontal, and transverse planes, respectively.

Force plate data (1000Hz) was used to compute the root-mean-square of the magnitude of COP position data (RMS-COP) during the 4SBT to measure variability of steady-state balance control. We averaged the margin of stability (MoS), as measured by Sivakumaran et al., to interpret balance control—i.e., control of the center of the pelvis (position and velocity) based on its distance relative to the BOS boundaries [50]. The woskspace area (cm2) was estimated with the in-built MATLAB function boundary(x,y, 0.05) based on maximal trunk excursion during the postural star-standing test. The RMS of the sum of angles across planes of motion of the ankles was computed to measure active range of motion (ROM). EMG (1000Hz) signals were band-pass filtered (60-500

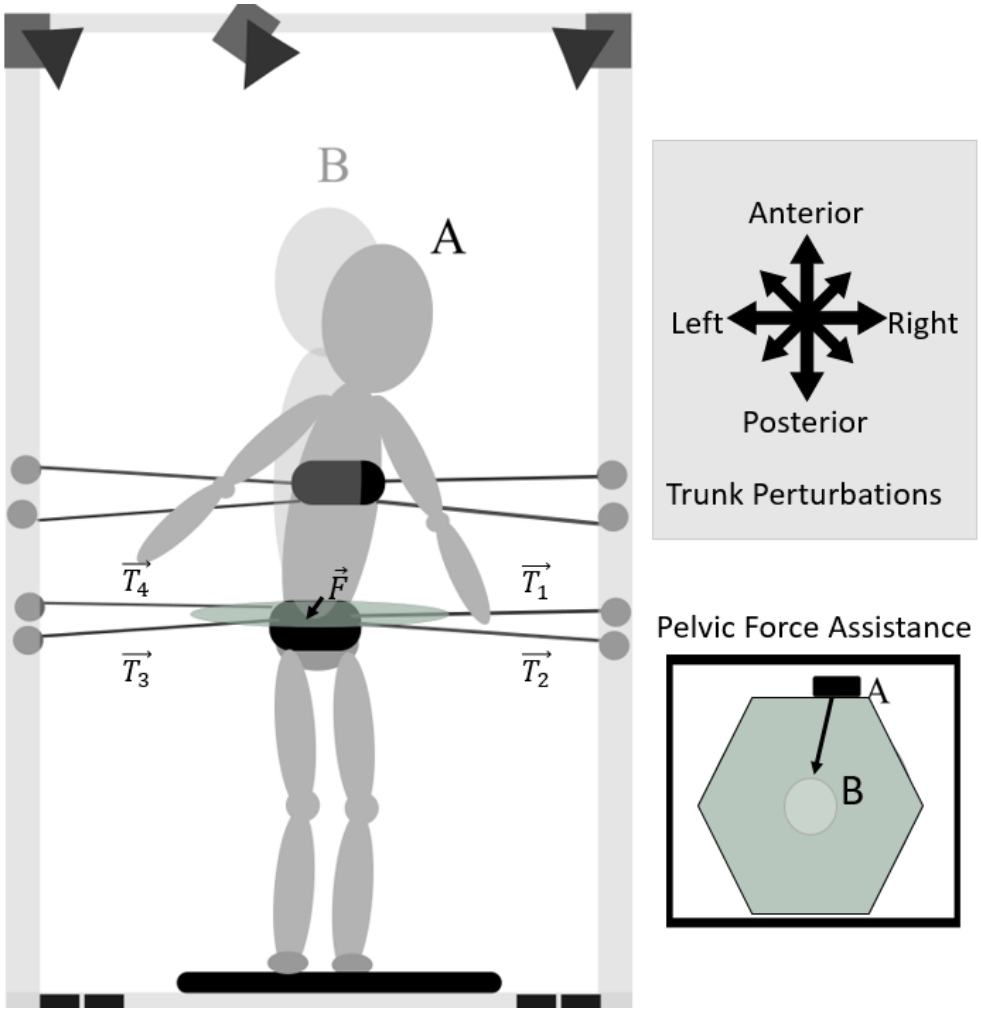

Figure 3.2: A participant inside the RobUST system with labeled parts of the device. The trunk and pelvis cables are attached to the respective belts on the user. During training, the SCI participant received trunk perturbations and assist-as-needed force field at the pelvis. The force field boundary was set to the irregular force field or set to the individual's base of support boundary.

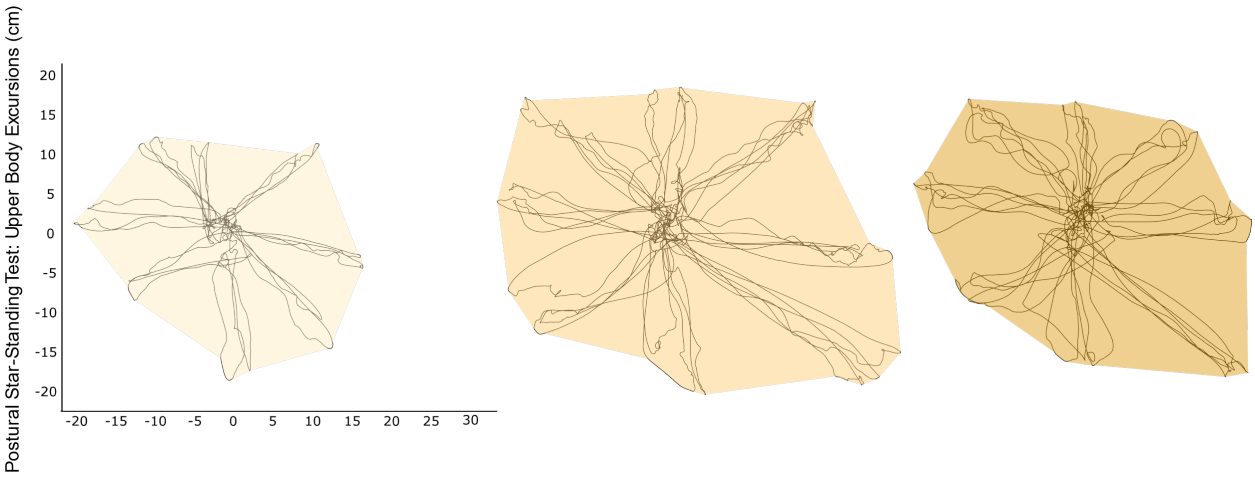

Figure 3.3: Shows postural star-standing test outcomes. The participant increased the workspace area and performed greater larger upper body excursions 1week after the 1st and 2nd training blocks with respect to baseline. However, these improvements did not meet the 2SD bandwidth criterion. BL = baseline. PT1 = 1week after the 1st training block. PT2 = 1week after the 2nd training block. cm = centimeters.

Hz), rectified, low-pass filtered at 100Hz, and normalized to the EMG baseline activity obtained when the participant received direction-specific perturbations. The integrated EMG (iEMG) data was calculated and normalized by the integrated EMG activity obtained while the participant stood still without postural disturbance (baseline EMG) [33].

3.4 Results

The participant expanded his workspace area and increased the length of upper body excursions during the postural star-standing test. Nonetheless, these improvements did not meet the 2SD bandwidth criteria (Fig. 3.3).

The participant tolerated higher levels of force intensity after RobUST-intervention during posterior, anterior and rightward perturbations (Fig. 3.4).

EMG responses were highly variable across study sessions. We could not establish measurement stability during baseline assessments and we did not find substantial changes after each training block. However, we observed a consistent increase in right gluteus medius activity (iEMG) during perturbative forces towards the more-impaired lower extremity (i.e., right side) (Fig. 3.5).

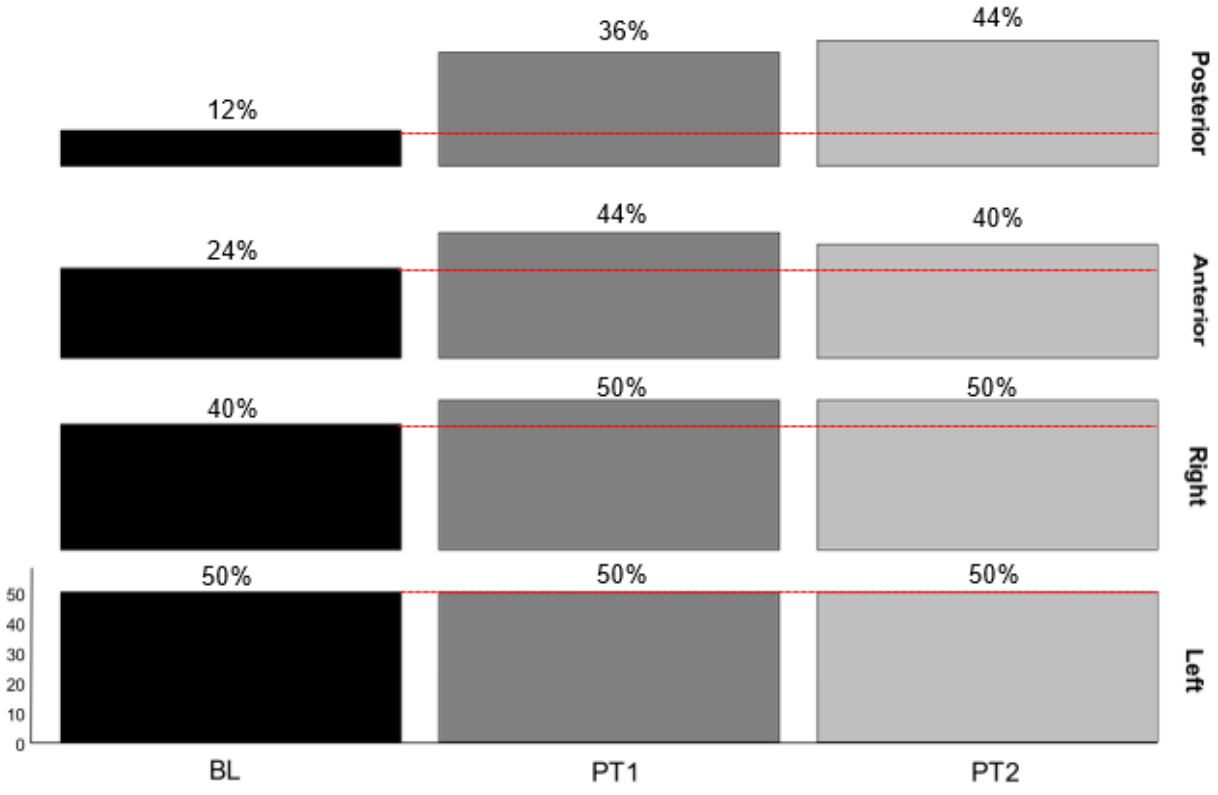

Figure 3.4: Outcomes of the direction-specific perturbations delivered by RobUST to examine reactive postural control. The subject was able to react against a higher reactive force intensity at the trunk after RobUST-intervention. However, this was not the case during leftwards perturbations since the participant achieved maximum intensity (50% of body weight) at baseline. BL = baseline. PT1 = 1week after 1sttraining block. PT2 = 1week after 2ndtraining block.

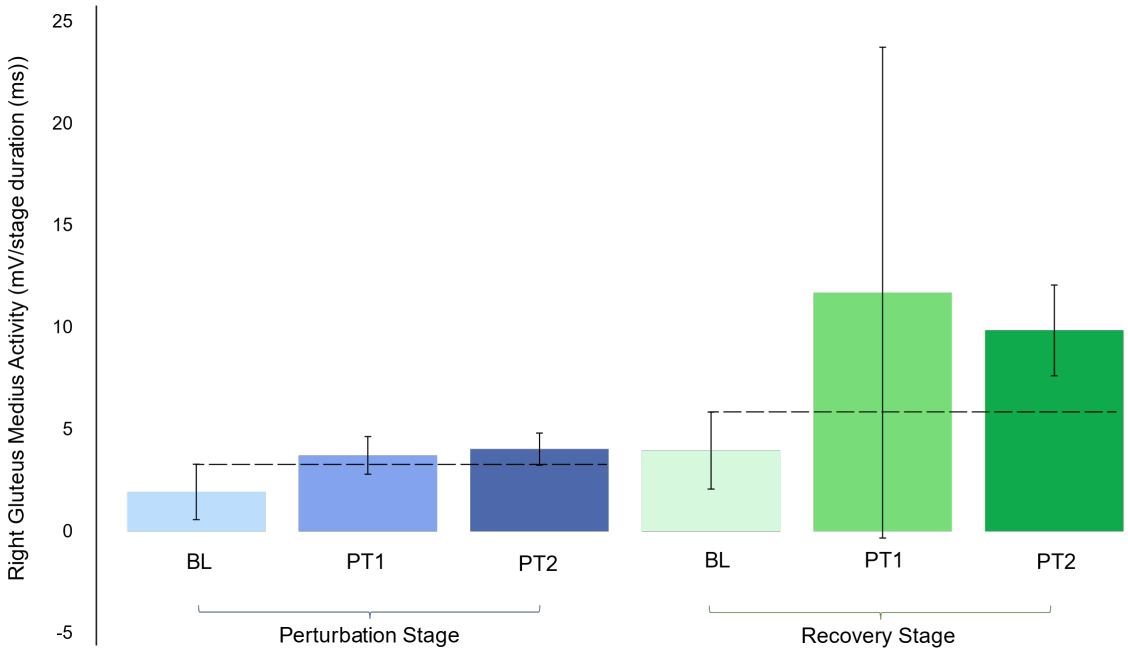

Figure 3.5: Outcomes of the iEMG of gluteus medius activity during the reactive postural control exam. A substantial increase in muscle activity was found during both the perturbation (650ms) and recovery (1500ms) events. mV = millivolts. BL = baseline. PT1 = 1week after 1sttraining block. PT2 = 1week after 2ndtraining block.

3.5 Discussion

This single-subject-research study shows preliminary efficacy of RobUST-intervention to train steady-state, proactive-active, and reactive postural standing control. The participant completed all the scheduled sessions, did not fall or report muscular or articular pain, and showed cardiovascular tolerance to RobUST-intervention.

Similarly, our pilot data shows that an activity-based postural training with RobUST technology is highly effective to train postural standing in ambulatory people with SCI. The participant of our study was a safe community-dwelling ambulator since his BBS score at baseline (55/56) was superior to the average 47.9 found in ambulatory people with SCI and AIS D [51]. Still, he improved his dynamic balance to pick up objects from the floor after RobUST-intervention.

Furthermore, the participant improved reactive postural control mechanisms by increasing activity of right gluteus medius; which was impaired in our clinical case—neurological level of

injury: L3—together with the muscles of the anterior, posterior, and lateral compartments of the leg. Gluteus medius is an important pelvic stabilizer, and during postural imbalance in the frontal plane, it had a critical contribution in accepting body weight support on the most-impaired right leg (perturbation stage) and restoring postural balance (recovery stage) during upright stance. These improved in-place postural control strategies are clinically relevant, because people with SCI often compensate with their arms to control the body during ADLs in standing [52]. In this line, we have also shown in healthy participants that "assist-as-needed" pelvic force fields improve postural sway during postural perturbations in unsupported standing at a similar level than holding a handlebar for body support [53].

3.6 Conclusion

Overall, our findings emphasize the therapeutic value of the dual application of trunk and pelvic force fields to train posture in people with SCI. However, a large sample size is necessary to generalize these outcomes to the ambulatory SCI population. Also, the inclusion of participants with severe balance deficits could address the full therapeutic potential of RobUST-intervention.

Chapter 4

Redistributing Ground Reaction Forces During Squatting

4.1 Introduction

Squatting requires movement coordination of the lower extremity and pelvic muscles to stabilize the spine, torso, and pelvis [54, 55]. Hence, considering the postural, biomechanical, and functional features of squatting, this movement sequence has fitness and rehabilitation value in increasing muscle strength [56, 57].

In rehabilitation, squatting is often prescribed for strengthening the lower body. In physical therapy, squat exercises are usually performed with additional resistance to the motion by applying external weight to the body. Song et al. [58] showed how a posterior load at the knee improved muscle strength and balance. Kaya et al. [59] showed that weight-bearing exercises targeting quadriceps significantly improved clinical outcomes in patients with knee dysfunction, e.g., patellofemoral pain syndrome. Pollock et al. [60] performed a review on how exercises aimed to improve sit-to-stand motion led to an improvement in symmetric weight-bearing among stroke survivors. Symmetrical weight bearing is preferred given that stroke-fallers had higher weight asymmetries than stroke non-fallers [12].

Able bodied adults maintain a relatively symmetric weight distribution on their feet while performing a squat [61]. Meanwhile, populations with lower extremity impairments, like adults after anterior cruciate ligament reconstruction (ACLr), unload their affected limb [62]. However, Chan et al. have shown that individuals with (ACLr) are capable of symmetric loading while squatting once instructed or with visual feedback [63]. Another approach to augment weight-bearing

symmetry is to apply a physical feedback, such as a force, as shown in robotic gait studies [64, 65]. To the best of our knowledge, none of the available squat assisting devices have been designed or utilized to redistribute users' body weight among the legs without restricting natural motion. Therefore, our goal is to analyze how a pelvic lateral force facilitates an asymmetric weight-bearing distribution in healthy adults.

Several exoskeletons have been developed to assist in squatting through body weight (BW) suspension or assisting joint actuation at the hip, knees, or ankles [66, 67, 68, 69]. Jeong et al. designed the Angel-suit, which has motors to actuate the hip and knee joints and provide assistance to the wearer based on their center of pressure [70]. Meanwhile, Jeon et al. utilized a squat assistance robot that can provide weight support to the user during the squat sequence [55]. However, a common issue with exoskeletons and robots like these is the added mass to the user and constrained movement during the task. The exoskeleton may alter the user's squat performance, as seen in studies by Jeong et al. [70] and Yu et al. [71]. Therefore, it is also essential to evaluate whether or not the robotic device augments the user's squat motion before applying a force on the participants. Motivated by this need, we evaluate our robotic device to ensure it does not hinder an individual's movement during the squat cycle.

4.1.1 Research Aims

Our Robotic Upright Stand Trainer, RobUST, is a cable-driven system capable of applying forces on the trunk and pelvis of the user while standing. RobUST has been used to characterize postural balance and improve stability in individuals when reacting to force perturbations [2, 53]. In this study, we adapt RobUST to apply forces on the human pelvis during squat movements with the goals to 1) evaluate the effect that cables attached to the pelvis have on participants' squat performances while RobUST is in transparent mode, and 2) characterize ground reaction forces during squatting by applying a lateral pelvic force to the participants. These results will provide an insight into how to achieve body-weight distribution within the feet without restricting natural range of movement during squatting.

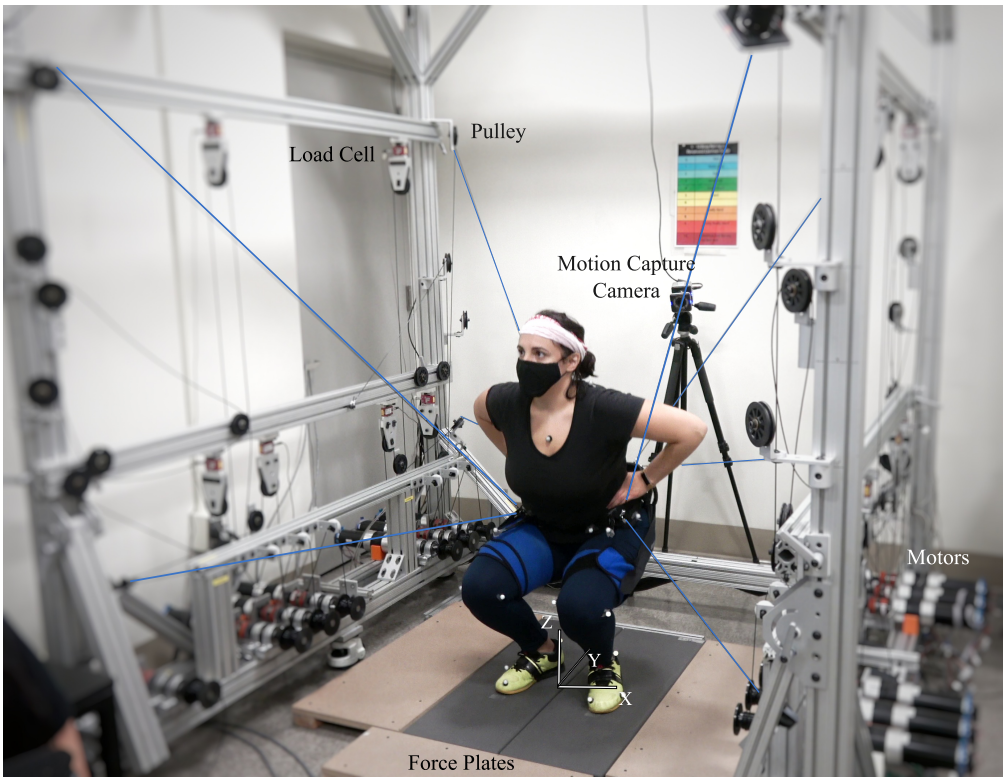

Figure 4.1: A participant inside RobUST performing a squat. Cables, highlighted in blue, are routed to the pelvis, four from above and four from below. Twenty-two markers are used to track and compute body kinematics. Force plates are used to measure ground reaction forces.

4.2 System Description

RobUST applies forces on the pelvis using a custom designed belt (Misty Mountain Threadworks, North Carolina) worn by the participant. To apply three-dimensional forces on the pelvis during a squat movement, eight cables were used, Fig. 4.1. Each cable is actuated by a motor (Maxon Motor, Switerzland) while connected to the pelvic belt. The cables are routed from cable spools attached at each motor to load cell tension sensors (LSB302 Futek, California). Each cable is then passed through a pulley and routed to the pelvic belt. Nine motion capture cameras (Vicon Vero 2.2, Denver) are mounted on the RobUST's 80/20 aluminum frame (80/20 Inc., Indiana) and one vicon camera is mounted on a tripod. The motion capture system is used to track the location of the belt and the body segments in real-time. To measure ground reaction forces, the participant stands on two force plates, one under each foot (Bertec Force Plate V1, Ohio).

4.3 Experiment Design

4.3.1 Study Design

Seven healthy participants (4F/3M) completed the experiment. All participants were right hand and right leg dominant: average weight 75.1±9kg, average height 170±13cm, average age 27.9±3yrs. The experiment consisted of three different squat conditions. In the first baseline, participants squatted without RobUST (No Cables). In the second baseline test, participants squatted with RobUST in transparent zero force mode (Cables). During the third condition (Lateral F), participants were asked to squat while receiving a lateral (5%BW) force on the pelvis towards their non-dominant side, their left side. The load was applied throughout the entire squat cycle. A 5%BW was chosen to reduce risk of injury. The average force vector output by RobUST for the seven participants during their eight squat cycles is shown in Fig. 4.2.

To reduce joint-related shear and prevent injury, participants were advised to squat in a slow and controlled manner, as recommended [56]. King et al. determined that 5-9 squats were sufficient to measure reliable coordination variability [72]. Therefore, for each condition, participants were asked to squat 8 times, with a 3s pause in between squats. Participants were given a 5min break and sat between the three conditions. Each participant chose a preferred foot placement while squatting which was marked with tape to ensure that placement remained the same across conditions.

4.3.2 Data Acquisition

All data were processed offline using MATLAB (Mathworks Inc.). Force plate data were recorded at 1000Hz and processed using a 4th order low-pass filter with a 6Hz cut off frequency. Tension sensor data were recorded at 200Hz. Kinematic data were recorded at 100Hz with Vicon cameras. Body markers were placed on each participant, five on the upper trunk (cervical region c7, one at each shoulder, mid back and upper chest), four around the pelvic belt, two at the hips (right and left side), two at each knee (lateral and medial part of the knee), one at the ankle near the lateral malleoulus, and three markers per foot (great toe, outer foot metatarsal, and heel), Fig. 4.3.

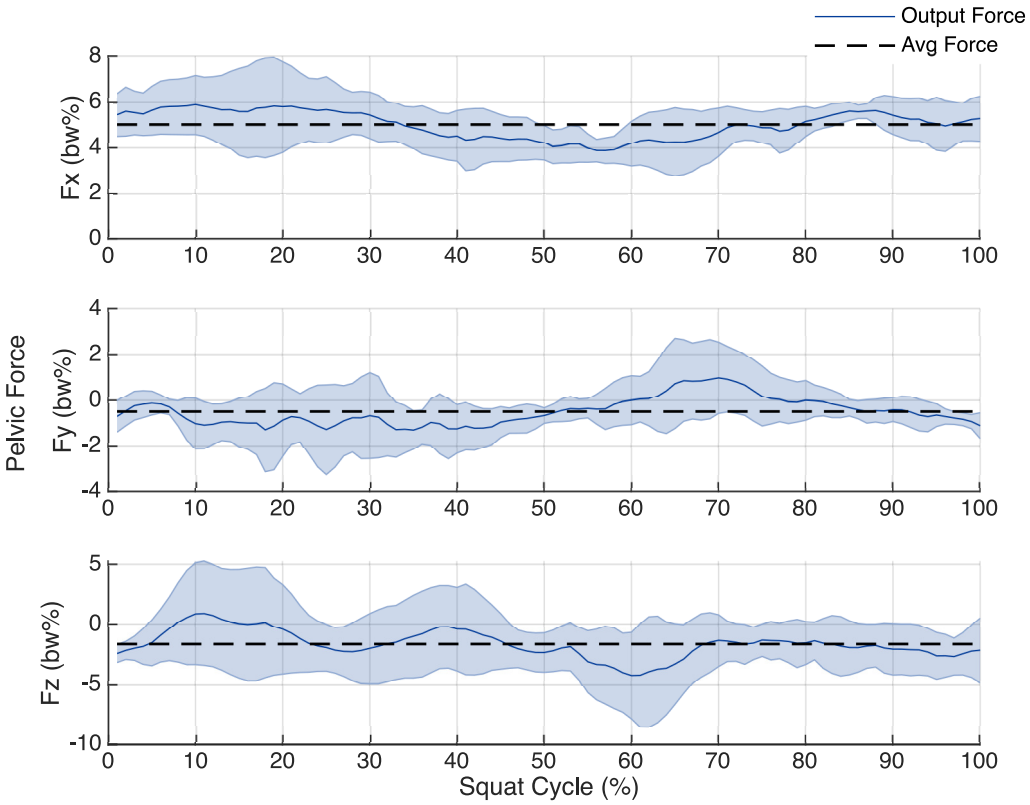

Figure 4.2: During the lateral force condition, the RobUST output force for the seven participants, across squat cycles, was averaged and is labeled Output Force. The overall force magnitude was 5.3%BW, with an intended cycle average (Avg Force) of 5%BW along the lateral left x direction, -0.5%BW in the anterior y direction, and -1.6%BW in the downward vertical z direction.

4.3.3 Data Analysis

Marker data were passed through a 4th order low-pass filter with a 6Hz cut off frequency. The global frame was centered at the participant's base of support (BOS), Fig. 4.1. Data were segmented to squat cycles using the vertical center of pelvis position and velocity in the global z direction. A squat cycle is defined so that the beginning of the squat cycle occurs when the participant is standing upright. The participant then squats to the minimum pelvic vertical height, which corresponds to 50 percent of the squat cycle. The participant then returns back to the upright standing position, i.e. 100 percent of the squat cycle. When the participant is in an upright neutral stance, the pelvis is at a maximum vertical height. This position was found using the Matlab function findpeaks (Matlab 2019). When the pelvis velocity in the vertical direction is greater than 20mm/frame, the beginning of each squat is initiated. To identify the end of a squat cycle, the pelvis velocity had to slow down to 20mm/frame. Each squat cycle was visually inspected to ensure correct segmentation.

After squat cycles were segmented, the marker and force plate data were resampled from 1 (onset of squat) to 50 (minimum vertical height of the center of pelvis). The participant then returned from this minimum position to the neutral upright position, interpolated as 50 to 100 percent of the squat cycle.

Joint angles were calculated according to the International Society for Biomechanics (ISB) guidelines [28]. Local coordinate frames were created for each foot, shanks, thighs, pelvis and torso, Fig. 4.3. The joint angles between the segments were calculated using a zyx decomposition of the rotation matrix. Pelvis position data were normalized during the cycle by dividing the current pelvic height by the height at the beginning of that cycles' pelvic position. Time variables were calculated for the total squat duration, for the time to descend to minimum position, and for the time to ascend from minimum position to standing. Vertical ground reaction forces were normalized using participants' weights. Center of pressure (COP) values were normalized based on the BOS, lateral COP by the width of the BOS, and anterior-posterior COP by the length of BOS [73].

The ranges were calculated for pelvis position and joint angles to characterize any differences in range of motion between squat conditions. The average symmetry index (SI) [74] was calculated using the left (Fz_l) and right (Fz_r) vertical ground reaction forces:

$$SI = \frac{|Fz_l - Fz_r|}{0.5 * (Fz_l + Fz_r)} * 100\% \tag{4.1}$$

The SI characterizes how participants distributed their weight among their two legs while squatting. A SI value close to zero indicates symmetric weight-bearing distribution. SI peaks and SI averages were calculated.

The average coefficient of variation (CV) [75] was calculated for the pelvic center in the three directions: lateral, anterior-posterior, and vertical directions, i.e. x, y, z, respectively. For each test condition, the participant's pelvic center position during a squat was averaged for the eight repetitions. The CV was calculated for the entire squat cycle:

$$CV = \frac{1}{n} \sum_{i=1}^{n=100} \frac{\sigma_i}{\mu_i} \tag{4.2}$$

where σ_i is the standard deviation of the pelvic center at i% of the squat cycle, and μ_i is the average position of the pelvic center at i%of the squat cycle. CV was used to characterize pelvic variability in the eight squats performed.

4.3.4 Statistical Analysis

Statistical analysis was performed using a statistical software (SPSS, version 28, IBM, 2021). For normally distributed data (n=7), as determined by the Shapiro-Wilk Test and visual Q-Q, a one-way repeated measurements ANOVA was performed. If the model was significant, a Bonferroni post-hoc test was applied. For significant models, the means of the measures are reported in the results as (M=mean ±std).

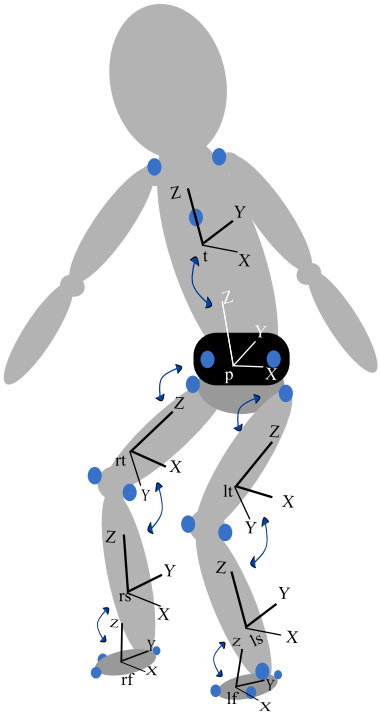

Figure 4.3: The blue circular dots represent where markers were placed on participants. The markers were used to create local coordinate frames: right foot-rf, right shank-rs, right thigh-rt, pelvis-p, trunk-t, left foot-lf, left shank-ls, and left thigh-lt. Joint angles were calculated based on the rotation between adjacent local frames.

4.4 Results

4.4.1 Baseline Squat Results

The addition of the cables did not cause significant difference in average and peak SI values between the No Cables and Cables condition, ($p > 0.05$). The average and peak SI values are reported in Table 4.1. The normalized ground reaction forces for the entire squat cycle are shown in Fig. 4.4. The average lateral COP (COPx) range and anterior-posterior COP (COPy) are reported in Table 4.1. The COPx was not significant between No Cables and Cables. However, there was a significant difference in the COPy between No Cables and Cables ($p = .046$).

The flexion range of motion of trunk and lower extremity joints are reported in Table 4.1 for each condition. The left knee flexion range was the only joint that showed a significant difference. The left knee range was significantly less in the Cables condition compared to the No Cables condition ($p = .048$). This cable effect was not observed in the right knee, participants did not have significant decrease in the right knee range of motion. A lack of power due to the small sample size could be the reason. Therefore, a GPower analysis (3.1.9.7, Franz Faul) was performed on the right knee range of motion with the actual effect size of η_p^2=0.35 and with an estimated power of 85%. The analysis revealed that an estimated sample of 17 subjects could lead to statistical significance. All other joint angle rotations displayed lower effect sizes, η_p^2, and were not significantly different between conditions, Table 4.1.

The added cables did not significantly effect participants' pelvic variability CV in the lateral CVx, (F(2,12)=1.3, $p > .05$), anterior-posterior CVy, (F(2, 12)=1.8, $p > .05$), nor vertical CVz direction (F(2,12)=0.23, $p > .05$). Group averages are graphed in Fig. 4.5.

4.4.2 Lateral Force Results

The LateralF condition caused participants to have an asymmetric ground reaction response, the average and peak SI values were significant compared to the No Cables ($p = .013$) and Cables ($p = .027$) conditions. The normalized ground reaction forces for each test condition are shown

Table 4.1: Variable Means, (SD) and Statistical Results for SI, COP and Joint Angle Flexion (°) (*Indicates Exp. Condition compared to No Cables had p<.05, * Indicates Exp. Condition compared to Cables had p<.05, * Indicates Exp. Condition compared to LateralF had p<.05)

Variables	**No Cables**	**Cables**	**Lateral F**	**Test Result**	p	η_p^2
SI Mean	11.2* (8)	11.5* (8)	35.7** (11)	$F(2,12)=13.3$	<.001	0.69
SI Peak	9.9* (7)	12.6* (8)	42.7** (12)	$F(2,12)=22.2$	<.001	0.79
COPx Range	0.071* (.023)	0.096* (.023)	0.18** (.048)	$F(2,12)=37.5$	<.001	0.86
COPy Range	0.22* (.054)	0.33* (.057)	0.28 (.059)	$F(2,12)=9.0$	.004	0.6
R Ank Range	29.18 (5.1)	29.55 (6.2)	28.63 (7.3)	$F(2,12)=0.13$	.88	0.021
L Ank Range	25.9 (11.8)	29.9 (7.7)	30.5 (9.8)	$F(2,12)=1.1$	.37	0.18
R Knee Range	85.4 (17.4)	79.2 (16.8)	80.0 (18.1)	$F(2,12)=3.17$	.08	0.35
L Knee Range	87.8* (18.4)	78.1* (17.2)	81.2 (21.8)	$F(2,12)=4.37$	.038	0.42
R Hip Range	67.5 (11.8)	64.6 (11.7)	68.2 (13.5)	$F(2,12)=1.45$	.27	0.2
L Hip Range	70.4 (11.2)	64.5 (10.9)	67.7 (16.2)	$F(2,12)=2.09$	.17	0.26
Trunk Range	24.4 (12.9)	16 (3.9)	21.6 (9.2)	$F(2,12)=2.31$	.14	0.28

in Fig. 4.4. There was a significant increase in the LateralF COPx range compared to No Cables (p = .001) and Cables (p = .003). There was no significant difference in the LateralF COPy range compared to No Cables and Cables, (p > .05). The average and peak SI values, and COP ranges are reported in Table 4.1.

All joint angles range of motions were not significantly affected by the LateralF conditions. Group means and SD for joint angles are reported in Table 4.1.

The LateralF condition did not significantly effect participants' pelvic variability CV in the lateral CVx F(2,12)=1.3, (p > .05), anterior-posterior CVy F(2, 12)=1.8, (p > .05), nor vertical CVz direction F(2,12)=0.23, (p > .05). Group averages for each condition are graphed in Fig. 4.5.

4.4.3 Timed Results

Participants did not display a significant difference in the time they descended from standing to their minimum squat depth. However, there was a significant difference in the ascent time from minimum depth to standing, F(2,12)=11.8, p=.001. The average time participants took to ascend with No Cables (M = 1.6±0.7s) was significantly less than with Cables (M = 2.0±0.7s, p = .025) and with LateralF (M = 2.1 ± 0.7s, p = .027).

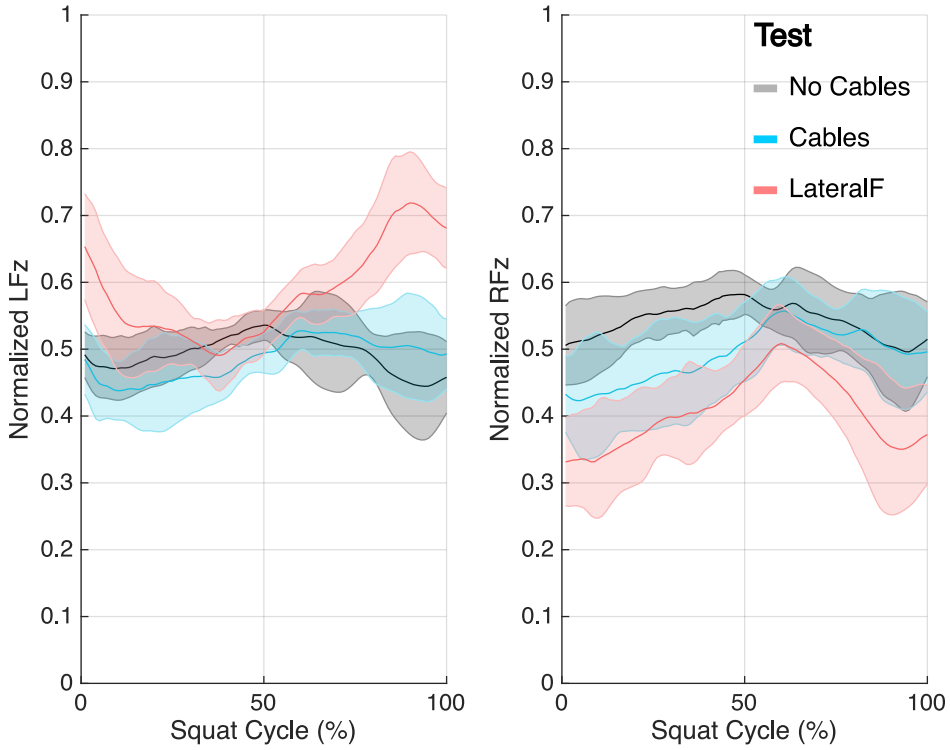

Figure 4.4: These are the group average and standard deviation of the left and right normalized ground reaction forces for the participants' squat cycles in the No Cables, Cables and the applied left Lateral Force condition. The ground reaction distributions are similar between the no cables and cables condition. For the left Lateral Force condition, participants displayed a greater ground reaction on the left foot, (left graph), and a decrease in the right foot ground reaction (right graph).

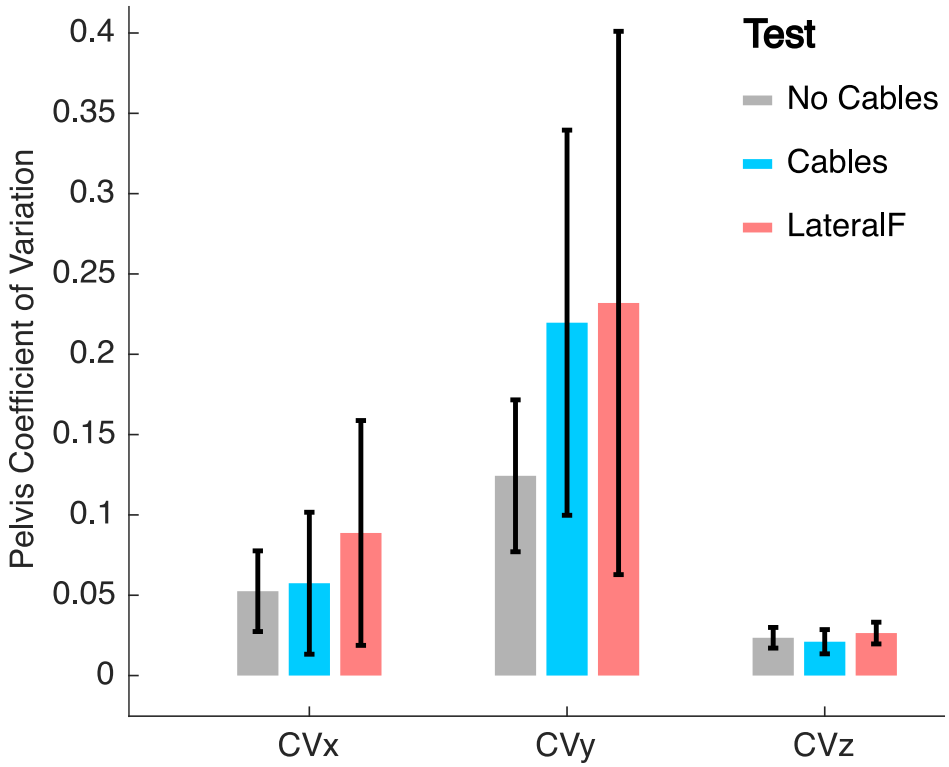

Figure 4.5: Group averages and standard deviations of the CV in the the lateral x, anterior-posterior y, vertical z directions for the pelvis during the squat cycles in No Cables, Cables and LateralF are shown. No significant differences were observed between test conditions.

4.5 Discussion

In this study, we investigated the applicability of RobUST to induce specific weight distribution during squatting in young adults with intact musculoskeletal and neurological systems. We experimentally verified that a lateral force of five percent BW on the pelvic segment is sufficient to create an asymmetric weight-bearing distribution throughout participants' squatting trajectories by increasing their left ground reaction forces and decreasing their right ground reaction forces. Consequent to the direction of the external force imposed on the body, the lateral force increased the lateral center of pressure amplitude range, as expected. Interestingly, the left lateral force did not increase pelvic variability between squat repetitions. Furthermore, our two baseline tests show that the added cables to the pelvis in RobUST transparent mode did not add pelvic variability to participants' movements during squatting. Therefore, we can conclude that the RobUST system does not add undesirable trajectories or movement errors inherent in squatting. These results are essential before implementing training programs with RobUST for people with neuromotor conditions, in which their movements may be highly variable.

4.5.1 Baseline Squat Comparisons

Participants performed eight free squats with no cables followed by eight squats in RobUST while connected with cables in transparent mode. In comparing the two baseline tests, we measured the potential interference the cable configuration and motor inertia might have on participants' squat movement. A minimum tension of 18N per cable applied throughout participants' squat motions did not significantly alter their pelvic trajectories, nor did it add any variability to their squat cycles, as indicated by the pelvic CV, Fig.4.5. However, the addition of cables to the pelvis increased participants' ascent time. Future studies utilizing surface electromyography could help us clarify whether a significant increase in muscle effort is associated with this increased ascent time.

The addition of the cables also affected the anterior-posterior COP range. The increase in range

indicates participants were brought further to their anterior-posterior BOS boundaries. Although the cables are low in inertia, the tension distribution applied to the cables may have caused the increase in range. One can lower the minimum tension but at a risk of the cables becoming slack, which would cause the system to be uncontrollable as the end-effector is outside of the feasible Wrench-Closure Workspace [76]. Since the squat motion is a cyclic movement, one can improve the transparency by tracking and predicting the motion to create a feed-forward signal that adjusts the tension distribution accordingly, as authors van Dijk et al. describe [77]. Nevertheless, RobUST can track the location of the pelvis throughout the squat cycles without losing tension or altering the natural cyclical pelvic motion of the participants as measured by the CV. This is a promising result for future applicability of RobUST in movements that involve the three planes of motion such as the one investigated in this study.

However, we found that the cables decreased participants' knee flexion-extension amplitude range of motion, i.e., participants did not squat to the same depth. Researchers showed that participants increased knee and hip range of motion when squatting while fatigued [78]. Therefore, the decrease in left knee range of motion may be due to a physical constraint from RobUST. The locations of the bottom four pulleys may not have been low enough for some participants' full depth squat. This can be easily overcome by moving the bottom pulleys further down in future experiments as the RobUST system is easily reconfigurable. Overall, the added cables to participants' pelvis in RobUST did not add variability to participants' pelvic squat motion. This finding is important because it allows one to isolate the force and trajectory control effects in future applications of RobUST.

4.5.2 Lateral Force Squat Condition

A lateral pelvic force is capable of redistributing a participant's weight through the lower extremities during the squat motion. The high SI values (Table 4.1) in the lateral force condition show participants had asymmetric vertical ground reaction loading between the left and right legs. These results can be utilized for motor practice and have potential to improve weight distribution among

the legs and feet. In other words, pelvic forces can be configured, via direction and force intensity, to augment lower limb loading responses and subsequently increase direction-specific ground reaction forces. This outcome may be of particular interest in the field of neuro-rehabilitation to train sit-to-stand functions via modified cyclical squatting with RobUST. Our results showed that RobUST can increase the peak ground reaction SI force in able bodied participants, Table 4.1. A Cochrane review on interventions to improve sit-to-stand found a lack of interventions to improve peak ground reaction forces and functional ability in the most severely impacted participants post stroke [60]. Therefore, the results obtained from able bodied participants are promising for future implementation on populations with asymmetrical weight-bearing, such as stroke survivors, to encourage loading on their affected leg.

A lateral force to the pelvis can augment participant's load distribution by applying as little as 5%BW force. This feature would allow clinicians to start at minimal augmented body weight forces and progressively increase as the participant improves across training sessions. An advantage of only applying a force at the pelvis is that it provides participants the freedom to adapt their kinematic response; their motion is not confined at the level of the joints. This can explain why participants' joints range of motion was not significantly affected, Table 4.1. In other robotic studies that have focused on squats [68, 70], the user is assisted at the hip and knee joint levels. The controllers of these robotic systems may be adaptable to provide a lateral load, but users may be constrained at the joints by the physical structure and motors or inertia of the mechanisms. Therefore, we recommend applying a lateral force on the pelvis because a lateral force on the pelvis is capable of directing the load and changing participants' lower extremity weight distribution without adding variability to the participants' natural squat motion.

4.5.3 Study Limitations

This study shows promising results in augmenting participant's weight distribution throughout their squats, as indicated by the increase in average SI values and mediolateral COP ranges, Table 4.1. The SI and COP values had high effect sizes, η_p^2, values above 0.6. The effect size is a

quantitative measure to evaluate the strength of the statistical value. A larger effect size provides higher confidence in the statistical claim. However, kinematic results, like the joint angle ranges, showed low effect sizes, η_p^2, values below 0.4. A study with a greater number of participants could increase the effect size and therefore generalize our kinematic results better.

Another limitation in this study, was not registering muscle activity of the lower extremity muscles. Muscle data could have provided information if participants were fatigued. In future studies, randomizing the order of the conditions could also minimize the outcome effects of fatigue. In addition, the muscle activity data could have expanded our understanding on how participants reacted to the additional load toward their non-dominant hemibody. The additional loading may promote muscle strength on their affected side, as researchers have shown resistance training intervention promoted muscular strengthening, [79]. Future studies should be performed to analyze the muscle responses.

4.6 Conclusion

In this squat study with healthy young adults, we first examined the impact of RobUST's transparent mode on undesirable movement effects. Investigating these interferences is essential for robotic rehabilitation systems in isolating the main effects before implementing a force training paradigm in the future. We found that the cable configuration and belt did not increase participants' pelvic motion variability, CV. Additionally, we characterize how the ground reaction force distribution was altered with a pelvic lateral force. Participants significantly increased their vertical ground reaction SI mean from 11.2% to 35.7% and SI peak from 9.9% to 42.7%. These results are encouraging for future studies that aim at redistributing participants' weight-bearing. Especially for populations with asymmetrical loading like stroke survivors or adults with ACLr. As a future extension, we recommend pelvic forces to induce symmetric loading, thus promoting greater stability and less risk of falls. In addition, the squat exercise can improve strength and balance in populations with weakened leg extremities.

Chapter 5

Characterizing Reactive Control in Sit-to-Stand

5.1 Introduction

Sit-to-stand is a fundamental everyday task that requires balance, and lower limb strength [80]. In people with sensorimotor impairments, rising from a chair can be difficult and has been reported as a frequent activity that leads to falls [81]. The task itself is destabilizing as it requires one to move from a greater base of support (BoS), on the feet and buttocks, to a narrower one, on the feet alone [82]. The risk of falls increases with age, but there are inadequate interventions to prevent falls and rehabilitation post-fall [83].

Exposing individuals to physical perturbations, i.e., perturbative forces that destabilize them, can improve balance control. These perturbations can be delivered by moving the BOS or applying external forces on specific body segments. Repeated exposures to perturbations have shown the benefit of improving balance and reducing the risk of falls in standing and gait studies [84, 85, 86].

Several lower limb robotics assist sit-to-stand movement by actuating the knees, hips, or ankles [87]. These systems reduce the effort of the user's load when transitioning from sitting to standing. However, sit-to-stand also requires participants to maneuver with stable coordination, an important rehabilitation factor often overlooked in these robotic assistive devices. To promote rehabilitation in sit-to-stand, robotic systems have the potential to improve the function, and there is a further need to investigate and assist in participants' reactive and active stability during the motion.

To the best of our knowledge, only Pavol et al. [88, 89] have studied reactive postural reactions while the participants transitioned from sit-to-stand. They showed that participants adapted and

recovered balance when exposed to slip perturbations from a platform.

In standing perturbation studies, it is well documented how individuals use different postural strategies to remain upright. One often invokes an in-place postural response without changing foot configuration to stay balanced. In platform standing studies, individuals flex the ankle to small perturbations, and as the perturbation increases, individuals may rely on the hips to regain balance [90]. Sometimes, one requires a change-in-support response by taking a step or reaching for support to regain stability [4, 24].

Identifying common control strategies used in maintaining balance may help better understand how the sensorimotor system performs a task [91]. Characterizing these strategies may also improve the evaluation to reduce the risk of falls. Motivated by this need and the lack of research on sit-to-stand perturbation responses, we aim to characterize how healthy individuals respond to different perturbations and intensities during the sit-to-stand motion.

5.1.1 Research Aims

We perform this study by modifying the Tethered Pelvic Assist device (TPAD), a cable-driven system that uses eight cables to apply a desired force on the user's pelvis [15]. The TPAD has been used in gait studies to show how pelvic forces can assist and augment individuals' motion [10, 92]. For this study, we use TPAD to apply pelvic forces during sit-to-stand motion.

Ten healthy participants underwent randomized perturbations delivered halfway during the sit-to-stand transition. Perturbations were produced either by moving the treadmill's belt or by applying a force using TPAD's cables. The intensity of the perturbations increased during the experiment until the individual failed to stay balanced, hence requiring a change-in-support reaction. We aim to characterize the postural responses and identify any strategies participants ultilized to recover from the perturbations. We measured muscle activity, via surface electromyography, kinematic joint movements, and ground reaction forces to evaluate participants' postural reactions. Studies on reactive balance control have shown that postural strategies vary depending on the context, motor task constraints, and type of perturbations [93]. Therefore, because of the perturbation location,

we expect that pelvic and treadmill perturbations will cause different postural responses. In addition, previous research has shown that participants have reduced stability to greater perturbation intensities [11], thus, we hypothesize that the higher the perturbation intensity, the greater the kinematic joint amplitudes and muscle activity will be required to regain balance. In the sit-to-stand transition, participants are moving anteriorly and vertically [94]. Therefore, due to the direction of the movement, we also expect that the anterior perturbation direction will cause different postural responses than posterior perturbations.

5.2 System Description

TPAD actuates eight cables attached around a pelvic belt. Four of the cables are routed up from the pelvic belt and four are routed down from the pelvic belt. All cables are routed to load cells (mlp200, Transducer Techniques, California), then passed to AC motors with gearboxes (Kollmorgen, Pennsylvania). The motors are all mounted on an aluminum frame (80/20 Inc., Indiana). The TPAD system has an instrumented force plate treadmill (Bertec, Ohio), two handrails along the sides, and a visual dome, Fig.5.1. For this study, a bar was secured across the center of the treadmill and mounted on the aluminum frame. A rowing seat cushion (Kohree Rowing Seat, Amazon Store) was attached to the bar. The height of the top of the bar from the treadmill was set to 46.5cm, and the height of the seat cushion was 7cm. The visual dome displayed the interior of a train, developed in Unity 3D[95]. Ten motion capture cameras detected markers placed around the pelvic belt and on the participant's joints to get real-time position data (Bonita-10 series from Vicon, Colorado).

5.3 Experiment Design

5.3.1 Study Design

The study consisted of a baseline condition and sets of perturbations. The baseline was performed with TPAD in transparent mode, with minimal tension of 15N per cable applied to the

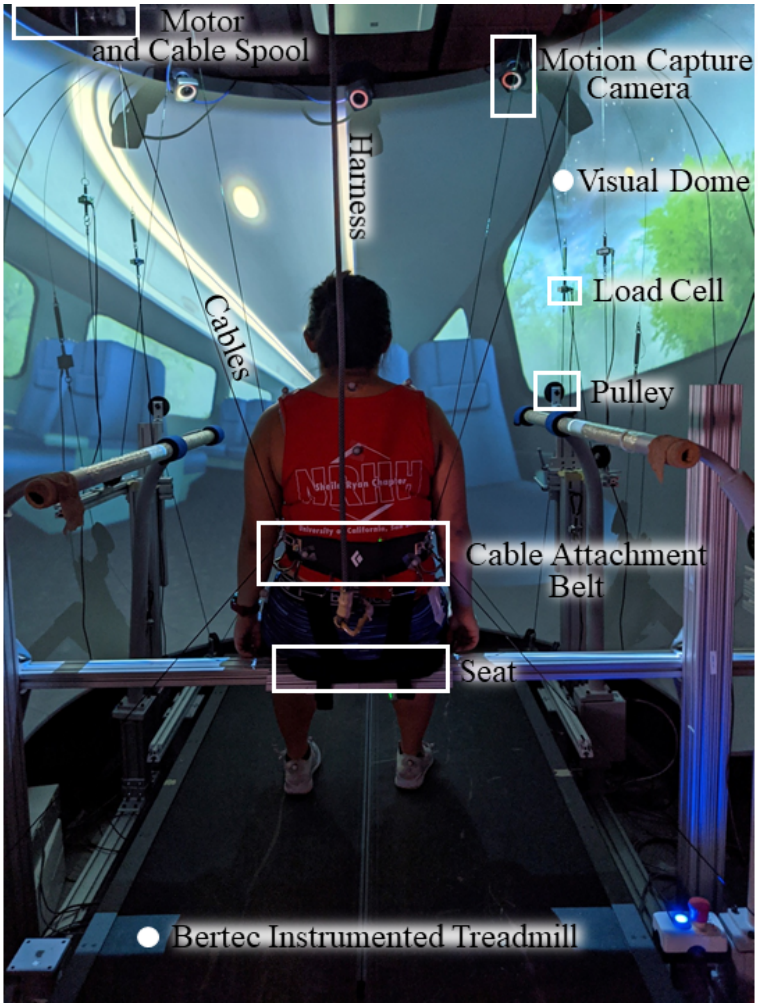

Figure 5.1: A seated participant within the TPAD system. The participant's feet are on the instrumented treadmill. A pelvic cable attachment belt has a harness and has 8 cables attached, routed through pulleys to load cell sensors. The cable is then routed to a cable spool on a rotating motor shaft. Motion capture cameras surround the TPAD system to track in real-time the position of the belt and body markers. A visual of the interior of a train compartment is shown to the user when conducting the experiment.

pelvic belt. Participants were instructed to rise from the TPAD seat at a self-selected pace, remain standing for about 1-2s, and then return back to the seated position. The sit-to-stand transition was performed five times, similar to the five repetition sit-to-stand test, which is a clinical assessment done to evaluate functional impairment [96]. After the baseline test, participants were given a break of approximate 3 minutes.

Perturbations were randomized in terms of the type (treadmill or pelvic) and direction (anterior or posterior). Perturbations were given near the middle of the participant's sit-to-stand transition, about 50% of the cycle, where 0% is seated, and 100% is standing upright. Perturbations lasted 0.5s, with 0.15s of perturbation rise time, 0.2s of constant perturbation intensity, and 0.15s of fall time.

In the first set of perturbations (First), participants received a peak of 5% body weight (BW) force on the pelvis and a peak acceleration of $0.4 m/s^2$. Afterward, the peak intensities and peak accelerations would increase by 5%BW and $0.2 m/s^2$, respectively. The force and acceleration profiles would continue to increment until the participant failed to maintain stability. Once the participant took a step or reached for a handrail, this was labeled as a failed attempt (Fail) because the individual failed to remain in an *in-place* postural strategy and required a *change-in-support* strategy. The Fail perturbation intensity was the maximum perturbation intensity for that direction and type, the intensity would no longer increase for that perturbation direction and type. The previous level of intensity was labeled as the participant's threshold level (Threshold), which is the maximum they could withstand using an *in-place* strategy.

The perturbation test was continued until the participant failed, i.e. required a change-in-support, in each type of perturbation and direction. For safety purposes, the maximum pelvic force TPAD would deliver was 50%BW, and the maximum acceleration the treadmill would go was $2.2 m/s^2$. The session ended if a participant reached the maximum force or acceleration peaks. A visual description of the perturbation tests are shown in Fig. 5.2. Participants were also instructed to rise from the TPAD seat at their own controlled pace and keep their arms at their sides unless they needed to stabilize with a handrail. A represented response to each perturbation delivered is

shown in Fig. 5.3.

5.3.2 Data Acquisition

Kinematic data were recorded at 200Hz with Vicon cameras and filtered through a low-pass filter of 4th order and 10Hz cut-off frequency. Twenty-three markers were placed around the body to calculate offline the joint angles: five were used on the upper trunk (one at each shoulder, mid-back, upper chest, and cervical region C7), four around the pelvis, two at the hips (right and left lateral sides), two at each knee (inner and outer part of the knee), one at each ankle, and three at each foot (toe, outer foot, and heel). A visual of the marker locations is shown in Fig. 5.2.

Force plate ground reaction data were collected at 1000Hz and passed through a 4th order low-pass filter with 10Hz cut-off frequency [97].

Muscle activity was measured using surface electromyography (EMG) with Delsys (Delsys Trigno Avanti Sensor, Massachusetts). Data were detrended then filtered using a 4th order band-pass filter with 20 to 500 Hz. Data were rectified and low-passed with a 4th order filter at 3Hz cut-off to obtain the linear envelope [98]. In healthy participants, researchers have shown no significant difference in muscle activity during sit-to-stand between dominant and non-dominant legs [99]. Therefore, muscle EMG data were obtained from the participant's self reported dominant side: rectus abdominis (RA), lower back erector spinae (ES), bicep femoris (BF), rectus femoris (RF), medial gastrocnemius (MG), and tibialis anterior (TA).

5.3.3 Data Analysis

All data were processed offline using Python. Data were segmented first by sit-to-stand cycle. The vertical component of the pelvis center position was used to determine if the individual was seated or standing. To identify between seated and standing the local maxima and minima of the vertical pelvis center were used. The python function scipy.signal.find_peaks() was used to find the local maxima and minima in the dataset with a distance of 400 data points between each, which would equate to 2s between sit-to-stands. The vertical velocity of the pelvis was calculated

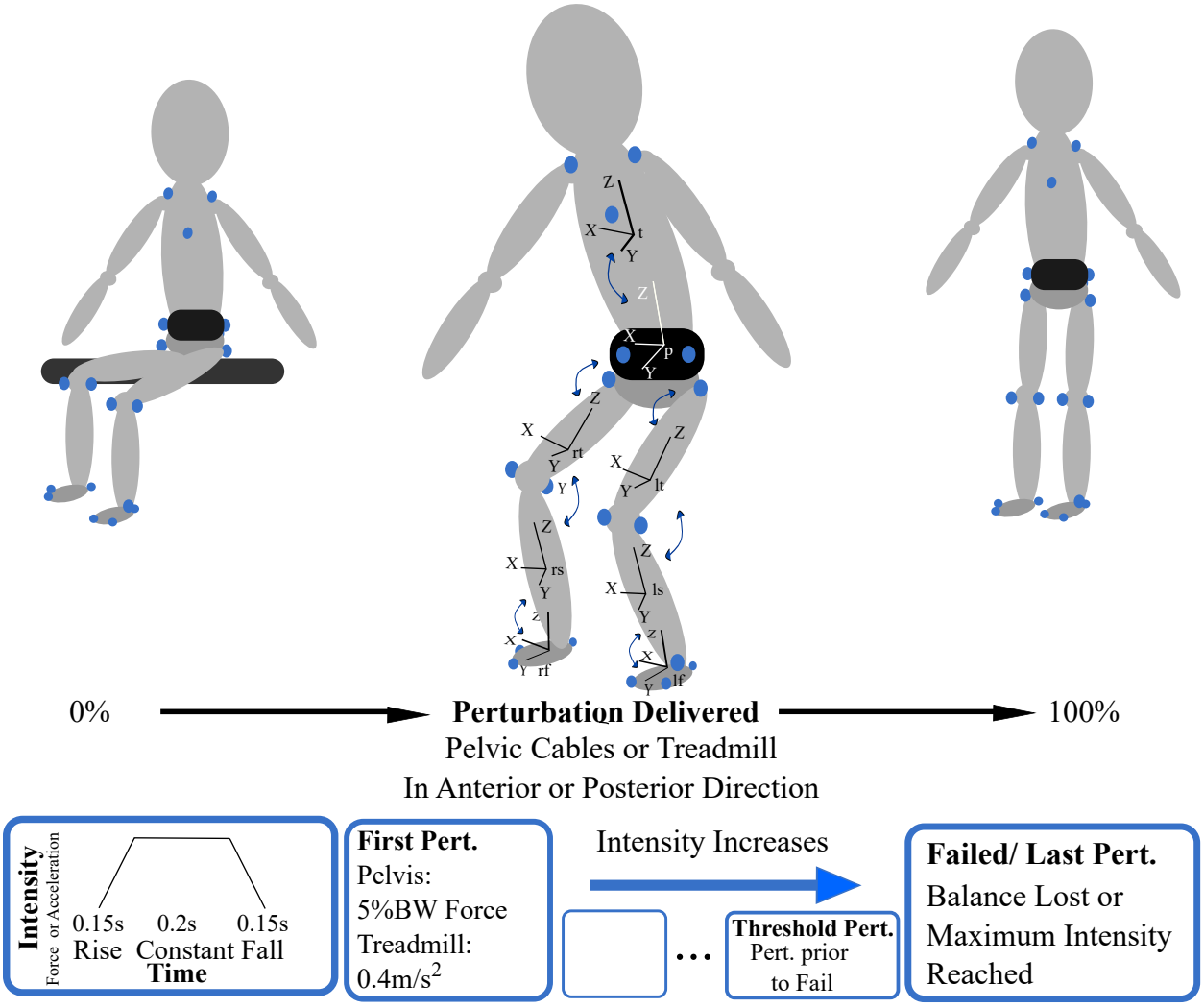

Figure 5.2: The sit-to-stand perturbation experiment design. Participants received perturbations about 50% of the transition cycle. The perturbation was random in terms of type and direction. Joint angles were calculated based on the rotation between adjacent local frames. The local coordinate frames are identified by segment labels: right foot-rf, right shank-rs, right thigh-rt, left foot-lf, left shank-ls, left thigh-lt, pelvis-p, and trunk-t. The blue circular dots represent the retroreflective motion capture markers that were placed to create the local coordinate frames.

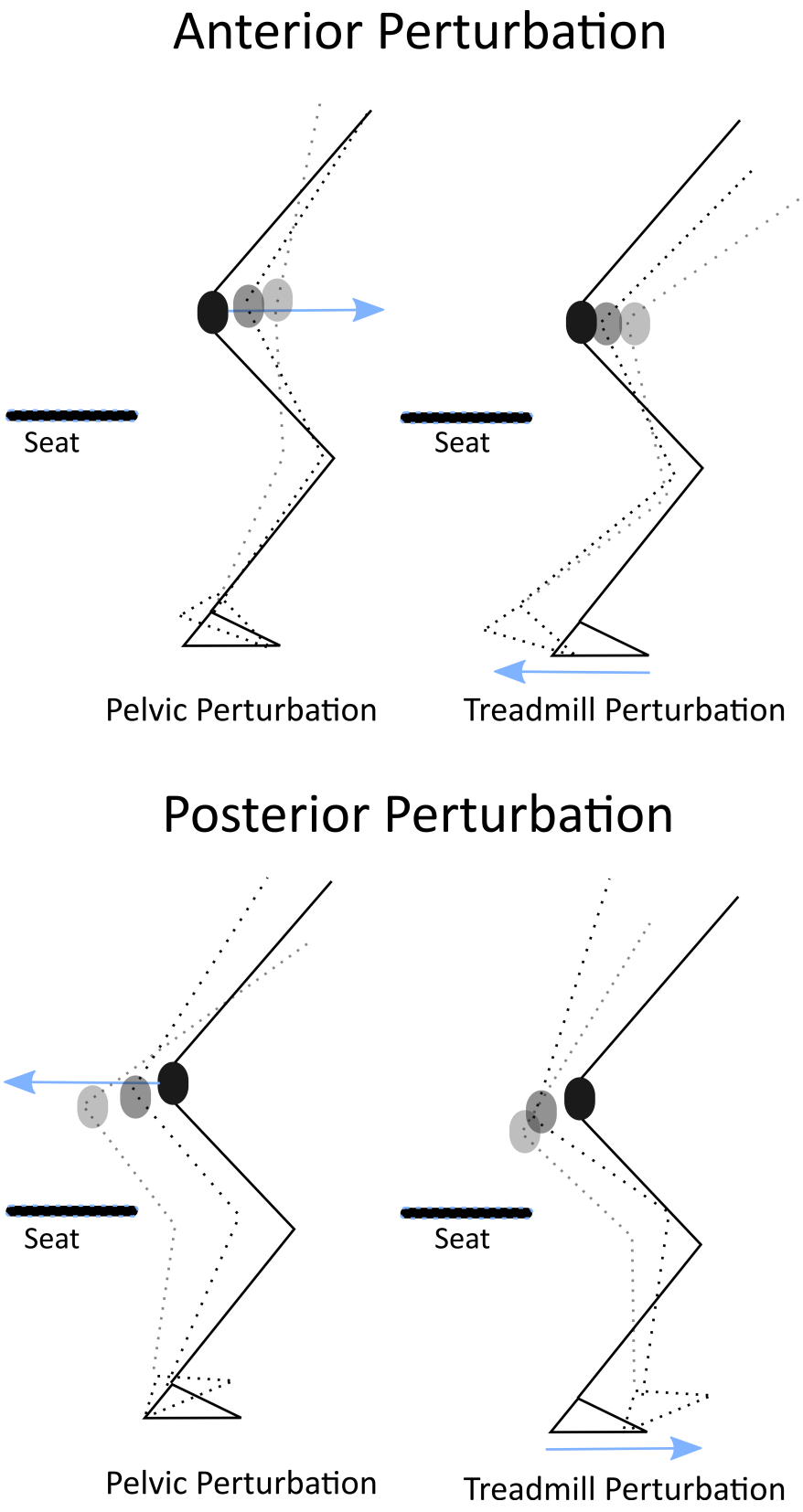

Figure 5.3: Representative reactions to sit-to-stand perturbations as they increase in intensity.

to determine the true onset and end of sit-to-stand transition points. The pelvic vertical velocity threshold was chosen as 20 mm/frame to indicate the start and end of the sit-to-stand trial. The threshold values were chosen based on a heuristic approach. Each sit-to-stand cycle was graphed to ensure correct segmentation. Afterward, the data were segmented to the perturbation duration.

Joint angles, Fig.5.2, were calculated for right and left ankles, knees, hips, and trunk based on ISB [28]. Each joint angle's total excursion (TE) was calculated, where the TE is the total distance traveled throughout the duration of the segmented data. The average symmetry index (SI) was calculated as defined in [100] for the vertical ground reaction forces between the right and left feet. EMG data were normalized by the muscle's maximum values obtained during baseline. Each muscle's peak EMG and integrated EMG (iEMG) were then calculated during the perturbation.

5.3.4 Statistical Analysis

Statistical analysis was performed with SPSS (IBM, v28). Data were normally distributed as determined by Shapiro-Wilk test and Q-Q plots. A three-way repeated measures ANOVA was used to explore statistical significance. Cases with missing experimental conditions were removed from the analysis resulting in a sample size of n=10. The three within-subject factors were the perturbation intensity levels (first, threshold, fail), the type of perturbation (treadmill, pelvic), and the perturbation direction (anterior, posterior). For variables that failed to meet Mauchly's Test of Sphericity, the Greenhouse-Geisser corrected F values were used. In the case of a significant ANOVA model, p-value < 0.05, post-hoc comparisons were followed up with Bonferroni's inequality correction. Interaction effects were prioritized to report results (means±SD). Moreover, Pearson's correlation coefficients were calculated to determine any associations between participants' height or weight and their perturbation threshold.

Table 5.1: Perturbation Thresholds Pearson's correlation coefficients, (p-value)

	Pel-Ant	**Pel-Post**	**Tread-Ant**	**Tread-Post**
Height	-0.54 (0.10)	0.31 (0.39)	-0.13 (0.72)	0.39 (0.26)
Weight	-0.32 (0.37)	0.32 (0.37)	-0.11 (0.77)	0.17 (0.63)

5.4 Results

5.4.1 Perturbation Threshold Results

Ten healthy adults (6 female, 4 male, 10 right-handed and right-legged dominant) participated in this study. The average participant weight was 69 ± 17kg, average age 28 ± 5yrs, and average height 171 ± 15cm. The average threshold perturbation intensities were: pelvis anterior 14.0±6.1%BW, pelvis posterior 13.5±3.4%BW, treadmill anterior 0.90±0.2m/s^2, and treadmill posterior 0.88±0.3m/s^2. No significant correlation was found between participants' height and threshold intensities nor between participants' weight and threshold intensities, Table 5.1.

5.4.2 Muscle Activity Results

The perturbation type and direction had significant interaction effects on the MG iEMG $F(1,9)=5.6$, $p<0.05$. Participants had greater MG iEMG during anterior perturbations in both types of perturbation (pelvic, treadmill) compared to posterior perturbations $p<0.005$. During anterior perturbations, pelvic perturbations caused the greatest MG iEMG compared to treadmill perturbations $p<0.05$. The perturbation direction and intensity had a significant interaction effect on the MG iEMG $F(2, 18)=3.7$, $p<0.05$. Participants had greater MG iEMG during anterior perturbations at Fail intensity compared to anterior perturbations at First intensity, $p<0.05$. In all intensity levels, participants had greater MG iEMG during anterior perturbations compared to posterior perturbations $p<0.05$. MG iEMG results are shown in Fig. 5.4.

Similarly, for RF, iEMG had a significant interaction effect between perturbation intensity and direction, $F(2,18)=5.0$, $p<0.05$. Participants had greater RF iEMG during posterior perturbations at Fail intensity (865±504) compared to anterior perturbations at Fail intensity (607±327). Averages per condition are depicted in Fig. 5.5.

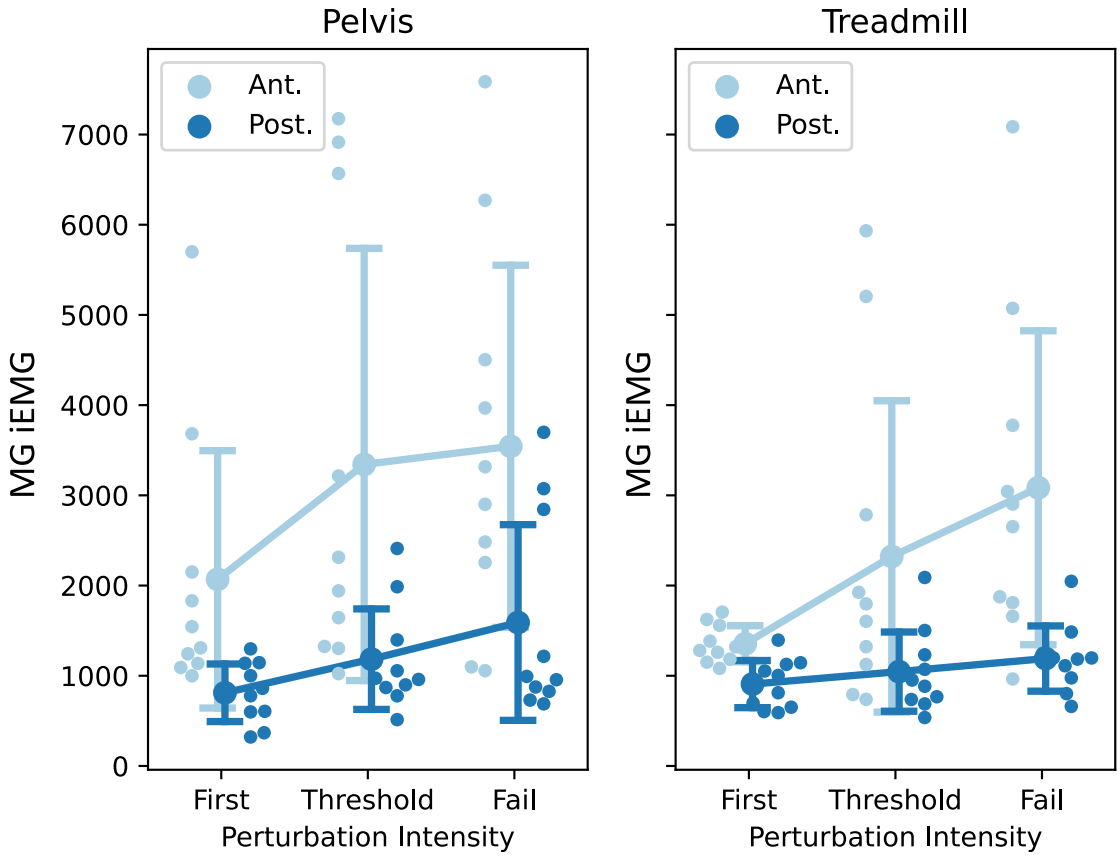

Figure 5.4: Means and SD of participants' MG iEMG results per perturbation direction, type and intensity. Individual dots are participants individual responses. Anterior pelvic perturbations (2985±2048) caused significantly greater MG iEMG than posterior pelvic perturbations (1195±689), $p<0.005$. Anterior treadmill perturbations (2253±1288) caused significantly greater MG iEMG than posterior treadmill perturbations (1048±373), $p<0.005$. Anterior pelvic perturbations caused significantly greater MG iEMG than anterior treadmill perturbations, $p<0.05$.

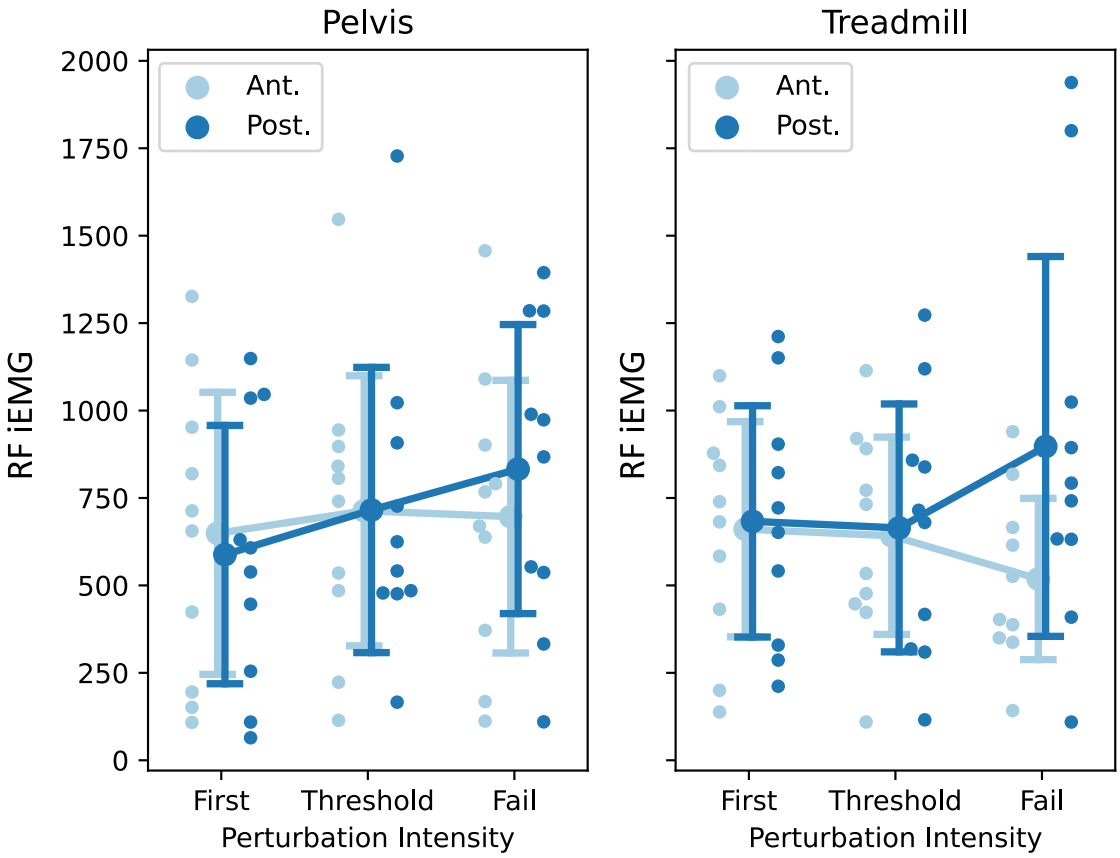

Figure 5.5: Means and SD of participants' RF iEMG results per perturbation direction, type and intensity. Individual dots are participants individual responses. At Fail intensity, posterior perturbations produced greater RF iEMG than anterior perturbations, $p<0.05$.

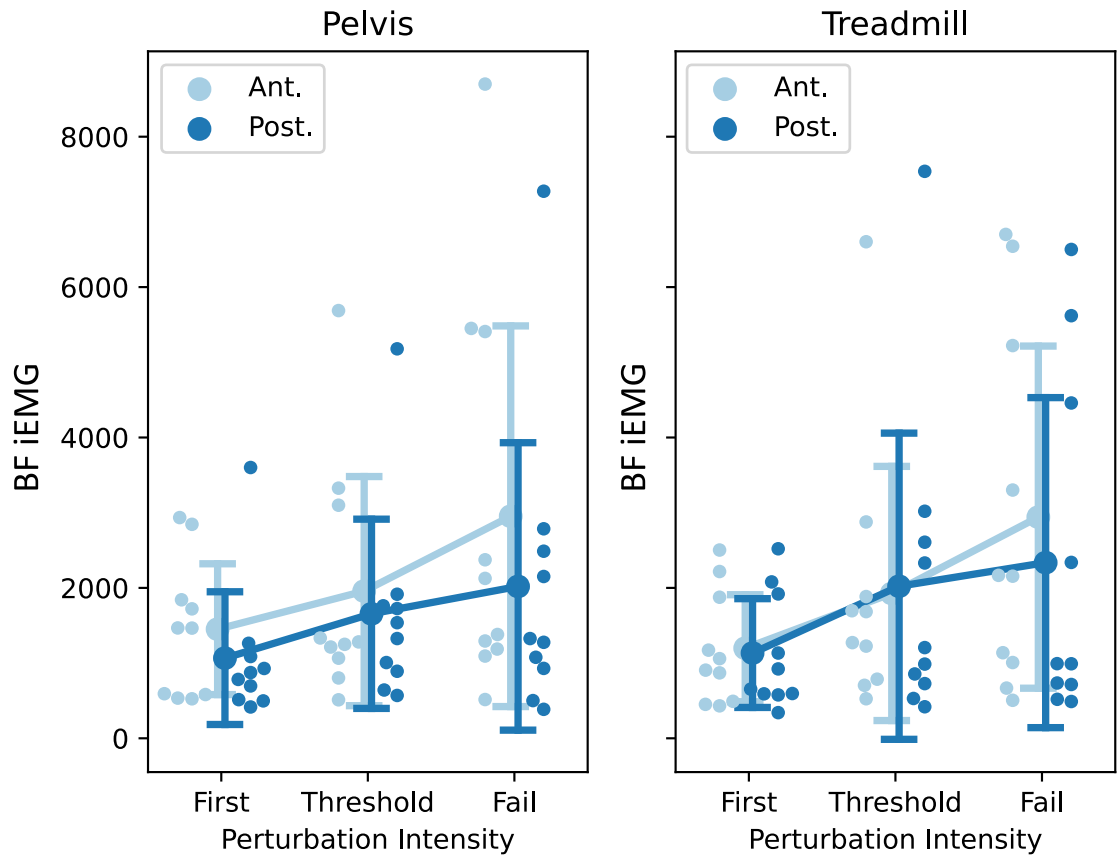

Figure 5.6: Means and SD of participants' BF iEMG results per perturbation direction, type and intensity. Individual dots are participants individual responses. Anterior perturbations (2071±1687) produced greater iEMG responses than posterior perturbations (1706±1582), $p<0.05$.

The perturbation direction had a main effect on participants' BF iEMG $F(1,9)=6.3$, $p<0.05$, and on ES iEMG $F(1,9)=17$, $p<0.005$. Anterior perturbations, compared to posterior, produced greater BF iEMG, $p<0.05$, and ES iEMG, $p<0.005$, (Fig. 5.6-5.7).

The perturbation intensity had a main effect on participants' BF iEMG $F(2, 18)=5.0$, $p<0.05$, and on ES iEMG $F(2,18)=6.7$, $p<0.01$. Participants had greater ES iEMG at perturbation Fail intensity compared to the First intensity, $p<0.05$, (Fig. 5.7).

The perturbation intensity had a main effect on the TA iEMG $F(2,18)=4.8$ $p<0.05$. However, post-hoc comparisons did not reveal significant differences. An additional statistical power analysis showed that a lack of power could be masking a significant effect between the perturbation

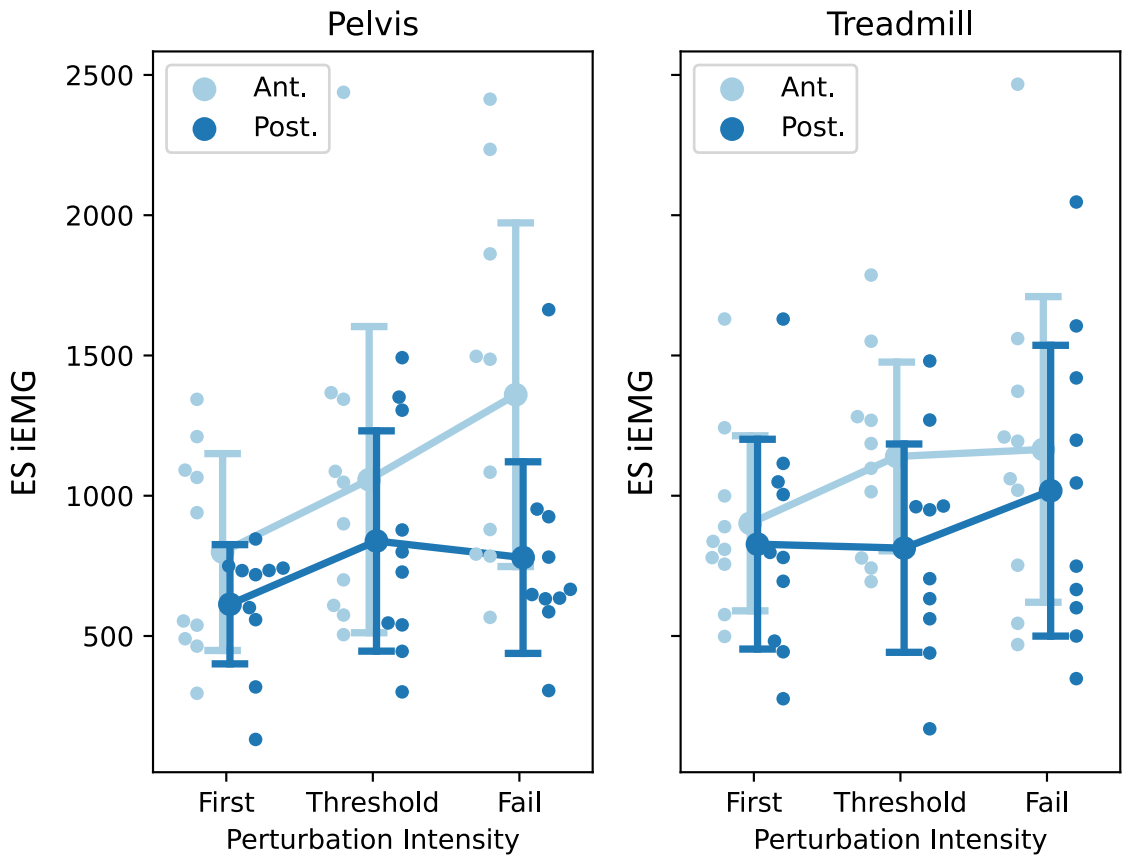

Figure 5.7: Means and SD of participants' ES iEMG results per perturbation direction, type and intensity. Individual dots are participants individual responses. Anterior perturbations (1071±475) caused greater ES iEMG responses than posterior perturbations (815±388), $p<0.005$. In addition, the Fail Intensity (1053±517) had greater ES iEMG than the first perturbation intensity (747±329), $p<0.05$.

intensities for iEMG of TA. G-power (v3.1.9.7, Dusseldorf University) was used to estimate the required sample to find a significant effect. The actual effect size ($\eta_p^2 = 60\%$) and a estimated power = 80% were used to compute the sample size estimation. Our analysis estimated that a total of 16 participants would be required.

5.4.3 Kinematic Results

Perturbation direction had a main effect on participants' trunk flexion TE $F(1,9)=5.9$, $p<0.05$. Anterior perturbations produced greater trunk flexion TE compared to posterior perturbations $p<0.05$ (Fig.5.8). No interaction effects were observed. Perturbation intensity had a main effect on trunk vertical rotation $F(2,18)=15.2$, $p<0.001$. Participants had greater trunk rotation TE at the perturbation Fail intensity compared to the First intensity, $p<0.005$, (Fig.5.9). No interaction effects were observed.

Perturbation type had a significant effect on the left knee TE flexion $F(1,9)=9.3$, $p<0.05$. Treadmill perturbations (43.4±14.8°) produced greater left knee TE flexion compared to pelvic perturbations (37.4±14.8°), $p<0.05$. No interaction effects were observed.

Perturbation type and direction had significant interaction effects on the left ankle TE flexion $F(1,9)=5.55$, $p<0.05$. In the posterior direction, treadmill (16.4±6.5°) produced greater left ankle TE flexion compared to pelvic (12.6±5.2°) $p<0.05$. In pelvic perturbations, the anterior direction (17.0±6.8°) produced greater left ankle TE flexion compared to posterior (12.6±5.2°), $p<0.05$.

Perturbation direction had a significant effect on the right knee TE flexion $F(1,9)=39.9$, $p<0.001$. Anterior perturbations (45.1±16.4°) produced greater right knee TE flexion than posterior (35.9±14.6°). No interaction effects were observed.

The perturbation intensity had a significant effect on the right ankle TE flexion $F(2,16)=4.93$, $p<0.05$. Perturbation Fail intensity (17.4±7.0°) produced greater right ankle TE flexion compared to First intensity (13.3±5.9°), $p<0.05$. No interaction effects were observed. No significant effects were observed in the right or left hip TE flexion values.

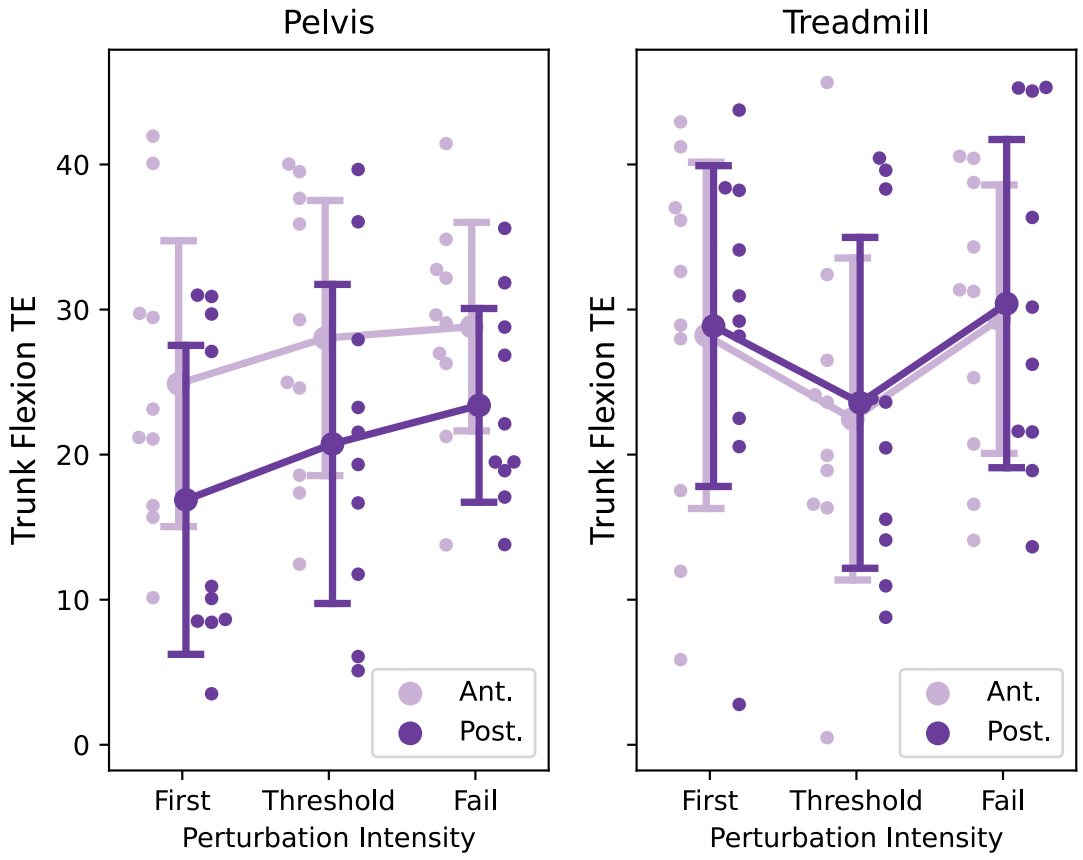

Figure 5.8: Means and SD of participants' trunk TE flexion per perturbation direction, type and intensity. Individual dots are participants individual responses. Anterior perturbations (26.7±10°) caused significantly greater trunk flexion TE compared to posterior perturbations (24.0±11°), $p<0.05$.

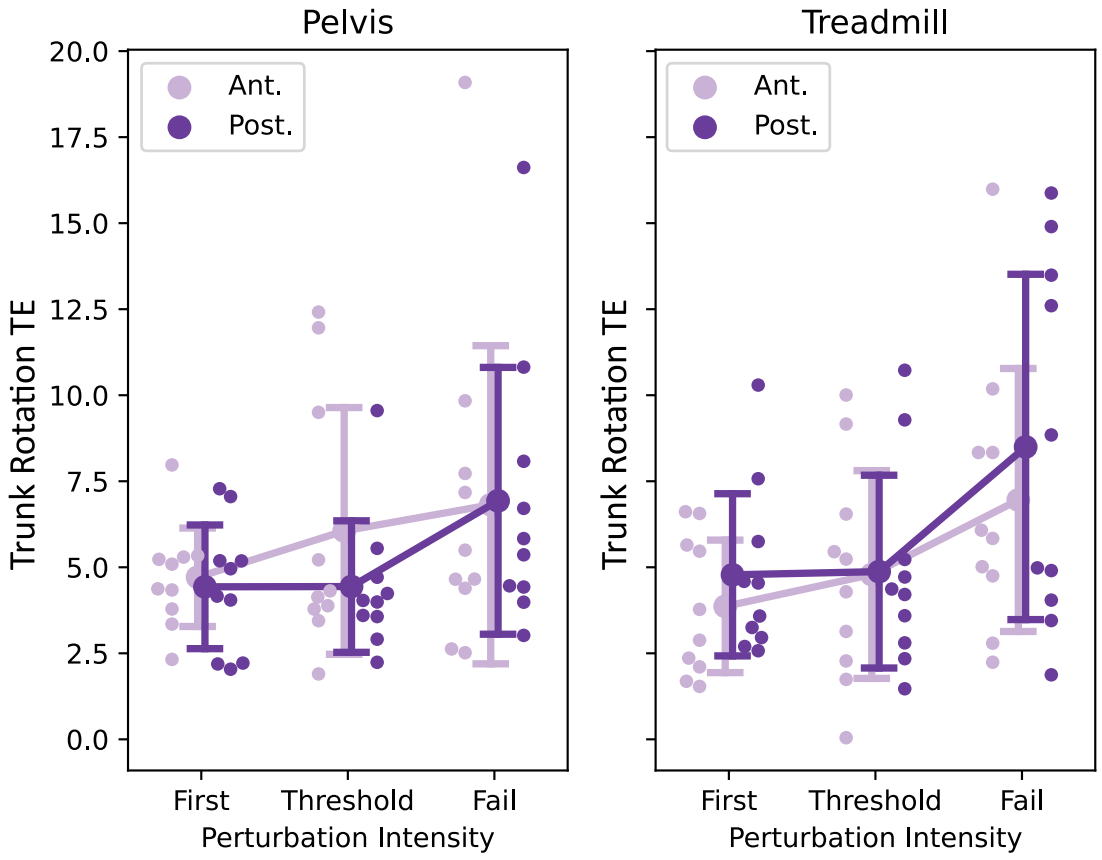

Figure 5.9: Means and SD of participants' trunk TE rotation per perturbation direction, type and intensity. Individual dots are participants individual responses. Participants had greater trunk rotation TE at the Fail intensity (7.3±4.6°) compared to the First perturbation intensity (4.4±2.0°), $p<0.005$.

5.4.4 Ground Reaction Results

The ground reaction average symmetry index was not significantly affected by the perturbation intensity $F(2, 18)=0.42$, $p>0.05$, type $F(1,9)=5.1$, $p>0.05$, or direction $F(1,9)=0.09$, $p>0.05$; no interaction effects were significant.

5.5 Discussion

This study used a robotic system to characterize how healthy participants responded to perturbations during a sit-to-stand movement. Few studies have characterized postural strategies in sit-to-stand motion, and no study before had investigated muscle and joint angle reactive responses, which is important in improving the evaluation and interventions to reduce the risk of falls. Various robotic platforms have been designed to assist in the transfer from sit-to-stand, however, none have investigated reactive rehabilitation strategies to assess stability. With the TPAD, our results showed I) participants displayed direction-specific postural responses, they had greater muscle activity and kinematic TE to oppose the perturbation direction, II) the highest perturbation intensity promoted greater muscle activity and kinematic responses, and III) perturbation type with the interaction of direction affected participants' MG activity and their left knee TE flexion.

5.5.1 Perturbation Direction

Perturbation direction had the most distinct effect on participants' postural responses. Participants responded to anterior perturbations by having a greater level of activity in posterior muscles that extend the trunk, hip, and knee (ES, BF, MG). As we expected, these muscles help participants restore equilibrium by opposing the direction of the perturbation. Similarly, posterior perturbations required greater activity from an anterior muscle, hip flexor RF. However, participants did not display significant changes in the remaining front muscles, TA and RA, during posterior perturbations. We would have expected significantly higher TA and RA activation during posterior perturbations. Although, since sit-to-stand is a dynamic motion that requires lower leg and trunk

coordination and requires an initial activation from the TA [101], distinguishing significant differences in the anterior muscles may be masked.In this study, we investigated the overall activity during the perturbation period. Further research is required to characterize the timing of muscle responses.

Participants relied on their torso to maintain stability when an unexpected ground or body displacement compromised their balance. Participants regained balance by increasing trunk flexion and rotations. In addition, participants required greater trunk control when receiving anterior perturbations or perturbations past their threshold, as indicated by the increase in ES activity. However, no changes in the RA were observed, this may have been due to the location of the pelvic belt or any adipose tissue present [102]. Trunk control is a necessity to remain upright and to perform movements that maintain the center of mass within the base of support [103]. Rehabilitation of trunk control has shown improved balance and gait in patients with stroke [103, 104]. Sit-to-stand perturbations encouraged trunk movement; this can potentially be a future method to train trunk control.

5.5.2 Perturbation Type

In standing perturbation studies, receptors near the area of the perturbation respond first [90]. Thus, platform perturbations would initially cause ankle flexion with TA and MG muscle responses. Likewise, pelvic cable-based perturbations would cause initial hip motion with RF and BF muscle responses. However, participants engaged the MG more during anterior pelvic perturbations than during anterior treadmill perturbations. A possible explanation may be related to the timing and postural configuration at which the perturbation was delivered. Perturbations were delivered at 50% of the sit-to-stand cycle, with ankles, knees, and trunk flexed (Fig.5.2). A treadmill perturbation displaces participants' feet, not constricting other joint movements it could allow participants to maintain their knee and trunk flexed configuration. Meanwhile, a pelvic perturbation physically displaces their pelvis and thus requires joint movement compensation, as indicated by the increase in the right knee TE during anterior perturbations. Therefore, participants required

greater muscle activity from their distal and proximal muscles to regain balance from pelvic perturbations.

To recover from treadmill perturbations, participants had higher left knee flexion compared to pelvic perturbations. As for posterior perturbations, the treadmill produced greater left ankle flexion than pelvic perturbations. Bhise et. al. [105] concluded that most able-bodied participants prefer their dominant leg for controlled movement but when the task is destabilizing participants choose their left leg regardless of dominance. This may explain why participants only had significant left knee and ankle TE. The increase in only the left total excursion indicates participants relied more on their left leg to recover from treadmill perturbations.

5.5.3 Perturbation Intensity

Surprisingly, participants displayed a similar response in muscle and kinematic results during the first and threshold perturbation levels. In this postural perturbation paradigm, we found an increase in muscle activity and an increase in trunk rotation when participants lost their balance at the Fail perturbation intensity. During this Fail perturbation intensity, participants used a *change-in-support* strategy to recover their stability. This change-in-support strategy required greater muscle activity to regain balance. According to Kam et. al. [106], able-bodied individuals may prefer to take a step at lower perturbation intensities rather than going to their extreme in-place base of support boundaries. This may explain why no significant differences were identified in the muscle activity between first perturbations and the threshold perturbations. Brauer et. al. confirmed that taking a reactive step is prioritized before an in-place response [107]. Thus, in able-bodied participants, one should train past the individual's threshold to promote increased muscle activation.

5.5.4 Sit-to-Stand Perturbations

Most postural strategy research has been performed on standing responses from platform perturbations. In these studies, participants do not rely on their knees as effectively. Researchers have documented that knee stiffness lowers postural stability and delays biomechanical responses [108,

109]. Meanwhile, the sit-to-stand perturbation task encourages participants to have a mixed postural strategy that includes knee flexion. Our outcome matches the nature of the motor task. Unlike a standing position, a sit-to-stand task requires knee control to move the upper body vertically.

Researchers Mak et al. have shown that the cause of falls in sit-to-stand was insufficient limb support of body weight when reaching maximum vertical velocity [82]. They suggest increasing rehabilitating strategies that strengthen lower limb muscles and improve body movement coordination. Lower limb and pelvic robotic systems have the capability to apply forces while participants transition from sit-to-stand. However, most systems are implemented for alleviating body weight or reducing joint torque. Further research is needed on improving participants' balance and coordination. Therefore, rehabilitating robotic systems should address this need to promote active stability. We suggest perturbative sit-to-stand paradigms, like the one investigated in this study, as a rehabilitation method; it encourages greater muscle activity and requires participants to overcome imbalance as they transition from seated to standing.

5.5.5 Study Limitations

A potential limitation was sensorimotor adaptations to the perturbation intensities. Whereas perturbations were randomized in type and direction to prevent individuals from anticipating the perturbation delivered, perturbation intensity increased gradually. Participants could have adapted and improved throughout the perturbation sets and thus had higher perturbation thresholds. Another study limitation was the number of participants. A larger number of participants would be needed to generalize TA iEMG responses further.

The ground reaction SI showed no significant differences between the left and right loading. However, discrepancies in symmetry may be present in populations with neurological conditions. Only the muscle activity from the dominant hemibody was recorded in this study. A bilateral EMG analysis would offer a more detailed study of neuromuscular responses. Further research is needed to distinguish any variance between dominant and non-dominant legs and would be necessary for people with balance disorders.

5.6 Conclusion

In this sit-to-stand perturbation study, we used a robotic system TPAD to characterize young adults' postural responses. Participants required greater trunk control against the sit-to-stand perturbations. Participants also experienced greater muscle activity to oppose the perturbation direction. During anterior perturbations, participants required higher MG activity when receiving a pelvic perturbation rather than a treadmill perturbation. Pelvic perturbations caused the greatest increase in distal and proximal muscles to regain balance. Overall, sit-to-stand perturbation results are encouraging as a potential for rehabilitation. A perturbation-based sit-to-stand training could promote greater muscle activity while requiring reactive coordination. Depending on the individual's therapeutic need, a sit-to-stand perturbation paradigm could regulate the perturbation intensity to target specific control strategies during either in-place or change-in-support reactions. The application of an incremental intensity protocol may promote greater motor flexibility and fine control of neuromuscular responses until the point of postural instability is reached, when the participant transitions from an in-place to a change-in-support strategy. Therefore, we recommend a sit-to-stand perturbation paradigm as a rehabilitation method.

Chapter 6

Characterizing Sit-to-Stand Reactive Responses in Young and Older Adults

6.1 Introduction

Falls are the highest cause of death in adults aged 65 and older [110]. Transferring from sit-to-stand has been reported as the cause of 41% of falls in an elderly population [111]. Sit-to-stand requires full body coordination, trunk control and lower limb strength. However, with the increase in age the task becomes more challenging and the risk of falling increases [83].

Providing perturbative forces to an individual has been shown as a method to reduce the chance of falls [112]. Although, only few studies have looked into individuals reactive postural responses in sit-to-stand motion [89, 113]. And only researchers Pavol et al. [88] have investigated the postural responses in young and older groups. However, they only characterized participants step and falling responses, they did not measure any muscle activity, kinematic joint angles, or ground reaction forces.

Characterizing reactive strategies may improve the evaluation to reduce the risk of falls and better train individuals against falling. Therefore, the aim of this study is to identify how age may affect reactive postural responses during sit-to-stand maneuvers. Healthy young and older adults were recruited to perform a set of sit-to-stand perturbations. To identify postural response differences, the muscle activity, kinematics and ground reaction forces were measured.

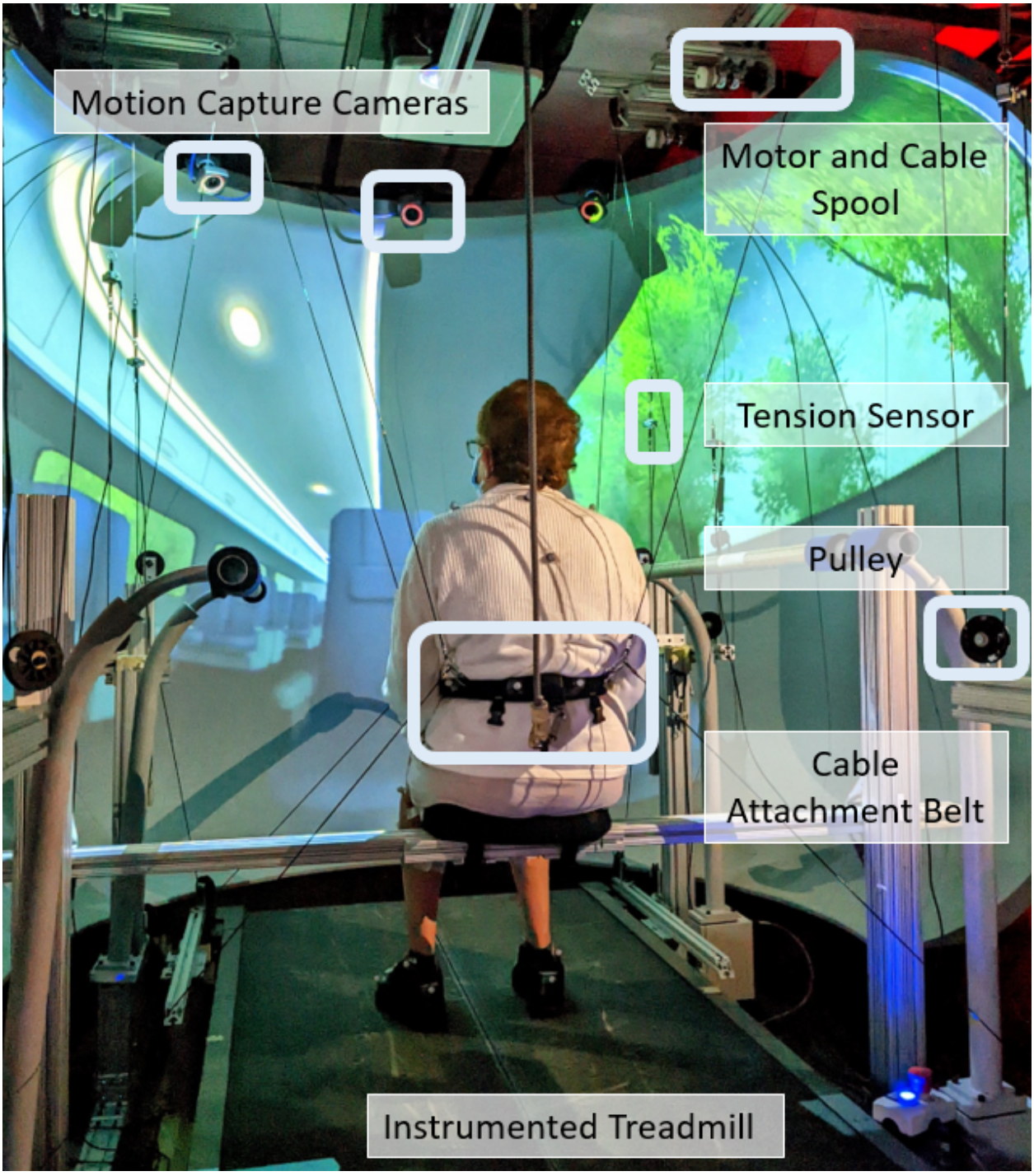

Figure 6.1: A participant seated in the TPAD system. The motion capture cameras track the position of reflective markers on the cable attachment belt and on markers across the body. Eight cables and a harness are connected to the cable attachment belt. Each cable is routed from a cable spool motor assembly to tension sensors to the cable attachment belt. Pulleys are used to direct the cables. Participants have each foot on the instrumented treadmill.

Table 6.1: Demographic Information for Sit-to-Stand Study Participants

Group	Age (yrs)	Height (cm)	Weight (kg)	Gender	Commuters	Total Participants
Young	29±5	172±13	74±18	8F(7M)	Daily:8 (Weekly:7)	15
Older	71±9	162±8	72±13	13F(6M)	Daily:13 (Weekly:1)	19

6.2 Experiment Design

6.2.1 Participant Information

Fifteen young adults and nineteen older community dwelling adults participated in this study. Demographic information is found in Table 6.1. All participants performed sit-to-stands and walked without any assistance. Commuters were defined as taking the bus or subway. Daily commuters used the bus or subway at least 5-7 times a week, weekly commuters took bus or subway 1-4 times a week.

6.2.2 Study Design

The study consisted of a baseline condition and sets of perturbations. The baseline was performed with TPAD in transparent mode, where a minimal tension of 15N per cable was applied to the pelvic belt. Participants were instructed to rise from the TPAD seat at a self-selected pace, remain standing for about 1-2s, and then return back to the seated position. The sit-to-stand transition was performed five times, similar to the five repetition sit-to-stand test, which is a clinical assessment done to evaluate functional impairment [96]. After the baseline test, participants were given a break of approximately 3 minutes.

Perturbations were randomized in terms of the type (treadmill or pelvic) and direction (anterior or posterior). Perturbations were given near the middle of the participant's sit-to-stand transition, about 50% of the cycle, where 0% is seated, and 100% is standing upright. The perturbation intensity had a trapezoidal profile to give the TPAD and treadmill time to ramp and up and ramp down in a smooth manner. Perturbations lasted 0.5s, with 0.15s of perturbation rise time, 0.2s of constant perturbation intensity, and 0.15s of fall time.

In the first set of perturbations, participants received a peak of 5% body weight (BW) force

on the pelvis and a peak acceleration of 0.4m/s^2. The first set of perturbations were labeled as Low perturbation intensities (Low). Afterward, the peak intensities and peak accelerations would increase by 5%BW and 0.2m/s^2, respectively. These values were chosen in order to limit the maximum of perturbation sets to 10, which would indicate a maximum of 50%BW and 2.2m/s^2. The force and acceleration profiles would continue to increment until the participant failed to maintain stability. This was labeled as a failed attempt (Fail) because the participant failed to stay *in-place* and required a *change-in-support* strategy, like taking a step or reaching for a handrail. The peak perturbation intensity in that direction and type would no longer increase once the participant failed. The previous level of intensity was labeled as their threshold level (Threshold), which is the maximum they could withstand using an *in-place* strategy.

In the case participants stepped at the low intensity, the trail was repeated an additional two times at the low intensity. The three trails were then categorized into Failed, Low and Threshold.

The perturbation test was continued until the participant failed, i.e. required a change-in-support, in each type of perturbation and direction. For safety purposes, the maximum pelvic force TPAD would deliver was 50%BW, and the maximum acceleration the treadmill would go was 2.2m/s^2. The session ended if a participant reached the maximum force or acceleration peaks. A visual description of the perturbation tests are shown in Fig. 6.2. Participants were also instructed to rise from the TPAD seat at their own controlled pace and keep their arms at their sides unless they needed to stabilize with a handrail.

6.2.3 Data Analysis

All data were processed offline using Python. Data were segmented first by sit-to-stand cycle. The vertical component of the pelvis center position was used to determine if the individual was seated or standing. The python function scipy.signal.find_peaks() was used to find the local maxima and minima in the dataset with a distance of 400 data points between each, which would equate to 2s between sit-to-stands. The vertical velocity of the pelvis was calculated to determine the true onset and end of sit-to-stand transition points. The pelvic vertical velocity threshold was

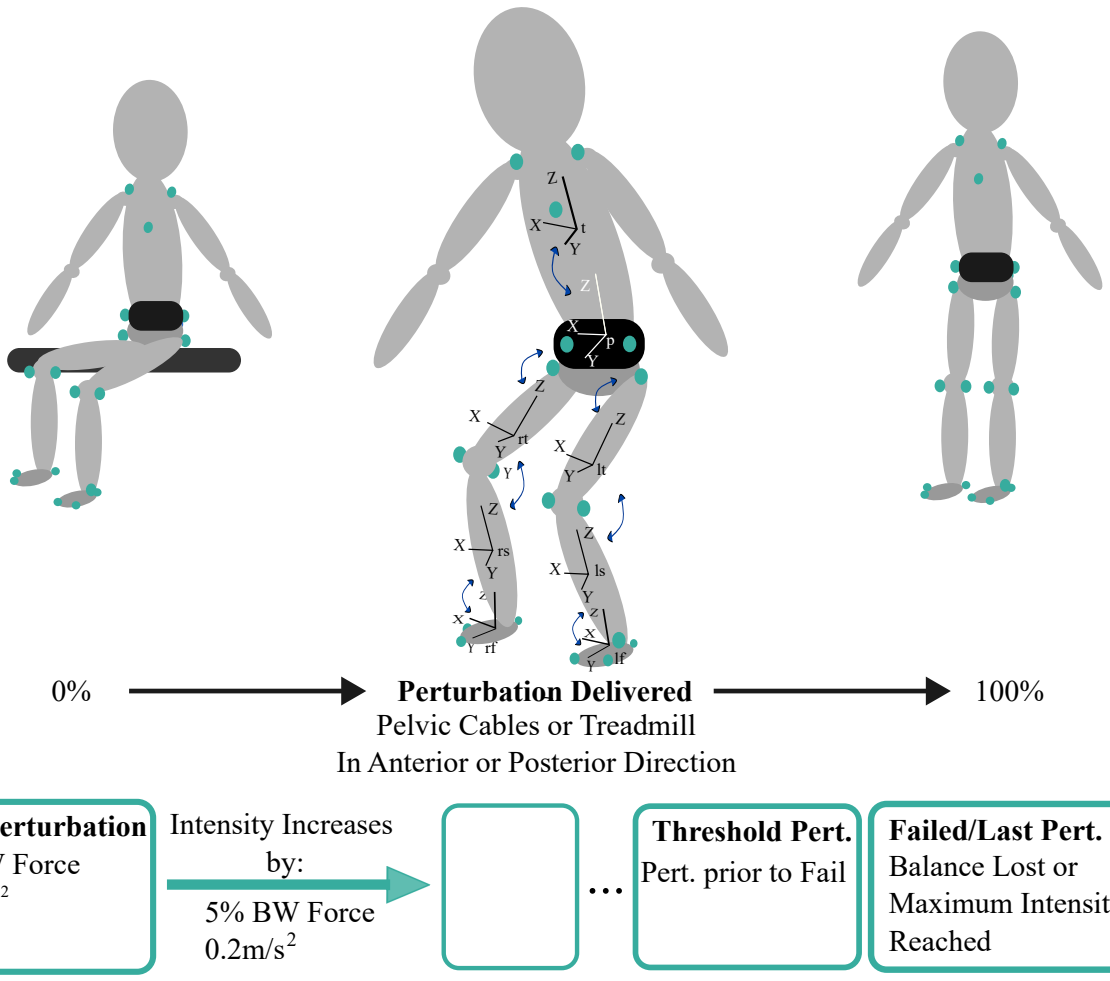

Figure 6.2: The sit-to-stand perturbation experiment design. Participants received perturbations about 50% of the transition cycle. The perturbation was random in terms of type and direction. Joint angles were calculated based on the rotation between adjacent local frames. The local coordinate frames are identified by segment labels: right foot-rf, right shank-rs, right thigh-rt, left foot-lf, left shank-ls, left thigh-lt, pelvis-p, and trunk-t. The circular dots represent the retroreflective motion capture markers that were placed to create the local coordinate frames.

chosen as 20 mm/frame to indicate the start and end of the sit-to-stand trial. The threshold values were chosen based on a heuristic approach. Each sit-to-stand cycle was graphed to ensure correct segmentation. Afterward, the data were segmented to the perturbation duration. Variables were then calculated and labeled for each type of perturbation and direction.

6.2.3.1 Kinematic Variables

Kinematic data were recorded at 200Hz with Vicon cameras and filtered through a low-pass filter of 4th order and 10Hz cut-off frequency. Twenty-three markers were placed around the body to measure joint angles: five were used on the upper trunk (one at each shoulder, mid-back, upper chest, and cervical region C7), four around the pelvis, two at the hips (right and left lateral sides), two at each knee (inner and outer part of the knee), one at each ankle, and three at each foot (toe, outer foot, and heel). A visual of the marker locations is shown in Fig. 6.2. Joint angles were calculated for right and left ankles, knees, hips, and trunk based on ISB [28]. Each joint angle's total excursion (TE) was calculated, where the TE is the total distance traveled throughout the duration of the segmented data.

To determine primary and secondary muscles participates utilized during the perturbation, the maximum and second maximum TE were categorized as primary and secondary, respectively. The left and right joints (ankles, knees and hips) TE were averaged before calculating maximum TE.

The margin of stability, MoS, was calculated as defined by Hof et al. [114], the minimum distance from the base of support (BoS) to the XCoM position. Where XCoM is:

$$XCoM = \vec{u} + \frac{\dot{\vec{u}}}{\sqrt{g/(l)}} \tag{6.1}$$

In which $\vec{u}$ is the CoM, estimated by the pelvic markers, $\dot{\vec{u}}$ is the CoM velocity, $g = 9.81 m/s^2$ and l is the subject's leg length while standing multiplied by 1.2 as suggested [114]. The leg length was estimated from the pelvic markers average vertical position to the foot markers average vertical position. The BoS was determined the by the feet marker positions in contact with the

ground. Ground reaction forces were checked to determine if participant had double stance or adjusted their weight to single stance on one foot. The MoS was calculated in the four directions, i) to the anterior BoS, calculated based on the toe markers, ii) to the posterior BoS based on the heel markers, iii) to the furthest right marker in the mediolateral direction and iv) to the furthest left marker in the mediolateral direction. A representation of the MoS and BOS is shown in 6.3. The anterior-posterior (AP) MoS direction was calculated as the minimum MoS in i) and ii). The mediolateral (ML) MoS was calculated as the minimum MoS in iii) and iv).

6.2.3.2 Ground Reaction Force Variables

Force plate ground reaction data were collected at 1000Hz and passed through a 4th order low-pass filter with 10Hz cut-off frequency [97]. The average symmetry index (SI) was calculated as defined in [100] for the vertical ground reaction forces between the right and left feet.

6.2.3.3 Muscle Variables

Muscle activity was measured using surface electromyography (EMG) with Delsys (Delsys Trigno Avanti Sensor, Massachusetts). Data were detrended then filtered using a 4th order band-pass filter with 20 to 500 Hz. Data were rectified and low-passed with a 4th order filter at 3Hz cut-off to obtain the linear envelope [98]. In healthy participants, researchers have shown no significant difference in muscle activity during sit-to-stand between dominant and non-dominant legs [99]. Therefore, muscle EMG data for young participants were obtained from the participant's self reported dominant side: lower back erector spinae (ES), biceps femoris (BF), rectus femoris (RF), medial gastrocnemius (MG), and tibialis anterior (TA). For the older participants, muscle EMG data was collected from both their left and right sides. A visual of the muscles of interest are shown in Fig. 6.4. EMG data were normalized by the muscle's maximum values obtained during baseline. The integrated EMG (iEMG) were then calculated during the perturbation period using trapezoidal rule.

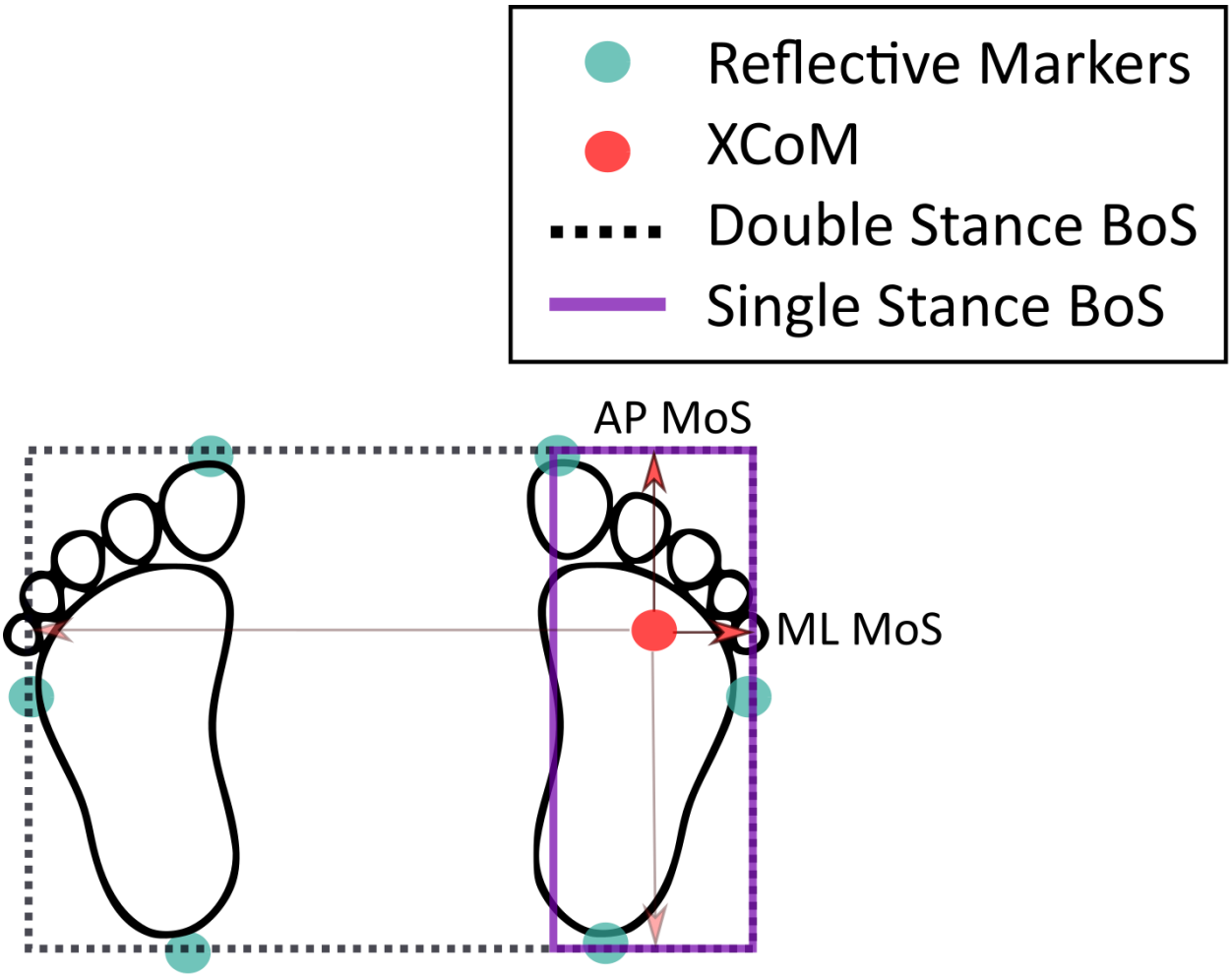

Figure 6.3: The BoS was dependent on the ground reaction forces and foot markers. If the participant was in double stance, the BoS was calculated using both feet markers. Otherwise, the BoS for single stance was calculated based on the foot in contact with the ground. The teal circular dots represent the reflective motion capture markers that were placed to create the BoS boundary. The MoS were calculated in the four directions, the minimum MoS in the AP and the ML directions were then selected for statistical analysis.

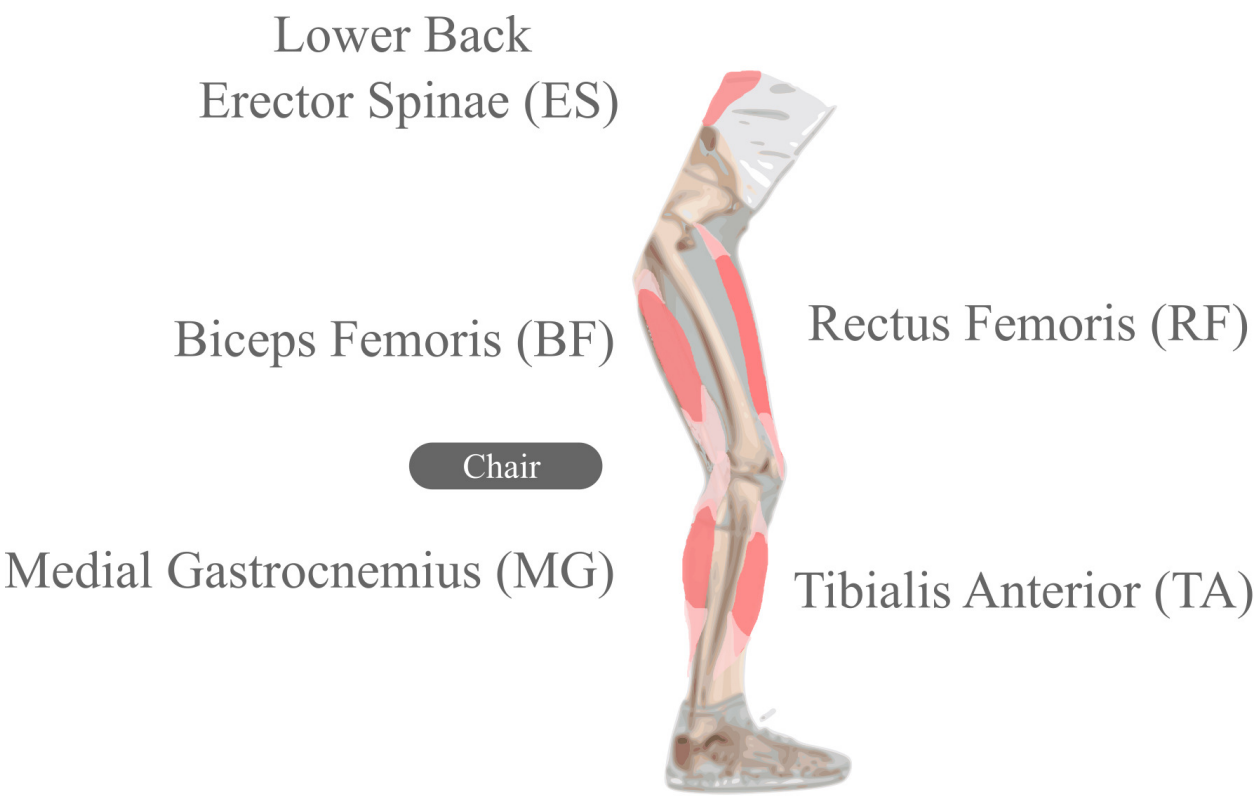

Figure 6.4: EMG data was collected from these muscles. The figure shows a representation of where the muscles are located in pink.

6.2.4 Statistical Analysis

Statistical analysis was performed with SPSS (IBM, v28). Data were normally distributed as determined by Shapiro-Wilk test and Q-Q plots. A three-way repeated measures ANOVA was used to explore statistical significance. Cases with missing experimental conditions were removed from the analysis. The two within-subject factors were the type of perturbation (treadmill, pelvic), and the perturbation direction (anterior, posterior). The between-subject factor was the group (young, older). The three-way repeated measures ANOVA was performed for each of the three perturbation intensities (low, threshold, fail). For variables that failed to meet Mauchly's Test of Sphericity, the Greenhouse-Geisser corrected F values were used. In the case of a significant ANOVA model, post-hoc comparisons were followed up with Bonferroni's inequality correction. Interaction effects were prioritized to report results (means±SD).

Older adults muscle iEMG results were compared between the right and left sides using a T-Test. For the two group comparison using three-way repeated measure ANOVA, the participants' dominant side muscle responses were analyzed.

A Cochrane Q test was performed to determine if there was significance in pattern with the primary and secondary joint used to remain stable during the perturbation. A Cochrane Q test is a non-parametric statistical test for categorical responses.

6.3 Results

6.3.1 Margin of Stability Results

6.3.1.1 Low Perturbation Intensity

At low perturbation intensities, the ML MoS was not significantly affected. Meanwhile, the AP MoS was significantly different among the two age groups, F=6.22, p<0.05. Older adults had higher AP MoS than the young group. Group averages are displayed in Fig. 6.5

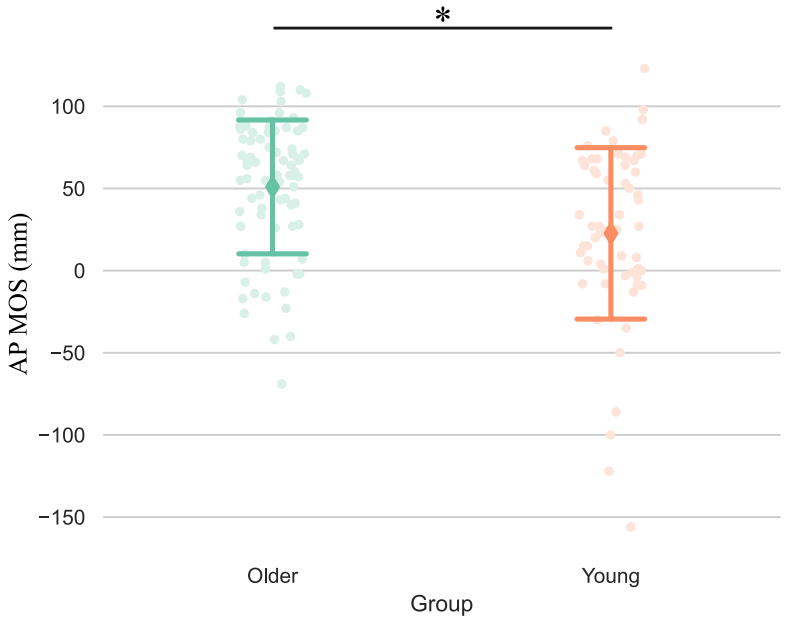

Figure 6.5: AP MoS at Low Perturbation Intensity. AP MoS was significantly different amongst the two age groups, F=6.22, p<0.05. Older adults had higher AP MoS than the young group.

6.3.1.2 Threshold Perturbation Intensity

The AP MoS had a significant interaction effect in the age group and perturbation direction, F=6.48, p<0.05. Group averages are displayed in Fig. 6.6

The ML MoS had a significant interaction effect between the perturbation type and perturbation direction, F=5.81, p<0.05. Group averages of ML MoS are in Fig. 6.7.

6.3.1.3 Fail Perturbation Intensity

During the fail perturbation intensity, the AP MoS was significantly affected by the three main effects. No interaction effects were observed. Posterior perturbations caused significantly smaller AP MoS compared to anterior perturbations, F=7.12, p<0.05, Fig. 6.8. Pelvic perturbations caused significantly smaller AP MoS compared to treadmill perturbations, F=8.96, p<0.01, Fig. 6.9. Young adults had significantly smaller AP MoS compared to older adults, F=15.76, p<0.001, Fig. 6.10. In the ML direction, there were no interaction effects observed. Group averages of MoS are in Fig. 6.11.

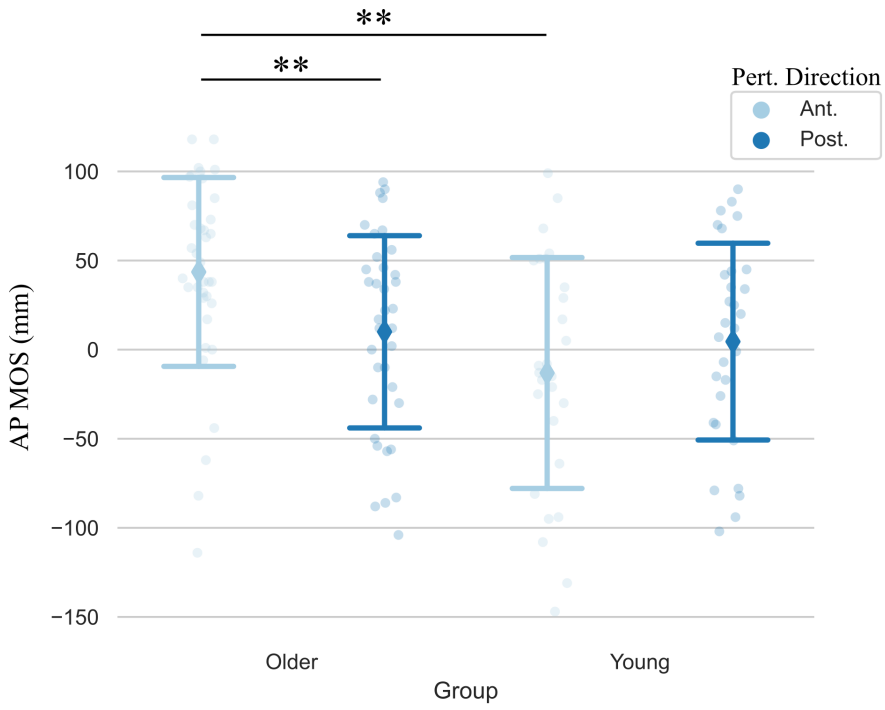

Figure 6.6: AP MoS at Threshold Perturbation Intensity. During anterior perturbations, older group had higher AP MoS compared to the young group, $p<0.001$. The older group also display significantly higher AP MoS during anterior perturbations compared to posterior perturbations, $p<0.005$. Significant differences are displayed with ** for $p<0.005$.

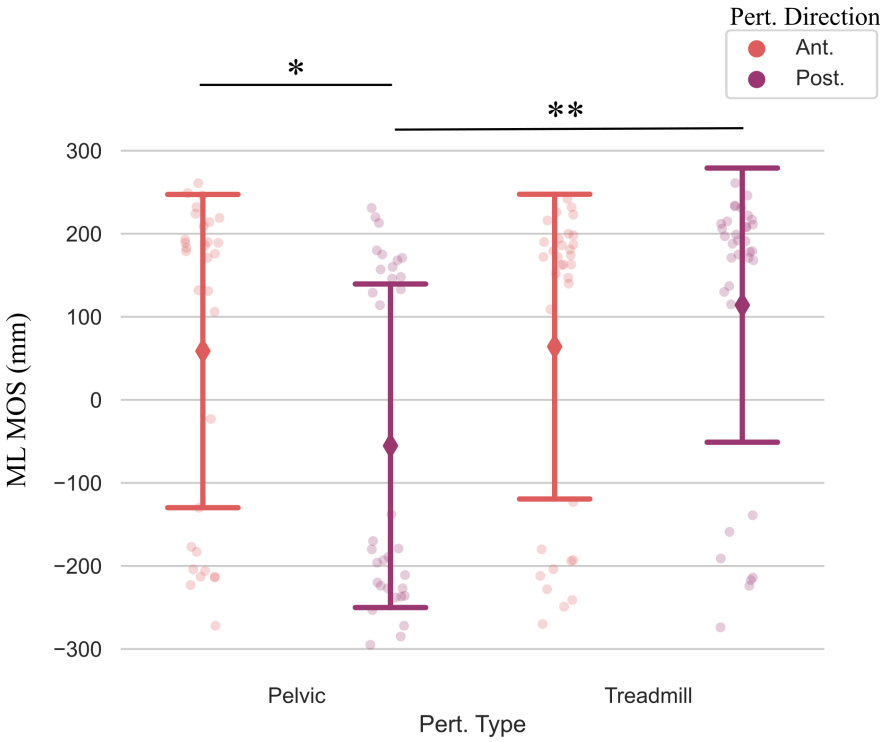

Figure 6.7: ML MoS at Threshold Perturbation Intensity. Participants had higher ML MoS during posterior treadmill perturbations compared to posterior pelvic perturbations, $p<0.001$. Participants also displayed higher ML MoS during anterior pelvic perturbations compared to posterior pelvic perturbations, $p<0.05$. Significant differences are displayed with * for $p<0.05$ and ** for $p<0.001$.

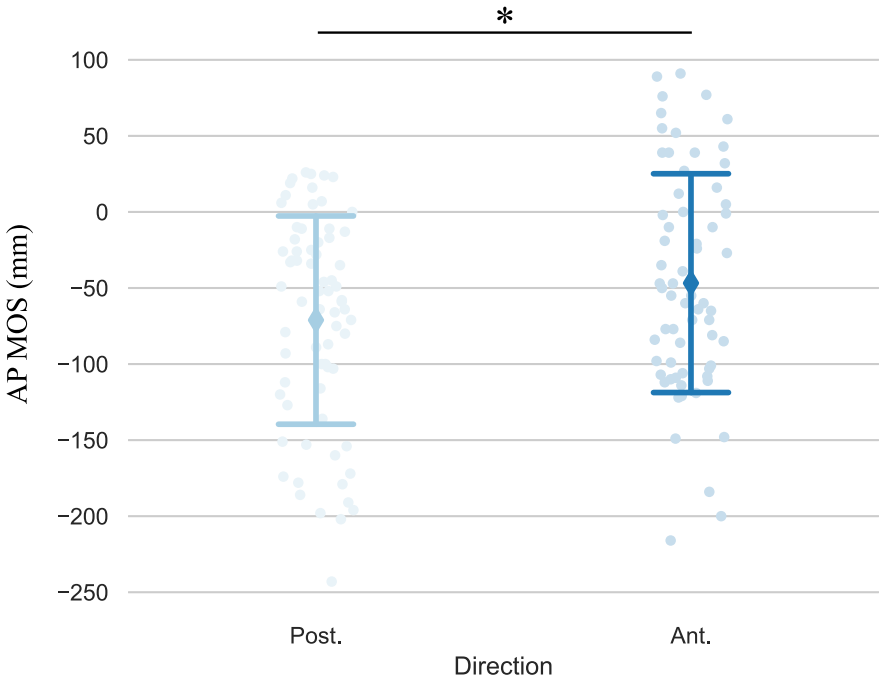

Figure 6.8: Posterior perturbations caused significantly smaller AP MoS compared to anterior perturbations, $F=7.12$, $^*p<0.05$, at Fail Perturbation Intensity.

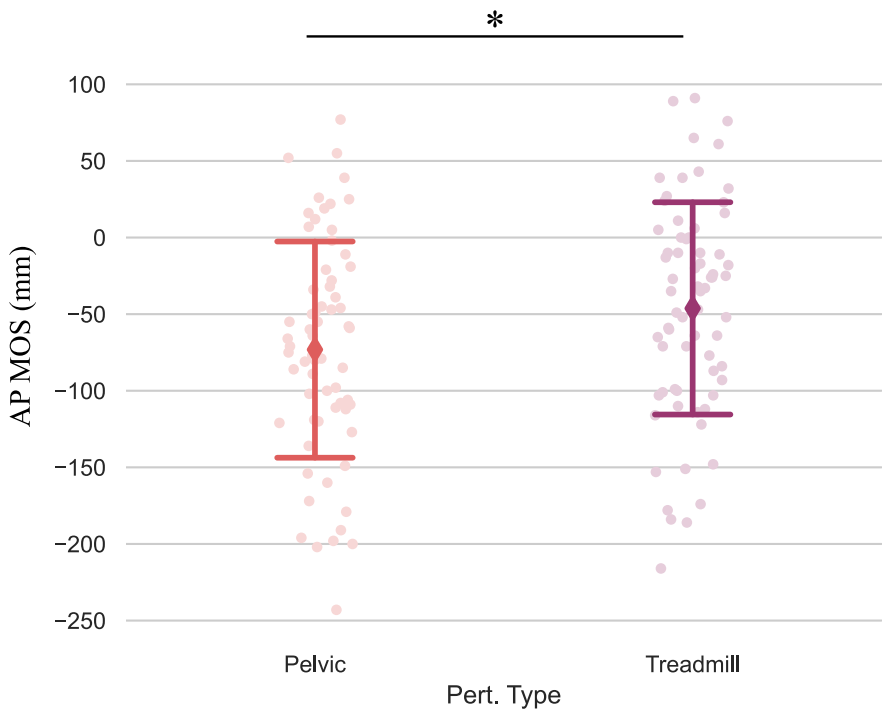

Figure 6.9: Pelvic perturbations caused significantly smaller AP MoS compared to treadmill perturbations, F=8.96, *p<0.01, at Fail Perturbation Intensity.

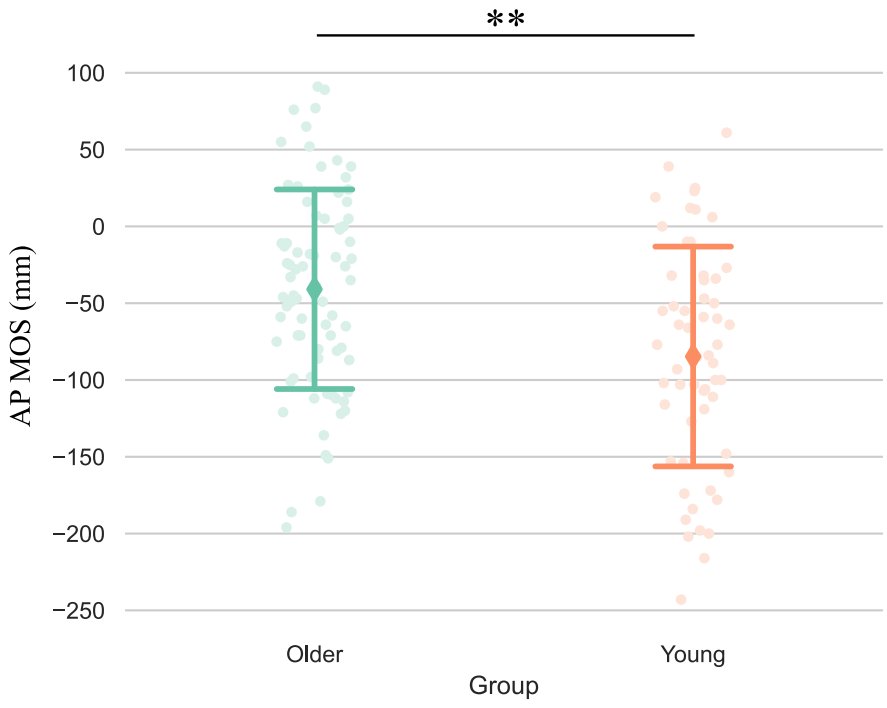

Figure 6.10: Young adults had significantly smaller AP MoS compared to older adults, F=15.76, **p<0.001, at Fail Perturbation.

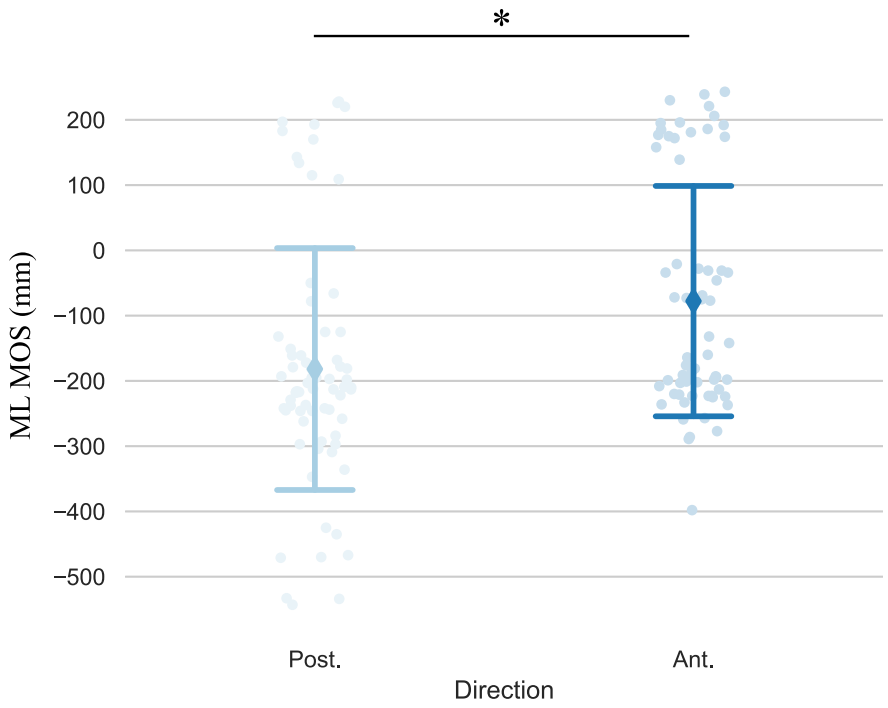

Figure 6.11: The perturbation direction had a main effect on the ML MoS at Fail Perturbation, F=5.5, *p<0.05. Posterior perturbations caused significantly smaller ML MoS compared to anterior perturbations.

6.3.2 Muscle Activity Results

The older adults showed no significant difference in the iEMG muscle responses between the left and right ES, BF, MG, and TA muscles. There was only significant difference between the right and left RF, p<0.05. The remaining muscle results are for participants' dominant side muscle responses.

6.3.2.1 Low Perturbation Intensity

At low perturbation intensity, the muscles that showed significant changes were BF (Fig. 6.12) and MG (Fig.6.13). No interaction effects were observed.

6.3.2.2 Threshold Perturbation Intensity

At participants' threshold perturbation intensity, all five muscles showed significant changes. The MG iEMG had a significant three way interaction between the perturbation type, perturbation

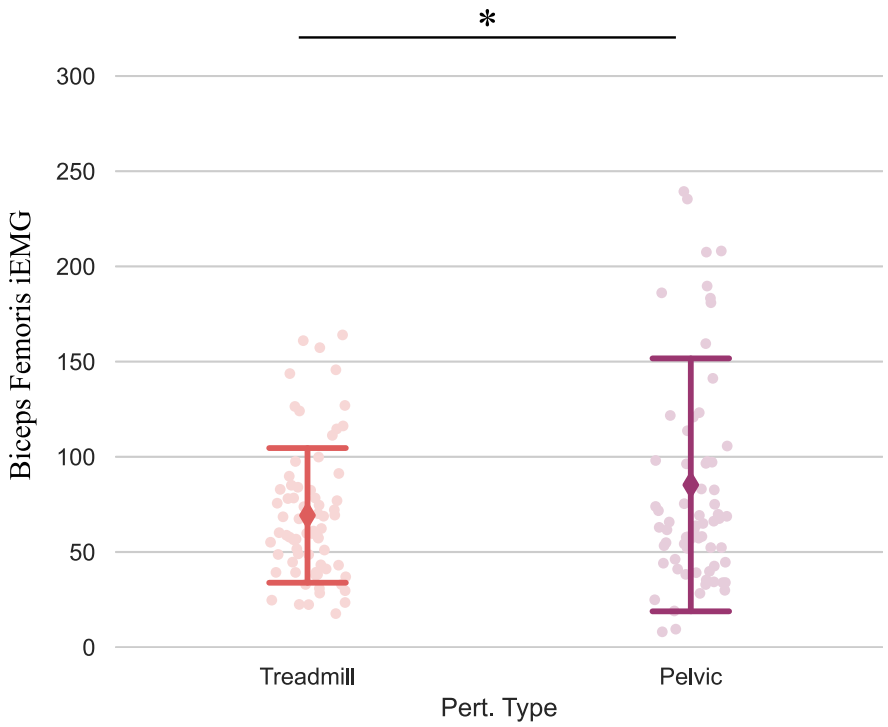

Figure 6.12: Biceps Femoris at Low Perturbation Intensity. Young and older participants had higher BF iEMG in response to pelvic perturbations compared to treadmill perturbations, F=5.21, *p<0.05.

direction and age group, F=5.23, p<0.05, Fig. 6.14.

The lower back ES iEMG results had significant two way interaction between perturbation direction and group F=5.59, p<0.05. The young group displayed higher ES iEMG responses to anterior perturbations compared to posterior perturbation, p<0.01, Fig. 6.15.

The RF iEMG results had significant two way interaction between direction and group, F=6.36, p<0.05. The older group had higher RF iEMG responses to posterior perturbations compared to anterior perturbation, p<0.005. Group averages for RF iEMG are graphed in Fig. 6.16.

The BF iEMG had significant main effect between the age groups, F=4.65, p<0.05. The young group had higher BF iEMG responses compared to the older group. Group averages of BF iEMG are in Fig. 6.17.

The TA iEMG had a significant main effect between the perturbation directions, F=16.62, p<0.001. Participants had higher TA iEMG responses during posterior perturbations compared to anterior perturbations. The TA iEMG results are graphed in Fig.6.18.

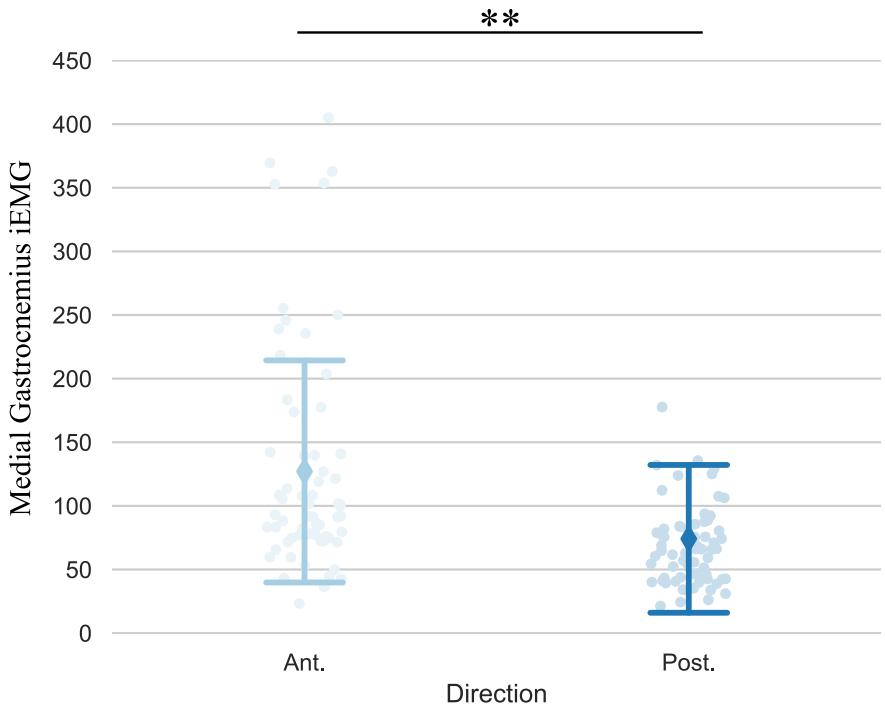

Figure 6.13: Medial Gastrocnemius at Low Perturbation Intensity. Young and older participants had higher MG iEMG responses during anterior perturbations compared to posterior perturbations, F=31, $^{**}p$<0.001.

6.3.2.3 Fail Perturbation Intensity

During the fail perturbation intensity, participants showed significant changes in all five muscles. No interaction effects were observed for either muscle. The perturbation direction had a significant main effect on all five muscles iEMG responses: the ES (Fig. 6.19), the RF (Fig. 6.20), the MG (Fig. 6.21), TA (Fig. 6.22) and BF (Fig. 6.23). Participants BF iEMG results had three significant main effects, perturbation direction (F=7.68, p<0.05), perturbation type (Fig. 6.24, F=5.34, p<0.05) and age group (Fig. 6.25, F=9.33, p<0.01).

6.3.3 Joint Total Excursion Results

6.3.3.1 Low Perturbation Intensity

The trunk TE flexion was significantly effected by two main effects, the age group (Fig. 6.26) and perturbation type (Fig. 6.27). No interaction effects were observed. The left ankle TE had

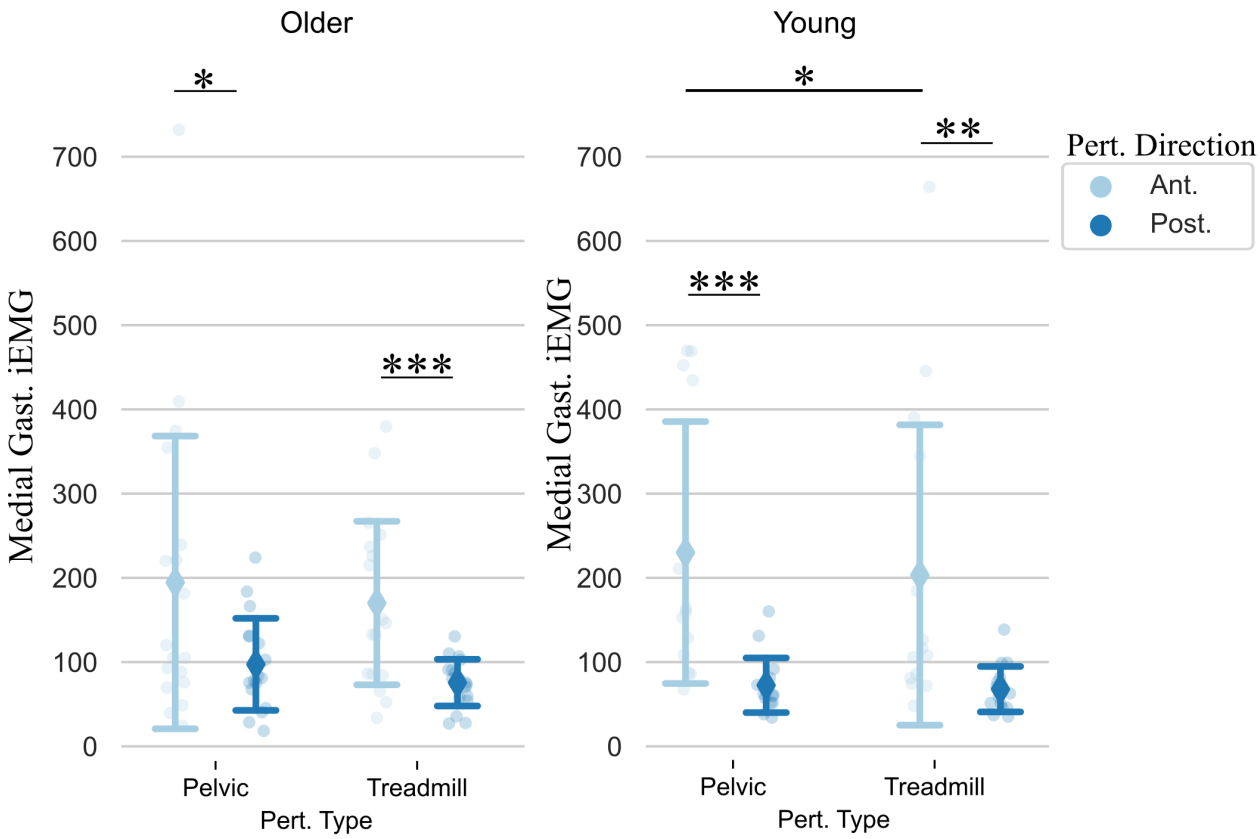

Figure 6.14: Medial Gastrocnemius at Threshold Perturbation Intensity. Young participants displayed higher MG iEMG responses during pelvic anterior perturbations than treadmill anterior perturbations, *p<0.05. Young participants also displayed higher MG iEMG responses during anterior perturbations than posterior perturbations, during both types of perturbations, pelvic and treadmill, ***p<0.001 and **p<0.01 respectively. Older participants also displayed higher MG iEMG responses during anterior perturbations compared to posterior perturbations, in both types of perturbations, pelvic and treadmill, *p<0.05 and ***p<0.001 respectively.

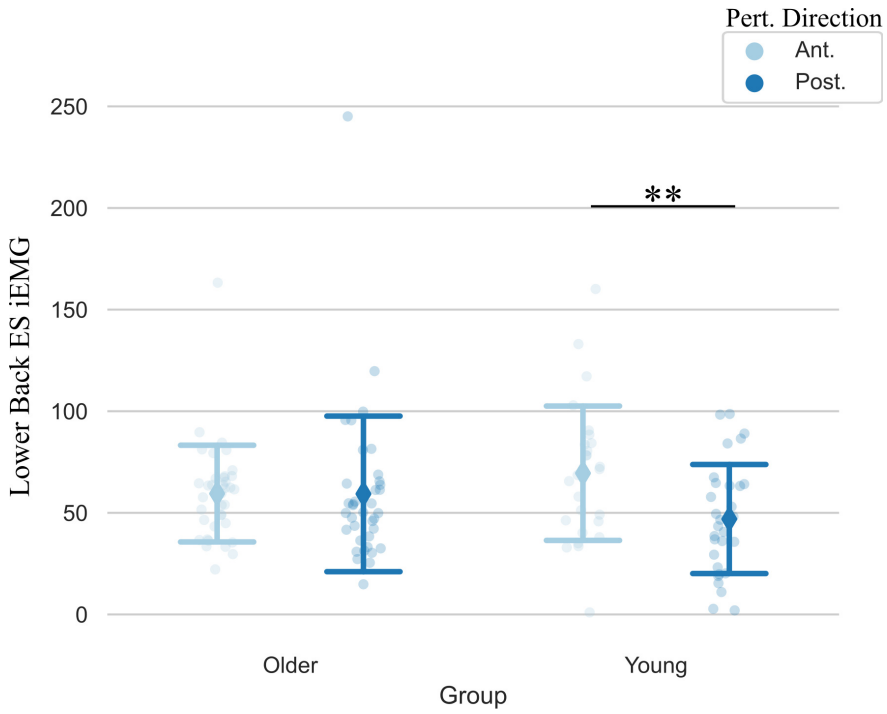

Figure 6.15: The lower back ES iEMG results at Threshold Perturbation Intensity. The young group displayed higher ES iEMG responses to anterior perturbations compared to posterior perturbation, $^{**}p<0.01$.

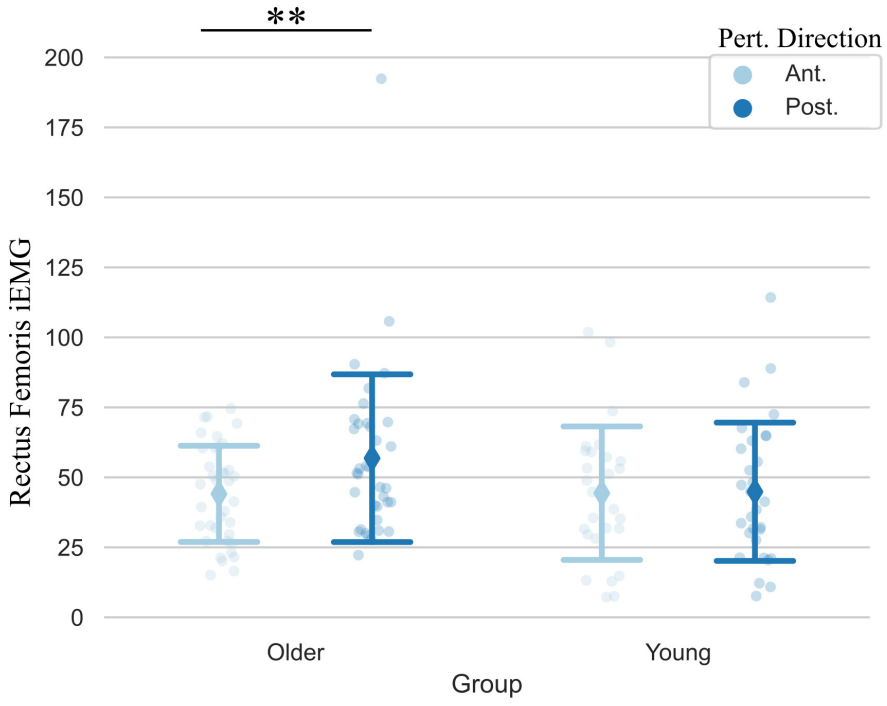

Figure 6.16: The RF iEMG results at Threshold Perturbation Intensity. The older group had higher RF iEMG responses to posterior perturbations compared to anterior perturbation, $^{**}p<0.005$.

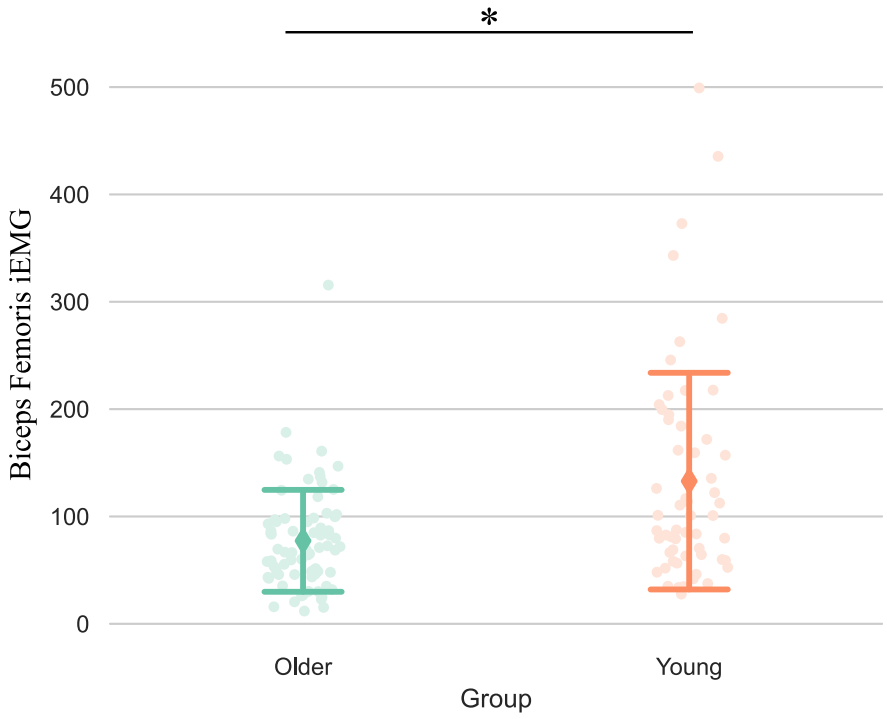

Figure 6.17: The BF iEMG results at Threshold Perturbation Intensity. The young group had higher BF iEMG responses compared to the older group, *p<0.05.

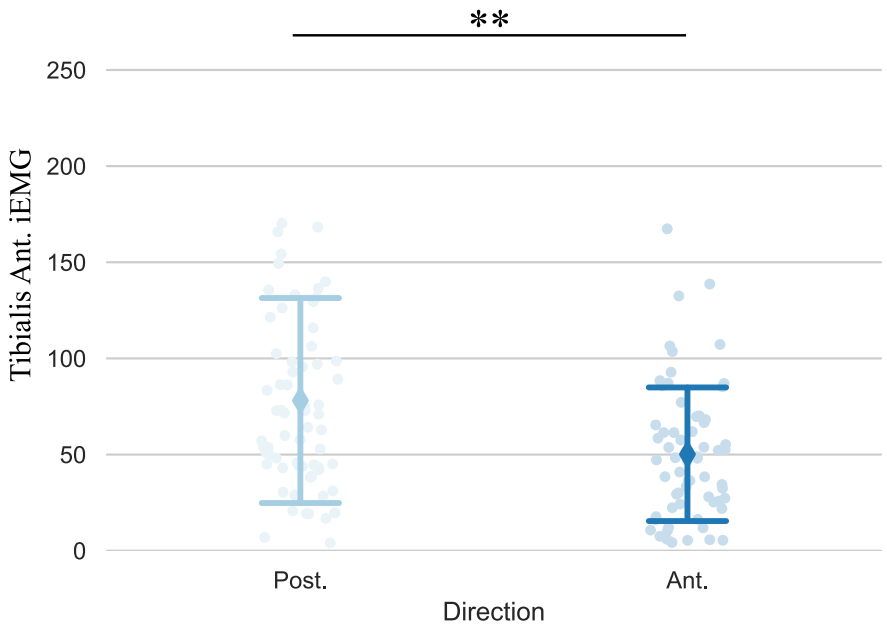

Figure 6.18: The TA iEMG results at Threshold Perturbation Intensity. Participants had higher TA iEMG responses during posterior perturbations compared to anterior perturbations, **p<0.001.

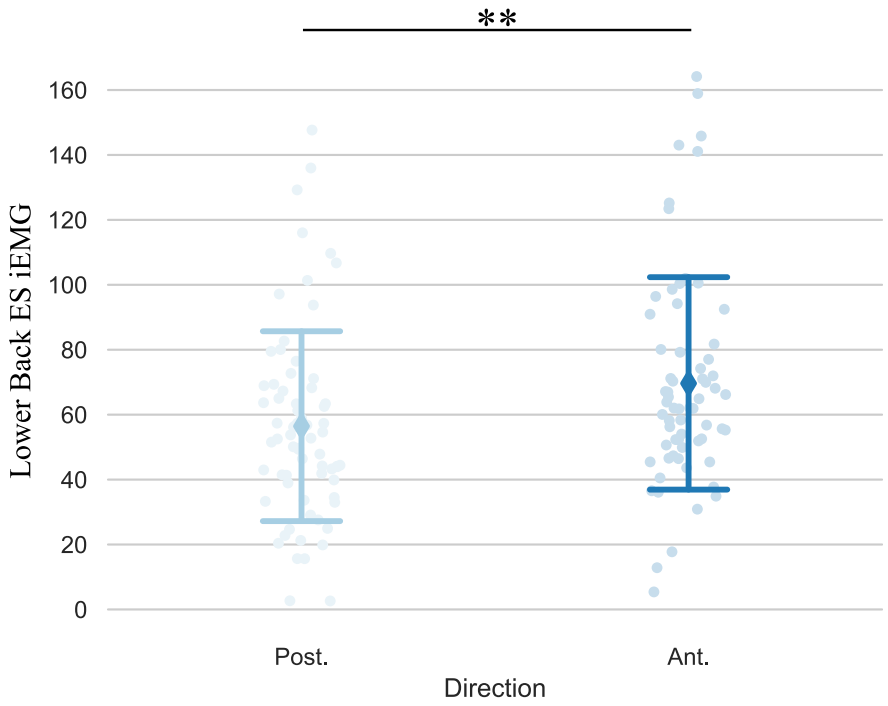

Figure 6.19: The lower back ES iEMG results at Fail Perturbation Intensity. The perturbation direction had a significant main effect on the ES iEMG responses, F=10.6, $^{**}p$<0.005. Participants had higher ES iEMG responses during anterior perturbations compared to posterior perturbation.

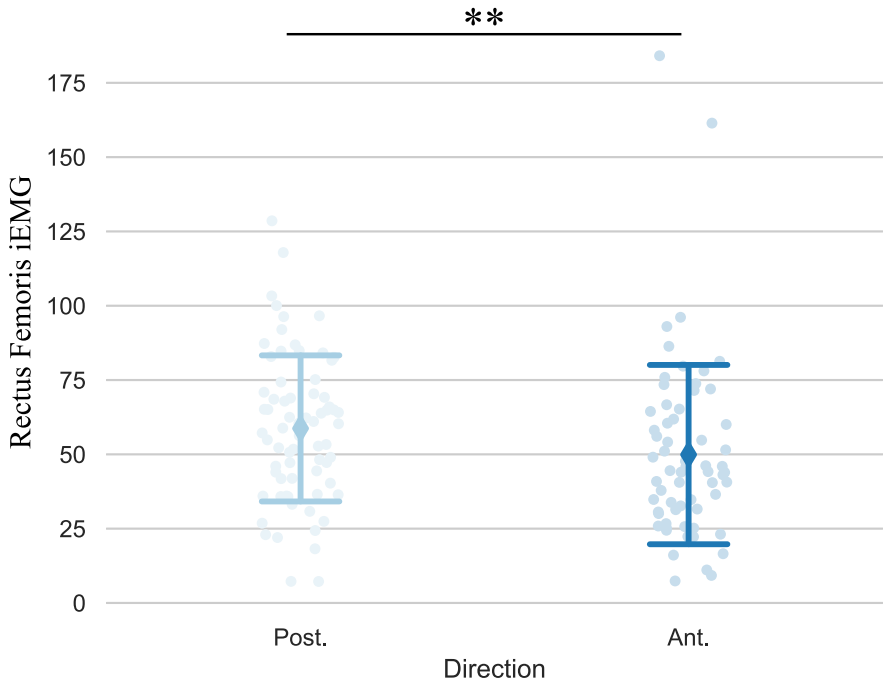

Figure 6.20: The RF iEMG results at Fail Perturbation Intensity. The perturbation direction also had a significant main effect on the RF iEMG responses, F=10.2, $^{**}p$<0.005. Posterior perturbations caused higher RF iEMG compared to anterior perturbations.

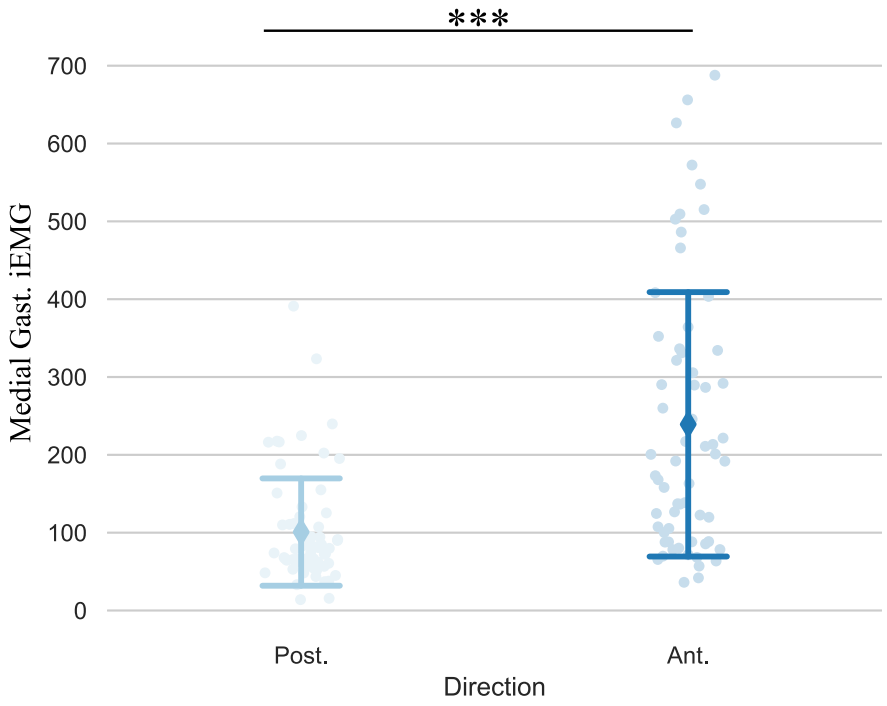

Figure 6.21: Medial Gastrocnemius at Fail Perturbation Intensity. The perturbation direction had a main effect on MG iEMG, F=32.47, ***p<0.001. Anterior perturbations caused greater MG iEMG responses compared to posterior perturbations.

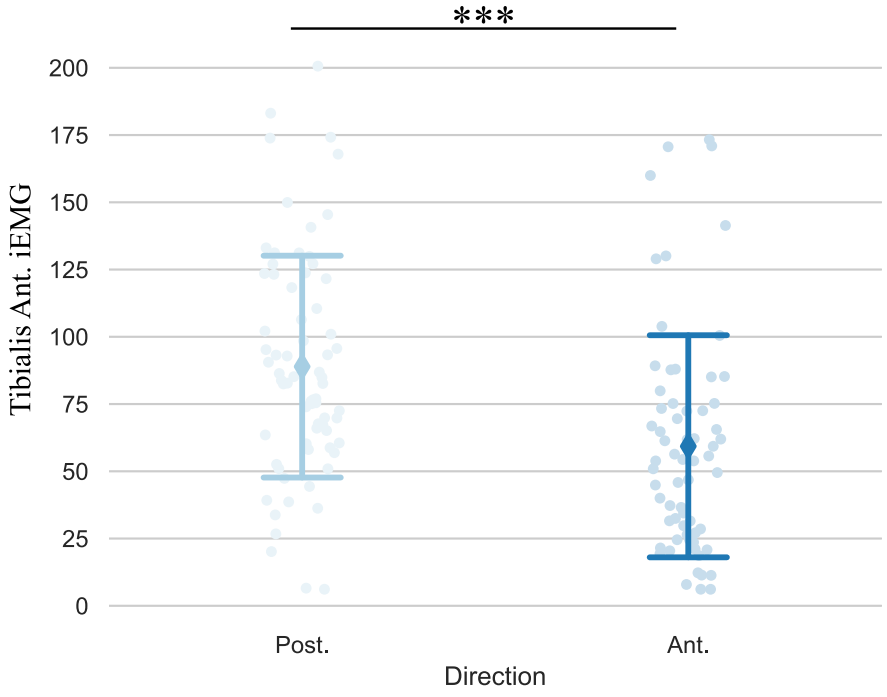

Figure 6.22: The TA iEMG results at Fail Perturbation Intensity. The perturbation direction also had a main effect on TA iEMG results, F=16.52, ***p<0.001. Posterior perturbations caused greater TA iEMG responses in participants compared to anterior perturbations.

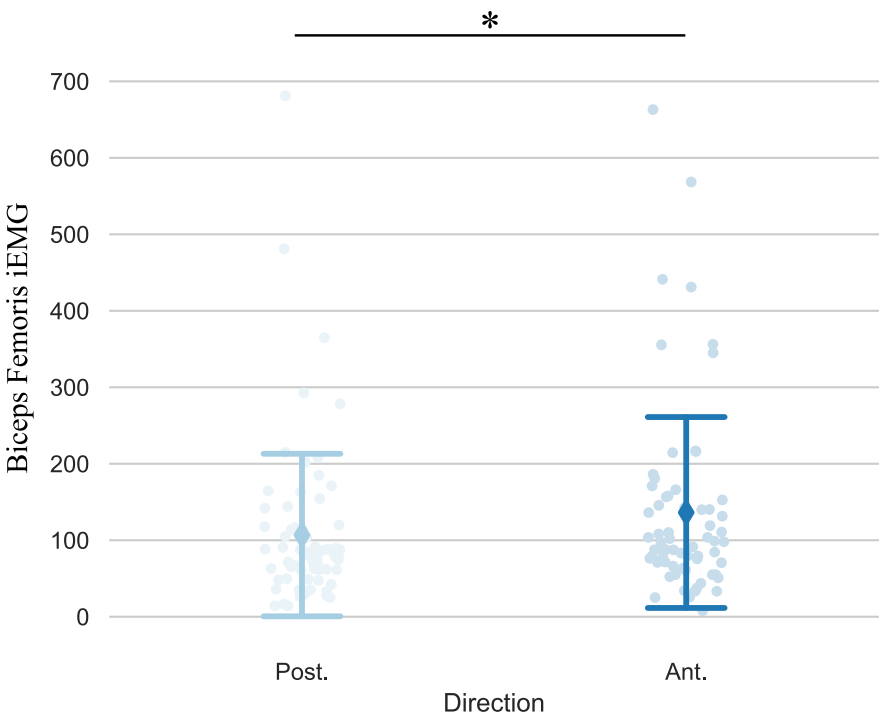

Figure 6.23: BF iEMG Responses at Fail Perturbation Intensity. Participants had higher BF iEMG during anterior perturbations compared to posterior perturbations, (F=7.68, *p<0.05).

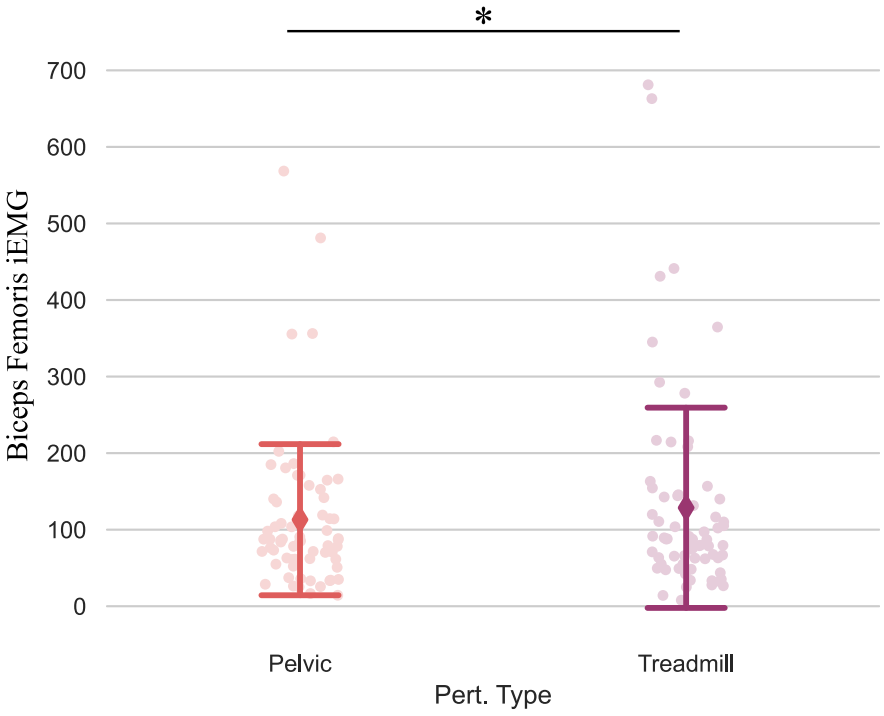

Figure 6.24: BF iEMG Responses at Fail Perturbation Intensity. Treadmill perturbations caused greater BF iEMG reactions compared to pelvic perturbations,(F=5.34, *p<0.05).

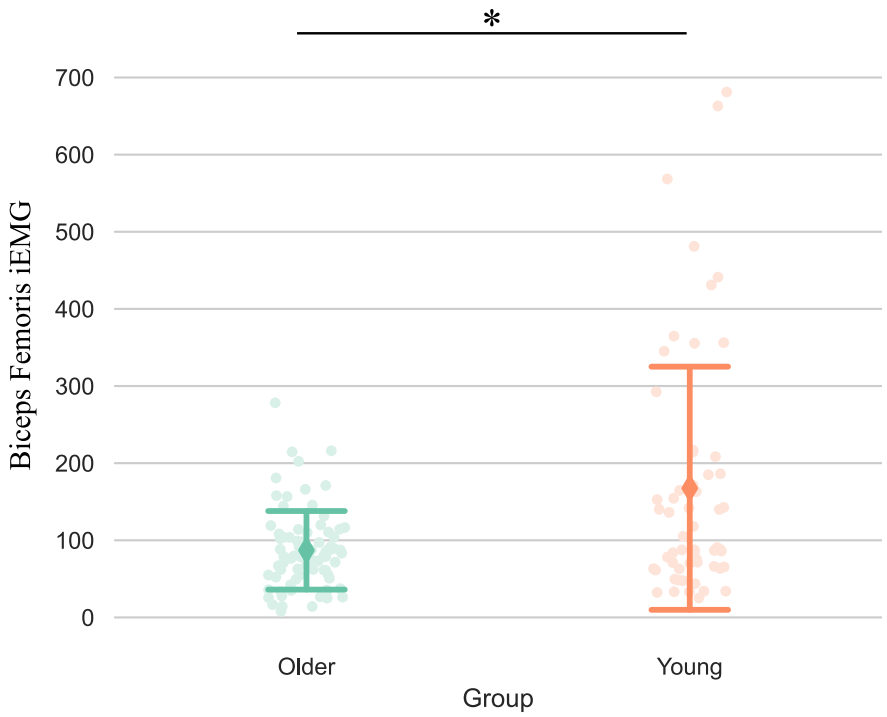

Figure 6.25: BF iEMG Responses at Fail Perturbation Intensity. The young group had higher BF iEMG responses compared to the older group, (F=9.33, *p<0.01).

significant interaction effects between the perturbation type and direction, F=4.42, p<0.05, (Fig. 6.28). The right knee TE had significant main effects. No interaction effects were observed. The right knee TE showed signficiant differences between age groups (Fig. 6.29), and between perturbation types (Fig. 6.30).

6.3.3.2 Threshold Perturbation Intensity

The trunk TE flexion had interaction effects between perturbation type and direction, F=5.16, p<0.05, Fig. 6.31. In addition, trunk TE had interaction effects between perturbation direction and age group, F=10.97 p<0.005, Fig. 6.32. The right ankle had interaction effects between the perturbation type and group, F=7.3, p<0.05, Fig. 6.33. The left ankle TE had two way interaction effects between the perturbation type and direction, F=5.2, p<0.05, Fig. 6.34. The right knee TE displayed two way interaction effects between the perturbation direction and group, F=6.84, p<0.05, Fig. 6.35. The left knee TE also displayed two way interaction effects between the perturbation direction and group, F=6.07, p<0.05, Fig. 6.36. The right hip TE had two way

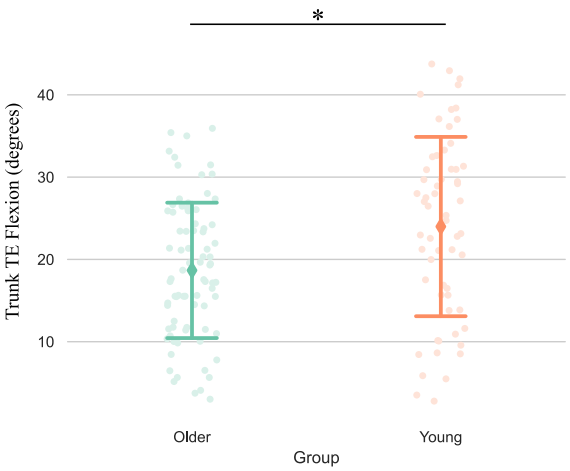

Figure 6.26: The trunk TE flexion was significantly effected by Age Group. Younger adults had higher trunk TE flexion than older adults, F=6.92, *p<0.05.

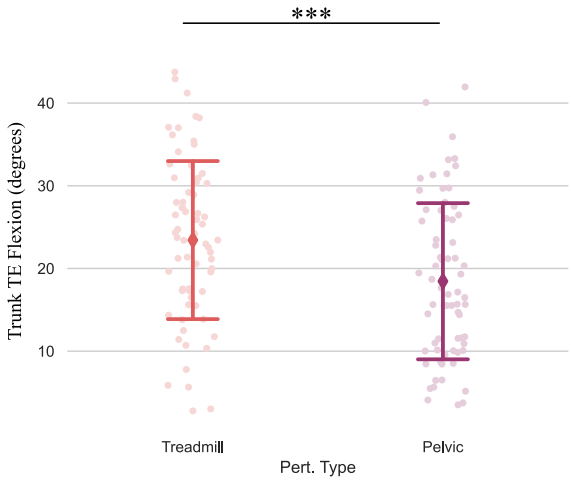

Figure 6.27: The trunk TE flexion was significantly effected by Perturbation Type. Treadmill perturbations caused greater trunk TE than pelvic perturbations, F=14.34, ***p<0.001.

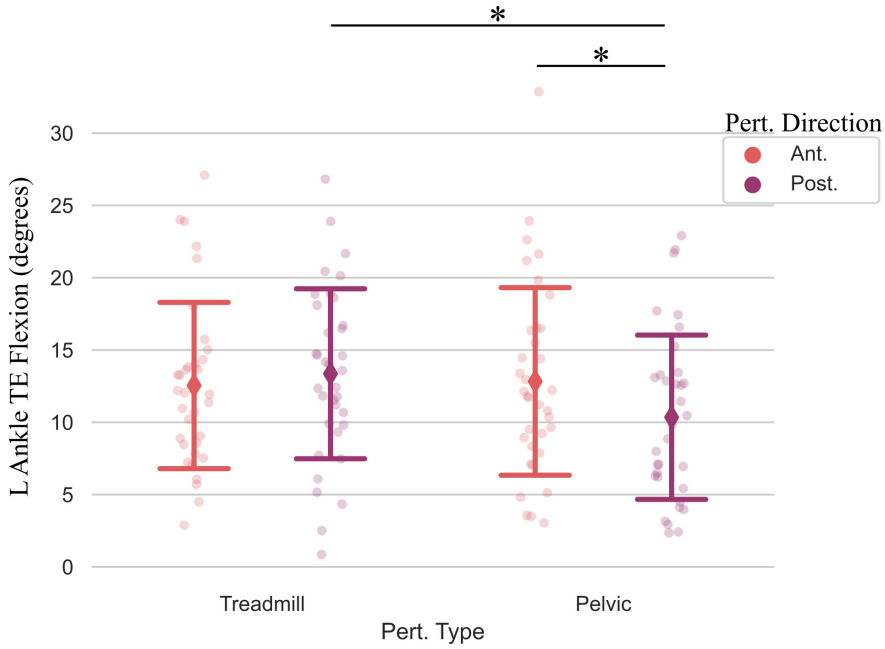

Figure 6.28: The left ankle TE had significant interaction effects at low perturbation intensity. Participants had higher left ankle TE during posterior treadmill perturbation compared to posterior pelvic perturbations, *p<0.05. During pelvic perturbations, participants had higher left ankle TE during anterior direction perturbations compared to posterior perturbations, *p<0.05.

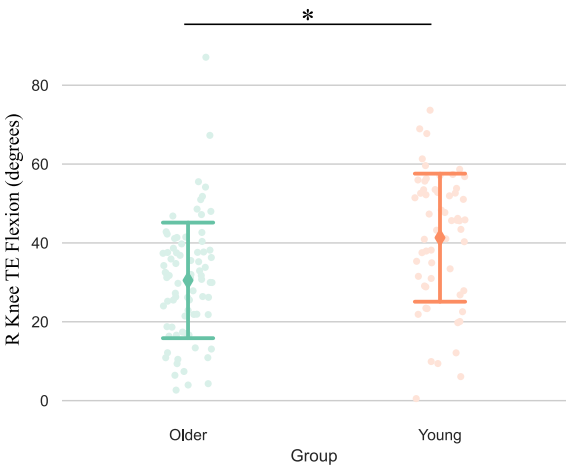

Figure 6.29: The right knee TE flexion was significantly effected by Age Group. Younger adults had higher right knee TE than older adults, F=6.91, *p<0.05.

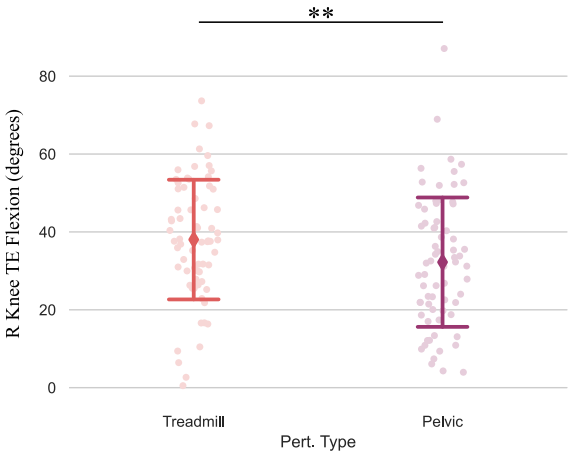

Figure 6.30: The right knee TE flexion was significantly effected by Perturbation Type. Treadmill perturbations caused greater right knee TE than pelvic perturbations, F=10.8, **p<0.005.

interaction effects between the perturbation direction and group, F=4.56, p<0.05, Fig. 6.37.

6.3.3.3 Fail Perturbation Intensity

The trunk TE had two way interaction effects between the perturbation type and direction, F=14.41, p<0.001, Fig. 6.38. The left ankle TE had two main effects, no interaction effects were observed. The age group also had a significant difference on the left ankle TE, F=8.8, p<0.01, Fig. 6.34. The perturbation direction had a significant effect on the left ankle TE, F=11.37, p<0.005, Fig. 6.40. The right knee TE responses had a two way interaction effect between the perturbation type and direction, F=5.92, p<0.05, Fig. 6.41. The left knee TE responses were mainly effected by age group (Fig. 6.42) and perturbation direction (Fig. 6.43), no interaction effects were observed.

6.3.4 Primary Joint Movement

No significant main effects were found in primary or secondary joint movement. This was the case for all three perturbation intensities.

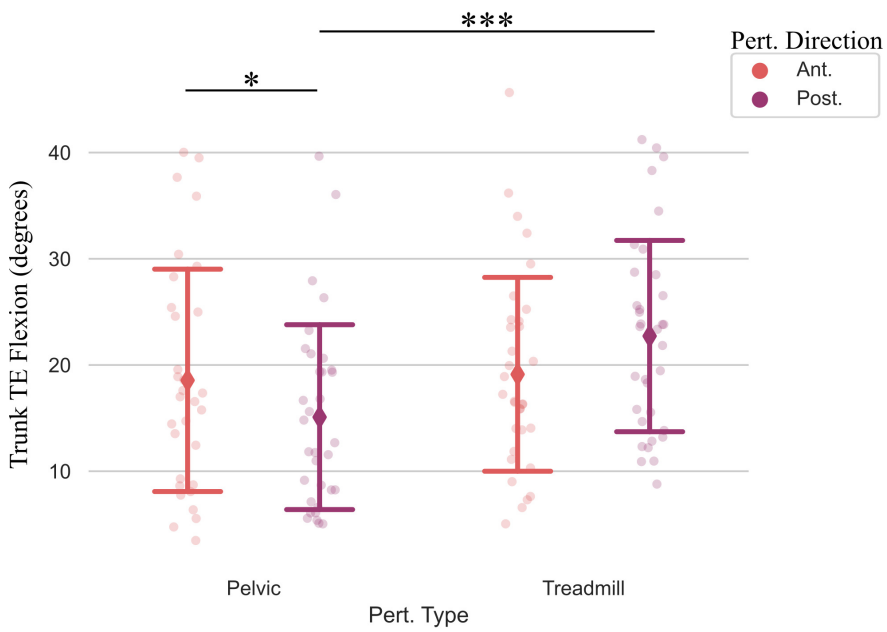

Figure 6.31: The trunk TE flexion had significant interaction effects between the perturbation type and direction at threshold perturbation intensity. Posterior treadmill perturbations caused greater trunk TE than posterior pelvic perturbations, ***p<0.001. During pelvic perturbations, anterior perturbations caused greater trunk TE than posterior perturbations, *p<0.05.

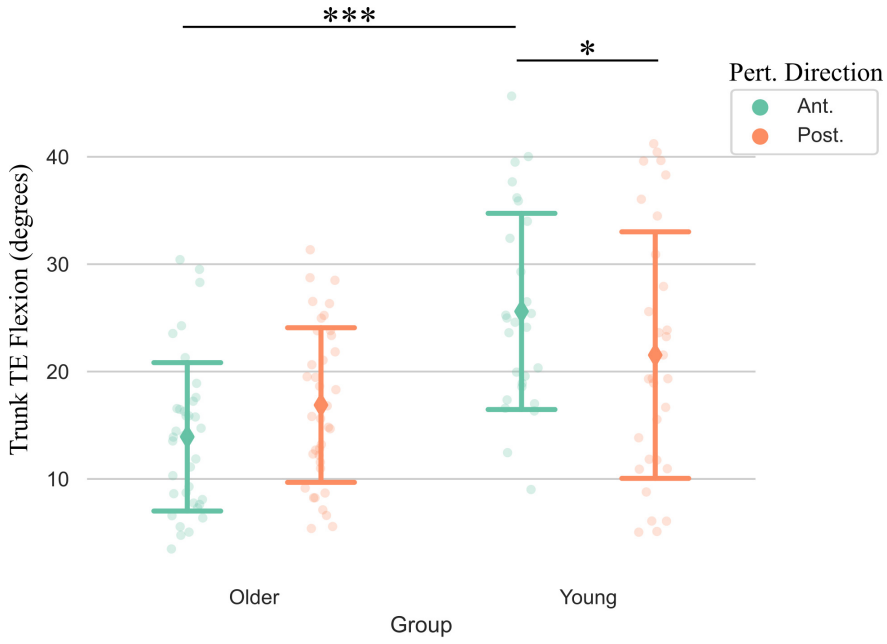

Figure 6.32: The trunk TE flexion had significant interaction effects between the perturbation direction and age group at threshold perturbation intensity. During anterior perturbations, younger adults had higher trunk TE than older adults, ***p<0.001. Young adults also had higher trunk TE during anterior perturbations compared to posterior perturbations, *p<0.05.

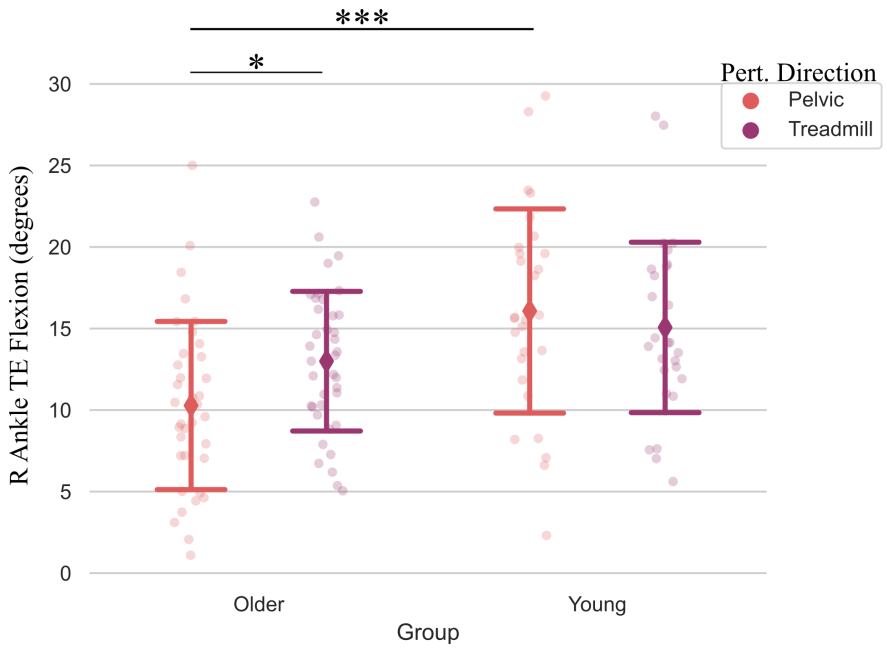

Figure 6.33: The right ankle TE flexion had significant interaction effects between the perturbation type and age group at threshold perturbation intensity. During pelvic perturbations, younger group had higher right ankle TE compared to the older group, ***p<0.001. In addition, the older group had higher right ankle TE during treadmill perturbations compared to pelvic perturbations, *p<0.05.

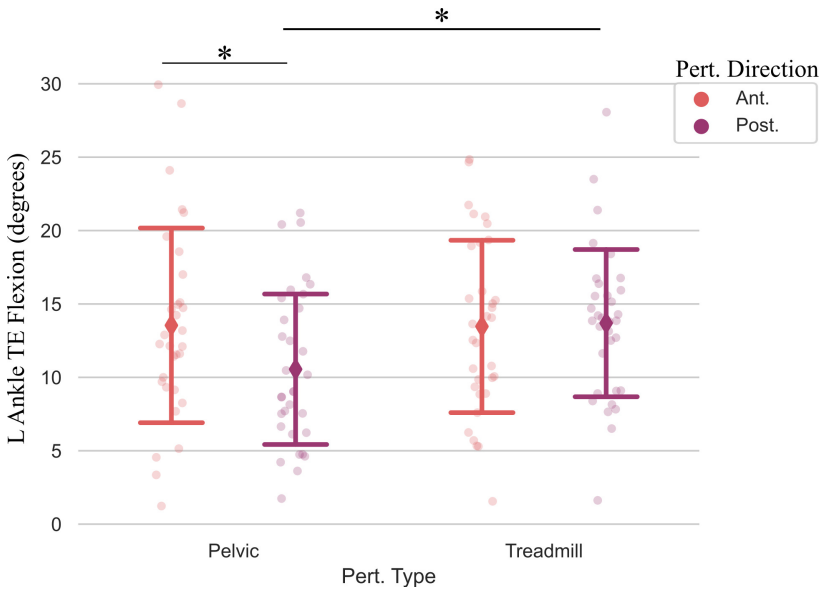

Figure 6.34: The left ankle TE flexion had significant interaction effects between the perturbation type and direction at threshold perturbation intensity. Participants had greater left ankle TE during posterior treadmill perturbations compared to posterior pelvic perturbations, *p<0.05. In terms of pelvic perturbations, participants had greater left ankle TE during pelvic anterior perturbations compared to pelvic posterior perturbations, *p<0.05.

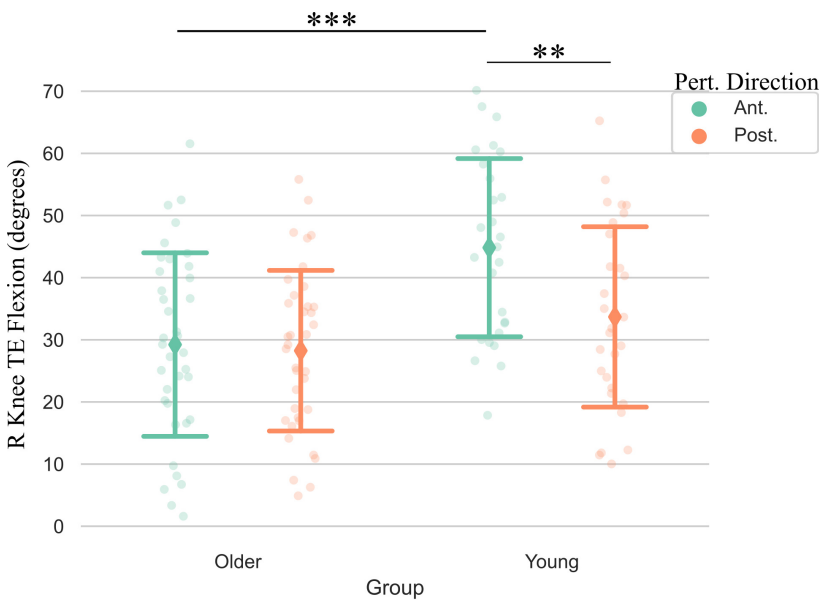

Figure 6.35: The right knee TE flexion had significant interaction effects between the perturbation direction and age group at threshold perturbation intensity. During anterior perturbations, the young group had higher right knee TE compared to the older group, ***p<0.001. In addition, the young group had higher right knee TE during anterior perturbations compared to posterior perturbations, **p<0.005.

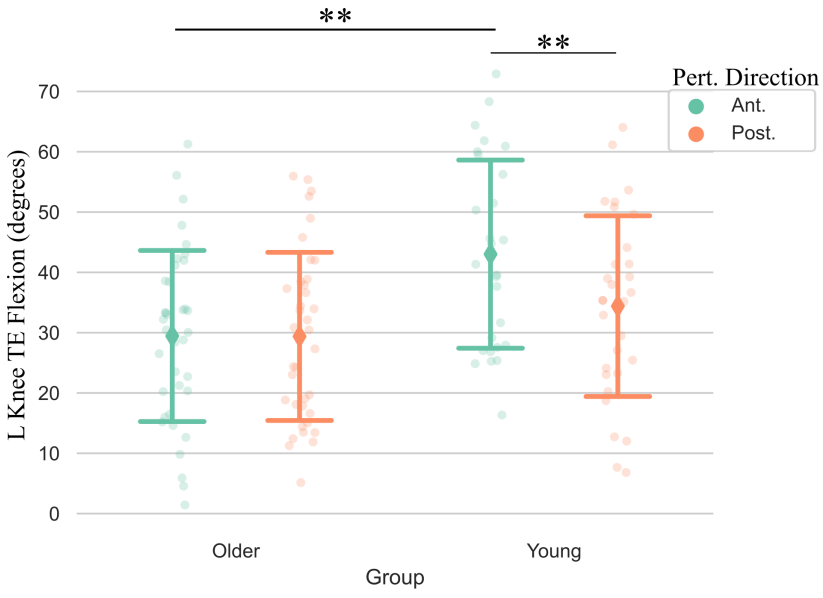

Figure 6.36: The left knee TE flexion had significant interaction effects between the perturbation direction and age group at threshold perturbation intensity. Similar to the right knee TE responses, during anterior perturbations, the young group had higher left knee TE compared to the older group, **p<0.005. The young group had significant higher left knee TE during anterior perturbations compared to posterior perturbations, **p<0.005.

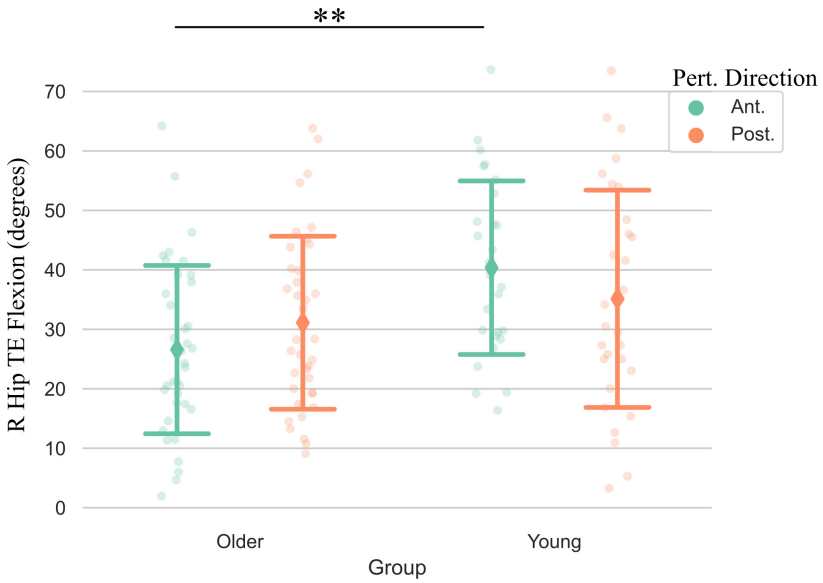

Figure 6.37: The right hip TE flexion had significant interaction effects between the perturbation direction and age group at threshold perturbation intensity. During anterior perturbations, the young group had higher right hip TE compared to the older group, $^{**}p<0.005$.

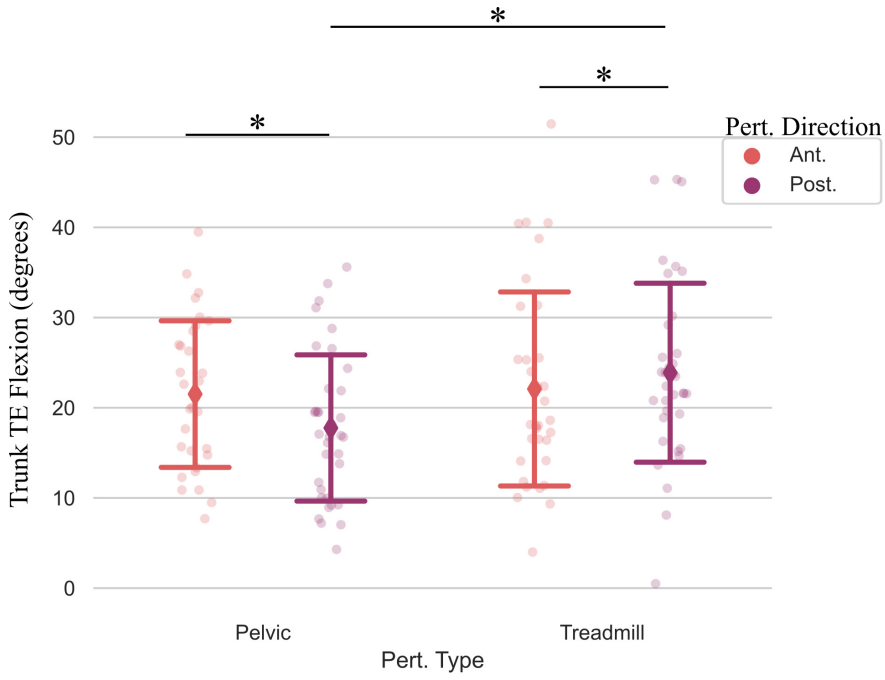

Figure 6.38: The trunk TE flexion had significant interaction effects between the perturbation type and direction at Fail perturbation intensity. During posterior treadmill perturbations, participants had higher trunk TE compared to posterior pelvic perturbations, $^{*}p<0.05$. In terms of pelvic perturbations, participants had higher trunk TE during anterior pelvic perturbations compared to posterior pelvic perturbations, $^{*}p<0.05$. Meanwhile, treadmill posterior perturbations caused greater trunk TE compared to treadmill anterior perturbations, $^{*}p<0.05$.

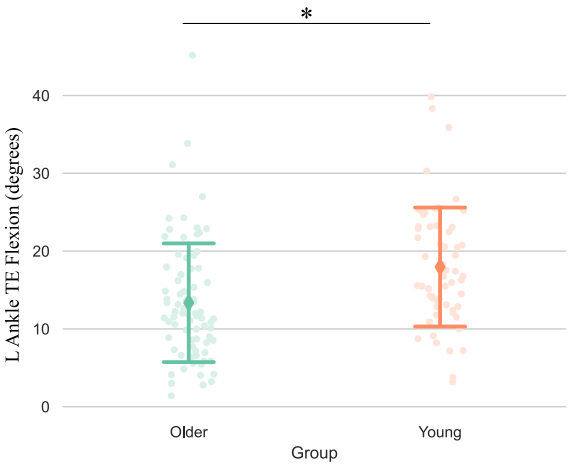

Figure 6.39: The left ankle TE flexion was significantly effected by Age Group at Fail perturbation intensity. The age group also had a significant difference on the left ankle TE, F=8.8, *p<0.01. The young group experienced higher left ankle TE compared to the older group.

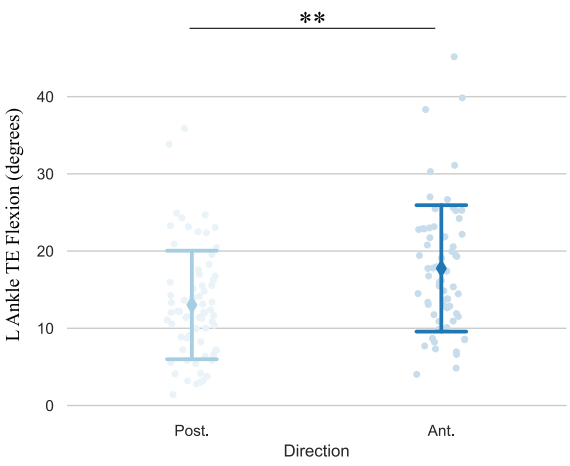

Figure 6.40: The left ankle TE flexion was significantly effected by Perturbation Direction at Fail perturbation intensity. The perturbation direction had a significant effect on the left ankle TE, F=11.37, **p<0.005. Anterior perturbations caused greater left ankle TE compared to posterior perturbations.

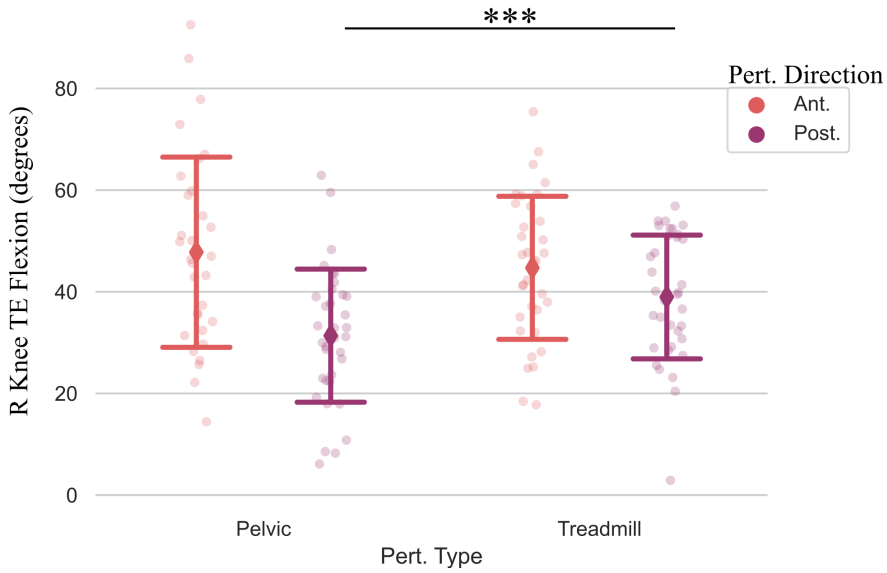

Figure 6.41: The right knee TE flexion had significant interaction effects between the perturbation type and direction at Fail perturbation intensity. Participants experienced higher right knee TE during pelvic anterior perturbations compared to pelvic posterior perturbations, ***p<0.001.

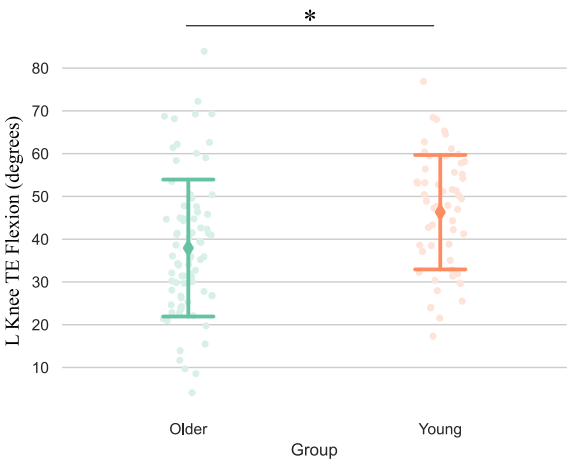

Figure 6.42: The left knee TE flexion was significantly effected by Age Group at Fail perturbation intensity. The young group responded with higher left knee TE compared to the older group, F=6.84, *p<0.05.

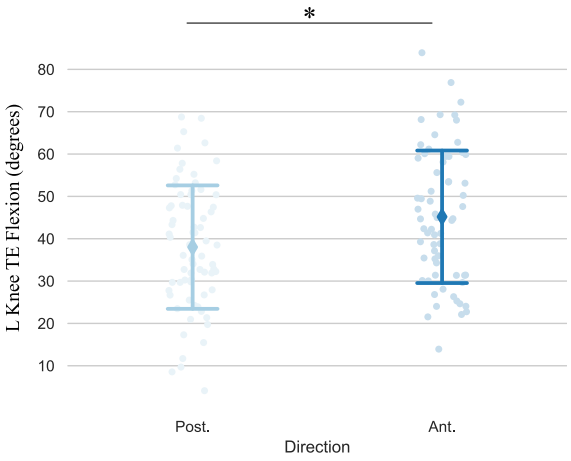

Figure 6.43: The left knee TE flexion was significantly effected by Perturbation Direction at Fail perturbation intensity. Participants had higher left knee TE during anterior perturbations compared to posterior perturbations, F=6.01, *p<0.05.

6.4 Discussion

6.4.1 Young versus Older Group Reactions

The younger group experienced higher joint TE compared to older adults. These results are expected, as a previous study has shown younger adults have higher hip and knee joint flexibility compared to older adults [115]. The higher joint motion also corresponds to the higher XCoM excursion, as identified by the smaller AP and ML margin of stability values. The higher joint movement and lower MoS in the young group is due to their flexibility and their stability confidence in greater areas of their BoS.

Interestingly, at perturbation threshold, the older group had higher MoS values, indicating older participants had a more conservative response. The older group stepped at higher MoS compared to the younger group, prioritizing stability with a *change-in-support* reaction instead of going to their BoS extreme boundaries. Similar to previous standing balance studies, it is documented that participants will elicit a *change-in-support* response before going to their maximum BoS values [106, 116]. The older group may have less confidence in their standing BoS area due to lower joint

flexibility and lower muscle strength. A *change-in-support* strategy can reduce the risk of falls however, *in-place* reactions are also important for regaining balance in situations where there is no external handrail or safe surface to take a step. Therefore, older adults should also be trained to improve their *in-place* responses.

In terms of iEMG muscle activity, the only muscle that was significantly different between the young and older group, was the BF. This was only observed during the perturbation threshold intensity and at the fail perturbation threshold intensity. The younger group showed higher BF muscle activity compared to the older group. The BF facilitates knee flexion and hip extension. The higher BF muscle activity corresponds with the younger group having higher knee and hip excursion compared to the older group. During the perturbation, the younger group utilize their knees and hip more for stability compared to the older group.

6.4.2 Perturbation Direction Effects

The muscle activity responses in both groups are correlated to the perturbation direction. Like witnessed in [113], the perturbation direction effects the muscle activity response. Anterior perturbations cause significant higher activity in posterior muscles to counter the movement of the perturbation direction. Similarly, for posterior perturbations, the higher muscle activity is witnessed in the anterior muscles.

6.4.3 Perturbation Type

Interestingly, the perturbation type had opposing muscle responses. Typically, in standing perturbations, the muscles near the area of the perturbation are more prominent [90]. For platform, like treadmill, perturbations, participants would utilize ankle flexion with TA and MG muscle responses. As for pelvic perturbations, participants would utilize hip and trunk movement, activating RF and BC muscles. In the previous study with healthy young adults, (Chp.5) participants engaged their MG muscles more during pelvic perturbations instead of during treadmill perturbations. In this study we see a similar pattern, the higher muscle activity are further from the perturbation

onsite. For treadmill perturbations at fail intensity, participants had higher BF activity compared to pelvic perturbations.

6.4.4 Study Limitations

The population gathered in this study are all city dwellers that often using a train or bus to commute. Therefore, the findings in this study are based on subjects that may encounter higher perturbations in day to day, from the subway or large crowds.

A limitation in this study, was how the primary and secondary joints utilized were determined. The use of joint TE may not have been sufficient to show participants' reactive response patterns. A further analysis on initial joint flexion or extension timings may provide more insight if there exists a reactive response pattern in participants' joint motion.

The repeated perturbations individuals underwent could have led to muscle fatigue. Although the breaks in between the sets tried to minimize the effects of fatigue, it is still a possibility and, therefore, a study limitation.

Conclusion

Contributions of the Current Work

In this dissertation we present methods to characterize and improve balance and stability in individuals during standing, squatting, and sit-to-stand transitions. This is achieved by utilizing different robotic control strategies in cable-driven systems. Assist-as-needed force control strategies in standing was presented to improve participants standing balance without decreasing their natural body weight loading. RobUST demonstrated potential as a training device since it enhances postural balance without significantly removing muscular control mechanisms that are of interest in re-training postural control strategies in standing.

Constant pelvic forces were utilized to demonstrate how they can redistribute participants' ground reaction force distributions. This was evaluated and achieved during a squat motion. We found that the cable configuration and belt did not increase participants' pelvic motion variability, CV. Additionally, participants significantly increased their vertical ground reaction SI mean from 11.2% to 35.7% and SI peak from 9.9% to 42.7%. These results are promising for future training paradigms to redistribute ground reaction forces and encourage specific weight distribution patterns in individuals who experience asymmetric limb loading, like stroke survivors.

Previous studies have shown that perturbation-based training can improve individuals' reactive control and reduce the risk of falls. However, few studies have investigated individuals' reactive control while transitioning from sit-to-stand. These studies only characterized step responses. Meanwhile, in this dissertation, we present how young and older adults react to sit-to-stand per-

turbations. Their muscular, kinematic, and ground force distribution reactions were analyzed. Patterns distincting the young and older groups were identified. This dissertation has shown that older adults prefer to take a step earlier than younger adults. These results can be utilized in targeting specific reactions in older age groups to reduce the risk of falls, such as encouraging *in-place* strategies that require and promote higher joint flexibility and muscle strength.

Suggestions For Future Work

A proof-of-concept training paradigm was presented in this dissertation with an individual who has spinal cord injury. This study identified the feasibility and future potential of using RobUST and mixed robotic strategies to improve standing postural control. An extension of this work is to perform such training with more individuals that require standing rehabilitation.

The squat exercise with pelvic constant forces can be utilized in future rehabilitation training to improve strength and balance in populations with weakened leg extremities. These results are encouraging for future studies that aim at redistributing participants' weight-bearing. Especially for populations with asymmetrical loading like stroke survivors or adults with ACLr. One can use pelvic forces to induce symmetric loading, promoting greater stability and less risk of falls. The squat motion can be adapted to modified squats or sit-to-stands depending on the rehabilitation goal.

In the sit-to-stand perturbation studies, we used a robotic system TPAD to characterize young and older adults' postural responses. Sit-to-stand perturbation results are encouraging as a potential for rehabilitation. A perturbation-based sit-to-stand training could promote greater muscle activity while requiring reactive coordination. Depending on the individual's therapeutic need, a sit-to-stand perturbation paradigm could regulate the perturbation intensity to target specific postural strategies during either in-place or change-in-support reactions.

References

[1] S. J. Harkema, C. K. Ferreira, R. J. van den Brand, and A. V. Krassioukov, "Improvements in orthostatic instability with stand locomotor training in individuals with spinal cord injury," *Journal of neurotrauma*, vol. 25, no. 12, pp. 1467–1475, 2008.

[2] M. Khan, T. Luna, V. Santamaria, I. Omofuma, D. Martelli, E. Rejc, J. Stein, S. Harkema, and S. Agrawal, "Stand trainer with applied forces at the pelvis and trunk: Response to perturbations and assist-as-needed support," *IEEE Transactions on Neural Systems and Rehabilitation Engineering*, vol. 27, no. 9, pp. 1855–1864, 2019.

[3] Y. Ivanenko and V. S. Gurfinkel, "Human postural control," *Frontiers in neuroscience*, vol. 12, p. 171, 2018.

[4] T. D. Luna, V. Santamaria, I. Omofuma, M. I. Khan, and S. K. Agrawal, "Postural control strategies in standing with handrail support and active assistance from robotic upright stand trainer (robust)," *IEEE Transactions on Neural Systems and Rehabilitation Engineering*, vol. 29, pp. 1424–1431, 2021.

[5] V Santamaria, T. Luna, and S. Agrawal, "Feasibility and tolerance of a robotic postural training to improve standing in a person with ambulatory spinal cord injury," *Spinal Cord Series and Cases*, vol. 7, no. 1, pp. 1–9, 2021.

[6] L. Z. Chiu and E. Burkhardt, "A teaching progression for squatting exercises," *Strength & Conditioning Journal*, vol. 33, no. 2, pp. 46–54, 2011.

[7] O. Pyoria, P. Era, and U. Talvitie, "Relationships between standing balance and symmetry measurements in patients following recent strokes (3 weeks) or older strokes (6 months)," *Physical therapy*, vol. 84, no. 2, pp. 128–136, 2004.

[8] P.-T. Cheng, S.-H. Wu, M.-Y. Liaw, A. M. Wong, and F.-T. Tang, "Symmetrical body-weight distribution training in stroke patients and its effect on fall prevention," *Archives of physical medicine and rehabilitation*, vol. 82, no. 12, pp. 1650–1654, 2001.

[9] V. Vashista, M. Khan, and S. K. Agrawal, "A novel approach to apply gait synchronized external forces on the pelvis using a-tpad to reduce walking effort," *IEEE robotics and automation letters*, vol. 1, no. 2, pp. 1118–1124, 2016.

[10] J. Kang, V. Vashista, and S. K. Agrawal, "On the adaptation of pelvic motion by applying 3-dimensional guidance forces using tpad," *IEEE Transactions on Neural Systems and Rehabilitation Engineering*, vol. 25, no. 9, pp. 1558–1567, 2017.

[11] D. Martelli, F. Aprigliano, P. Tropea, G. Pasquini, S. Micera, and V. Monaco, "Stability against backward balance loss: Age-related modifications following slip-like perturbations of multiple amplitudes," *Gait & posture*, vol. 53, pp. 207–214, 2017.

[12] P.-T. Cheng, M.-Y. Liaw, M.-K. Wong, F.-T. Tang, M.-Y. Lee, and P.-S. Lin, "The sit-to-stand movement in stroke patients and its correlation with falling," *Archives of physical medicine and rehabilitation*, vol. 79, no. 9, pp. 1043–1046, 1998.

[13] Y.-C. Pai, T. Bhatt, F. Yang, E. Wang, and S. Kritchevsky, "Perturbation training can reduce community-dwelling older adults' annual fall risk: A randomized controlled trial," *Journals of Gerontology Series A: Biomedical Sciences and Medical Sciences*, vol. 69, no. 12, pp. 1586–1594, 2014.

[14] S. K. Mustafa and S. K. Agrawal, "On the force-closure analysis of n-dof cable-driven open chains based on reciprocal screw theory," *IEEE Transactions on Robotics*, vol. 28, no. 1, pp. 22–31, 2011.

[15] V. Vashista, X. Jin, and S. K. Agrawal, "Active tethered pelvic assist device (a-tpad) to study force adaptation in human walking," in *2014 IEEE International Conference on Robotics and Automation (ICRA)*, 2014, pp. 718–723.

[16] A. Pott, T. Bruckmann, and L. Mikelsons, "Closed-form force distribution for parallel wire robots," in *Proceedings of the 5th International Workshop on Computational Kinematics*, Kluwer Academic Publishers, 2009, pp. 25–34, ISBN: 9783642019463.

[17] Alexis Fortin Cote, Philippe Cardou, and Clement Gosselin, "A Tension Distribution Algorithm for Cable-Driven Parallel Robots Operating Beyond their Wrench-Feasible Workspace," in *International Conference on Control, Automation and Systems*, 2016.

[18] M. I. Khan, V. Santamaria, J. Kang, B. M. Bradley, J. P. Dutkowsky, A. M. Gordon, and S. K. Agrawal, "Enhancing seated stability using trunk support trainer (trust)," *IEEE Robotics and Automation Letters*, vol. 2, no. 3, pp. 1609–1616, 2017.

[19] V. Santamaria, T. Luna, M. Khan, and S. Agrawal, "The robotic trunk-support-trainer (trust) to measure and increase postural workspace during sitting in people with spinal cord injury," *Spinal cord series and cases*, vol. 6, no. 1, pp. 1–7, 2020.

[20] D. A. Winter, *Biomechanics and motor control of human movement*. John Wiley & Sons, 2009.

[21] R. Park, H Tsao, A. Cresswell, and P. Hodges, "Anticipatory postural activity of the deep trunk muscles differs between anatomical regions based on their mechanical advantage," *Neuroscience*, vol. 261, pp. 161–172, 2014.

[22] A. Shumway-Cook and M. H. Woollacott, *Motor control: Translating research into clinical practice: Fourth edition*. 2014, ISBN: 9781469892610.

[23] F. B. Horak, J. Kluzik, and F. Hlavacka, "Velocity dependence of vestibular information for postural control on tilting surfaces," *Journal of neurophysiology*, vol. 116, no. 3, pp. 1468–1479, 2016.

[24] B. E. Maki, W. E. Mcilroy, and G. R. Fernie, "Change-in-support reactions for balance recovery," *IEEE Engineering in Medicine and Biology Magazine*, vol. 22, no. 2, pp. 20–26, 2003.

[25] Y. Okubo, D. Schoene, and S. R. Lord, "Step training improves reaction time, gait and balance and reduces falls in older people: A systematic review and meta-analysis," *British journal of sports medicine*, vol. 51, no. 7, pp. 586–593, 2017.

[26] A. Mansfield, A. L. Peters, B. A. Liu, and B. E. Maki, "Effect of a Perturbation-Based Balance Training Program on Compensatory Stepping and Grasping Reactions in Older Adults: A Randomized Controlled Trial," *Physical Therapy*, vol. 90, no. 4, pp. 476–491, Apr. 2010.

[27] J. Kang, V. Vashista, and S. K. Agrawal, "A novel assist-as-needed control method to guide pelvic trajectory for gait rehabilitation," in *2015 IEEE International Conference on Rehabilitation Robotics (ICORR)*, IEEE, 2015, pp. 630–635.

[28] G. Wu and P. R. Cavanagh, "Isb recommendations for standardization in the reporting of kinematic data," *Journal of biomechanics*, vol. 28, no. 10, pp. 1257–1261, 1995.

[29] A. C. Geurts, B. Nienhuis, and T. Mulder, "Intrasubject variability of selected force-platform parameters in the quantification of postural control," *Archives of physical medicine and rehabilitation*, vol. 74, no. 11, pp. 1144–1150, 1993.

[30] A. Ruhe, R. Fejer, and B. Walker, "The test–retest reliability of centre of pressure measures in bipedal static task conditions–a systematic review of the literature," *Gait & posture*, vol. 32, no. 4, pp. 436–445, 2010.

[31] R. M. Palmieri, C. D. Ingersoll, M. B. Stone, and B. A. Krause, "Center-of-pressure parameters used in the assessment of postural control," *Journal of Sport Rehabilitation*, vol. 11, no. 1, pp. 51–66, 2002.

[32] B. E. Maki, P. J. Holliday, and A. K. Topper, "A prospective study of postural balance and risk of falling in an ambulatory and independent elderly population," *Journal of gerontology*, vol. 49, no. 2, pp. M72–M84, 1994.

[33] A. S. Aruin and M. L. Latash, "The role of motor action in anticipatory postural adjustments studied with self-induced and externally triggered perturbations," *Experimental brain research*, vol. 106, no. 2, pp. 291–300, 1995.

[34] G. A. Ballinger, "Using generalized estimating equations for longitudinal data analysis," *Organizational research methods*, vol. 7, no. 2, pp. 127–150, 2004.

[35] F. Horak, L. Nashner, and H. Diener, "Postural strategies associated with somatosensory and vestibular loss," *Experimental brain research*, vol. 82, no. 1, pp. 167–177, 1990.

[36] L. Olivetti, K. Schurr, C. Sherrington, G. Wallbank, P. Pamphlett, M. Mun-San Kwan, and R. D. Herbert, "A novel weight-bearing strengthening program during rehabilitation of older people is feasible and improves standing up more than a non-weight-bearing strengthening program: A randomised trial," *Australian Journal of Physiotherapy*, vol. 53, no. 3, pp. 147–153, 2007.

[37] M. Bahramizadeh, M. E. Mousavi, M. Rassafiani, G. Aminian, I. Ebrahimi, M. Karimlou, and G. O. Toole, "The effect of floor reaction ankle foot orthosis on postural control in children with spastic cerebral palsy," *Prosthetics and orthotics international*, vol. 36, no. 1, pp. 71–76, 2012.

[38] C. Runge, "Shupert cl, horak fb, zajac fe," *Ankle and hip postural strategies defined by joint torques. Gait Posture*, vol. 10, pp. 161–170, 1999.

[39] L. M. Hall, S. Brauer, F. Horak, and P. W. Hodges, "Adaptive changes in anticipatory postural adjustments with novel and familiar postural supports," *Journal of neurophysiology*, vol. 103, no. 2, pp. 968–976, 2010.

[40] J. Allum and C. Pfaltz, "Visual and vestibular contributions to pitch sway stabilization in the ankle muscles of normals and patients with bilateral peripheral vestibular deficits," *Experimental Brain Research*, vol. 58, no. 1, pp. 82–94, 1985.

[41] H. Diener, J Dichgans, W Bruzek, and H Selinka, "Stabilization of human posture during induced oscillations of the body," *Experimental Brain Research*, vol. 45, no. 1-2, pp. 126–132, 1982.

[42] F. B. Horak, "Postural orientation and equilibrium: What do we need to know about neural control of balance to prevent falls?" In *Age and Ageing*, 2006.

[43] F. B. Horak and L. M. Nashner, "Central programming of postural movements: Adaptation to altered support-surface configurations," *Journal of neurophysiology*, vol. 55, no. 6, pp. 1369–1381, 1986.

[44] D. L. Sturnieks, J. Menant, K. Delbaere, J. Vanrenterghem, M. W. Rogers, R. C. Fitzpatrick, and S. R. Lord, "Force-controlled balance perturbations associated with falls in older people: A prospective cohort study," *PloS one*, vol. 8, no. 8, e70981, 2013.

[45] S. Henry, J Fung, and F. Horak, "Emg responses to multidirectional surface translations," in *Soc Neurosci Abstr*, vol. 21, 1995, p. 683.

[46] S. Phonthee, J. Saengsuwan, W. Siritaratiwat, and S. Amatachaya, "Incidence and factors associated with falls in independent ambulatory individuals with spinal cord injury: A 6-month prospective study," *Physical therapy*, vol. 93, no. 8, pp. 1061–1072, 2013.

[47] A. Kotecha, A. R. Webster, G. Wright, M. Michaelides, and G. S. Rubin, "Standing balance stability and the effects of light touch in adults with profound loss of vision—an exploratory study," *Investigative ophthalmology & visual science*, vol. 57, no. 11, pp. 5053–5059, 2016.

[48] V. Komisar, K. Nirmalanathan, E. C. King, B. E. Maki, and A. C. Novak, "Use of handrails for balance and stability: Characterizing loading profiles in younger adults," *Applied ergonomics*, vol. 76, pp. 20–31, 2019.

[49] S. Baudry and J. Duchateau, "Independent modulation of corticospinal and group i afferents pathways during upright standing," *Neuroscience*, vol. 275, pp. 162–169, 2014.

[50] S. Sivakumaran, A. Schinkel-Ivy, K. Masani, and A. Mansfield, "Relationship between margin of stability and deviations in spatiotemporal gait features in healthy young adults," *Human movement science*, vol. 57, pp. 366–373, 2018.

[51] J. Lemay and S Nadeau, "Standing balance assessment in asia d paraplegic and tetraplegic participants: Concurrent validity of the berg balance scale," *Spinal cord*, vol. 48, no. 3, pp. 245–250, 2010.

[52] M Moynahan, "Postural responses during standing in subjects with spinal-cord injury," *Gait & Posture*, vol. 3, no. 3, pp. 156–165, 1995.

[53] T. D. Luna, V. Santamaria, I. Omofuma, M. I. Khan, and S. K. Agrawal, "Postural Control Strategies in Standing with Handrail Support and Active Assistance from Robotic Upright Stand Trainer (RobUST)," *IEEE Transactions on Neural Systems and Rehabilitation Engineering*, vol. 29, pp. 1424–1431, 2021.

[54] S.-H. Kim, O.-Y. Kwon, K.-N. Park, I.-C. Jeon, and J.-H. Weon, "Lower Extremity Strength and the Range of Motion in Relation to Squat Depth," *Journal of Human Kinetics*, vol. 45, no. 1, pp. 59–69, Mar. 2015.

[55] Y. Jeon, M. Shin, C. Kim, B.-J. Lee, S. Kim, D. Chae, J.-H. Park, Y. So, H. Park, C. Lee, B. Kim, J. Chang, Y. Shin, and I. Kim, "Effect of Squat Exercises on Lung Function in

Elderly Women with Sarcopenia," *Journal of Clinical Medicine*, vol. 7, no. 7, p. 167, Jul. 2018.

[56] B. J. Schoenfeld, "Squatting kinematics and kinetics and their application to exercise performance," *The Journal of Strength & Conditioning Research*, vol. 24, no. 12, pp. 3497–3506, 2010.

[57] N. Wirtz, C. Zinner, U. Doermann, H. Kleinoeder, and J. Mester, "Effects of Loaded Squat Exercise with and without Application of Superimposed EMS on Physical Performance.," *Journal of sports science & medicine*, vol. 15, no. 1, pp. 26–33, Mar. 2016.

[58] J.-E. Song, H.-S. Choi, and W.-S. Shin, "Effect of applying resistance in various directions on lower extremity muscle activity and balance during squat exercise," *Physical Therapy Rehabilitation Science*, vol. 8, no. 2, pp. 61–66, Jun. 2019.

[59] D. Kaya, M. N. Doral, and M. Callaghan, "How can we strengthen the quadriceps femoris in patients with patellofemoral pain syndrome?" *Muscles, ligaments and tendons journal*, vol. 2, no. 1, pp. 25–32, Jan. 2012.

[60] A. Pollock, C. Gray, E. Culham, B. R. Durward, and P. Langhorne, "Interventions for improving sit-to-stand ability following stroke," *Cochrane Database of Systematic Reviews*, vol. 2014, no. 5, May 2014.

[61] S. J. Hodges, R. J. Patrick, R. F. Reiser, *et al.*, "Effects of fatigue on bilateral ground reaction force asymmetries during the squat exercise," *The Journal of Strength & Conditioning Research*, vol. 25, no. 11, pp. 3107–3117, 2011.

[62] K. E. Webster, D. C. Austin, J. A. Feller, R. A. Clark, and J. A. McClelland, "Symmetry of squatting and the effect of fatigue following anterior cruciate ligament reconstruction," *Knee Surgery, Sports Traumatology, Arthroscopy*, vol. 23, no. 11, pp. 3208–3213, 2015.

[63] M.-S. Chan and S. M. Sigward, "Loading behaviors do not match loading abilities postanterior cruciate ligament reconstruction.," *Medicine and science in sports and exercise*, vol. 51, no. 8, pp. 1626–1634, 2019.

[64] R. Hidayah, L. Bishop, X. Jin, S. Chamarthy, J. Stein, and S. K. Agrawal, "Gait Adaptation Using a Cable-Driven Active Leg Exoskeleton (C-ALEX) With Post-Stroke Participants," *IEEE Transactions on Neural Systems and Rehabilitation Engineering*, vol. 28, no. 9, pp. 1984–1993, Sep. 2020.

[65] B. Zhong, K. Guo, H. Yu, and M. Zhang, "Toward gait symmetry enhancement via a cable-driven exoskeleton powered by series elastic actuators," *IEEE Robotics and Automation Letters*, vol. 7, no. 2, pp. 786–793, 2021.

[66] K. Kiguchi and Y. Yokomine, "Perception-Assist with a Lower-Limb Power-Assist Robot for Sitting Motion," in *2015 IEEE International Conference on Systems, Man, and Cybernetics*, IEEE, Oct. 2015, pp. 2390–2394.

[67] Z. Wang, B. Wang, and D. Xu, "Design and simulation of a lower-limb power-assist exoskeleton for hip joint based on deep squat," in *2016 IEEE International Conference on Information and Automation (ICIA)*, IEEE, Aug. 2016, pp. 865–869.

[68] Y.-P. Hong, D. Koo, J.-i. Park, S. Kim, and K.-S. Kim, "The SoftGait: A simple and powerful weight-support device for walking and squatting," in *2015 IEEE/RSJ International Conference on Intelligent Robots and Systems (IROS)*, vol. 2015-Decem, IEEE, Sep. 2015, pp. 6336–6341.

[69] F. Parietti, K. Chan, and H. H. Asada, "Bracing the human body with supernumerary Robotic Limbs for physical assistance and load reduction," in *2014 IEEE International Conference on Robotics and Automation (ICRA)*, IEEE, May 2014, pp. 141–148.

[70] M. Jeong, H. Woo, and K. Kong, "A Study on Weight Support and Balance Control Method for Assisting Squat Movement with a Wearable Robot, Angel-suit," *International Journal of Control, Automation and Systems*, vol. 18, no. 1, pp. 114–123, Jan. 2020.

[71] S. Yu, T.-H. H. Huang, D. Wang, B. Lynn, D. Sayd, V. Silivanov, Y. S. Park, Y. Tian, and H. Su, "Design and Control of a High-Torque and Highly Backdrivable Hybrid Soft Exoskeleton for Knee Injury Prevention During Squatting," *IEEE Robotics and Automation Letters*, vol. 4, no. 4, pp. 4579–4586, Oct. 2019.

[72] A. C. King and K. B. Hannan, "Segment Coordination Variability during Double Leg Bodyweight Squats at Different Tempos," *International Journal of Sports Medicine*, vol. 40, no. 11, 2019.

[73] B. E. Maki, P. J. Holliday, and A. K. Topper, "A Prospective Study of Postural Balance and Risk of Falling in An Ambulatory and Independent Elderly Population," *Journal of Gerontology*, vol. 49, no. 2, pp. M72–M84, Mar. 1994.

[74] S. Nigg, J. Vienneau, C. Maurer, and B. M. Nigg, "Development of a symmetry index using discrete variables," *Gait & posture*, vol. 38, no. 1, pp. 115–119, 2013.

[75] D. A. Winter, *Biomechanics and Motor Control of Human Movement*. John Wiley & Sons, Inc., Sep. 2009, vol. 7, pp. 1–370.

[76] C. B. Pham, S. H. Yeo, G. Yang, M. S. Kurbanhusen, and I.-M. Chen, "Force-closure workspace analysis of cable-driven parallel mechanisms," *Mechanism and Machine Theory*, vol. 41, no. 1, pp. 53–69, 2006.

[77] W. van Dijk, H. van der Kooij, B. Koopman, and E. H. van Asseldonk, "Improving the transparency of a rehabilitation robot by exploiting the cyclic behaviour of walking," in *2013 IEEE 13th International Conference on Rehabilitation Robotics (ICORR)*, IEEE, 2013, pp. 1–8.

[78] B. Erman, M. Z. Ozkol, J. Ivanović, H. Arslan, M. Ćosić, Y. Yuzbasioglu, M. Dopsaj, and T. Aksit, "Assessments of ground reaction force and range of motion in terms of fatigue during the body weight squat," *International Journal of Environmental Research and Public Health*, vol. 18, no. 8, p. 4005, 2021.

[79] K. Häkkinen, W. J. Kraemer, R. U. Newton, and M. Alen, "Changes in electromyographic activity, muscle fibre and force production characteristics during heavy resistance/power strength training in middle-aged and older men and women," *Acta Physiologica Scandinavica*, vol. 171, no. 1, pp. 51–62, 2001.

[80] W. G. Janssen, H. B. Bussmann, and H. J. Stam, "Determinants of the sit-to-stand movement: A review," *Physical therapy*, vol. 82, no. 9, pp. 866–879, 2002.

[81] A. Boukadida, F. Piotte, P. Dehail, and S. Nadeau, "Determinants of sit-to-stand tasks in individuals with hemiparesis post stroke: A review," *Annals of physical and rehabilitation medicine*, vol. 58, no. 3, pp. 167–172, 2015.

[82] M. K. Mak, F. Yang, and Y.-C. Pai, "Limb collapse, rather than instability, causes failure in sit-to-stand performance among patients with parkinson disease," *Physical therapy*, vol. 91, no. 3, pp. 381–391, 2011.

[83] L. Z. Rubenstein, D. H. Solomon, C. P. Roth, R. T. Young, P. G. Shekelle, J. T. Chang, C. H. MacLean, C. J. Kamberg, D. Saliba, and N. S. Wenger, "Detection and management of falls and instability in vulnerable elders by community physicians," *Journal of the American Geriatrics Society*, vol. 52, no. 9, pp. 1527–1531, 2004.

[84] A. Mansfield, J. S. Wong, J. Bryce, S. Knorr, and K. K. Patterson, "Does perturbation-based balance training prevent falls? systematic review and meta-analysis of preliminary randomized controlled trials," *Physical therapy*, vol. 95, no. 5, pp. 700–709, 2015.

[85] Y. Moghadas Tabrizi, M. H. Mansori, and M. Karimizadeh Ardakani, "Postural control and risk of falling in people who are blind: The effect and durability of perturbation and vestibular exercises," *British Journal of Visual Impairment*, p. 02 646 196 211 067 355, 2022.

[86] S. Dusane and T. Bhatt, "Effect of multisession progressive gait-slip training on fall-resisting skills of people with chronic stroke: Examining motor adaptation in reactive stability," *Brain Sciences*, vol. 11, no. 7, p. 894, 2021.

[87] J. Zhou, S. Yang, and Q. Xue, "Lower limb rehabilitation exoskeleton robot: A review," *Advances in Mechanical Engineering*, vol. 13, no. 4, p. 16 878 140 211 011 862, 2021.

[88] M. J. Pavol, E. F. Runtz, B. J. Edwards, and Y.-C. Pai, "Age influences the outcome of a slipping perturbation during initial but not repeated exposures," *The Journals of Gerontology Series A: Biological Sciences and Medical Sciences*, vol. 57, no. 8, pp. M496–M503, 2002.

[89] M. J. Pavol, E. F. Runtz, and Y.-C. Pai, "Diminished stepping responses lead to a fall following a novel slip induced during a sit-to-stand," *Gait & posture*, vol. 20, no. 2, pp. 154–162, 2004.

[90] D. A. Winter, "Human balance and posture control during standing and walking," *Gait & posture*, vol. 3, no. 4, pp. 193–214, 1995.

[91] G. M. Blenkinsop, M. T. Pain, and M. J. Hiley, "Balance control strategies during perturbed and unperturbed balance in standing and handstand," *Royal Society open science*, vol. 4, no. 7, p. 161 018, 2017.

[92] D. Martelli, J. Kang, and S. K. Agrawal, "A perturbation-based gait training with multidirectional waist-pulls generalizes to split-belt treadmill slips," in *2018 7th IEEE International Conference on Biomedical Robotics and Biomechatronics (Biorob)*, 2018, pp. 7–12.

[93] K. Freyler, A. Gollhofer, R. Colin, U. Brüderlin, and R. Ritzmann, "Reactive balance control in response to perturbation in unilateral stance: Interaction effects of direction, displacement and velocity on compensatory neuromuscular and kinematic responses," *PLoS one*, vol. 10, no. 12, e0144529, 2015.

[94] S. Nuzik, R. Lamb, A. VanSant, and S. Hirt, "Sit-to-stand movement pattern: A kinematic study," *Physical therapy*, vol. 66, no. 11, pp. 1708–1713, 1986.

[95] J. K. Haas, "A history of the unity game engine," 2014.

[96] V. E. Staartjes and M. L. Schröder, "The five-repetition sit-to-stand test: Evaluation of a simple and objective tool for the assessment of degenerative pathologies of the lumbar spine," *Journal of Neurosurgery: Spine*, vol. 29, no. 4, pp. 380–387, 2018.

[97] J. J. Koltermann, M. Gerber, H. Beck, and M. Beck, "Validation of various filters and sampling parameters for a cop analysis," *Technologies*, vol. 6, no. 2, p. 56, 2018.

[98] B.-C. Chang, M. I. Khan, A. Prado, N. Yang, J. Ou, and S. K. Agrawal, "Biomechanical differences during ascent on regular stairs and on a stairmill," *Journal of biomechanics*, vol. 104, p. 109 758, 2020.

[99] W. Jeon, J. L. Jensen, and L. Griffin, "Muscle activity and balance control during sit-to-stand across symmetric and asymmetric initial foot positions in healthy adults," *Gait & posture*, vol. 71, pp. 138–144, 2019.

[100] R. A. Zifchock, I. Davis, J. Higginson, and T. Royer, "The symmetry angle: A novel, robust method of quantifying asymmetry," *Gait & posture*, vol. 27, no. 4, pp. 622–627, 2008.

[101] P.-T. Cheng, C.-L. Chen, C.-M. Wang, and W.-H. Hong, "Leg muscle activation patterns of sit-to-stand movement in stroke patients," *American journal of physical medicine & rehabilitation*, vol. 83, no. 1, pp. 10–16, 2004.

[102] P. Bartuzi, T. Tokarski, and D. Roman-Liu, "The effect of the fatty tissue on emg signal in young women," *Acta Bioeng Biomech*, vol. 12, no. 2, pp. 87–92, 2010.

[103] S Karthikbabu, S. John M, N Manikandan, R. Bhamini K, M Chakrapani, and N. Akshatha, "Role of trunk rehabilitation on trunk control, balance and gait in patients with chronic stroke: A pre-post design," *Neuroscience & Medicine*, vol. 2011, 2011.

[104] R. Cabanas-Valdés, C. Bagur-Calafat, M. Girabent-Farrés, F. M. Caballero-Gómez, M. Hernandez-Valiño, and G. Urrutia Cuchi, "The effect of additional core stability exercises on improving dynamic sitting balance and trunk control for subacute stroke patients: A randomized controlled trial," *Clinical rehabilitation*, vol. 30, no. 10, pp. 1024–1033, 2016.

[105] S. A. BHISE and N. K. PATIL, "Dominant and non dominant leg activities in young adults," *International Journal of Therapies and and Rehabilitation Research*, vol. 10,

[106] D. de Kam, J. M. Roelofs, A. K. Bruijnes, A. C. Geurts, and V. Weerdesteyn, "The next step in understanding impaired reactive balance control in people with stroke: The role of defective early automatic postural responses," *Neurorehabilitation and neural repair*, vol. 31, no. 8, pp. 708–716, 2017.

[107] S. Brauer, M Woollacott, and A Shumway-Cook, "The influence of a concurrent cognitive task on the compensatory stepping response to a perturbation in balance-impaired and healthy elders," *Gait & posture*, vol. 15, no. 1, pp. 83–93, 2002.

[108] D. Lee, S. Lee, J. Park, and H. Roh, "The effect of fixed ankle and knee joints on postural stability and muscle activity," *Journal of Physical Therapy Science*, vol. 25, no. 1, pp. 33–36, 2013.

[109] I. Di Giulio, V. Baltzopoulos, C. N. Maganaris, and I. D. Loram, "Human standing: Does the control strategy preprogram a rigid knee?" *Journal of Applied Physiology*, vol. 114, no. 12, pp. 1717–1729, 2013.

[110] E. Burns and R. Kakara, "Deaths from falls among persons aged 65 years—united states, 2007–2016," *Morbidity and Mortality Weekly Report*, vol. 67, no. 18, p. 509, 2018.

[111] K. Rapp, C. Becker, I. D. Cameron, H.-H. König, and G. Büchele, "Epidemiology of falls in residential aged care: Analysis of more than 70,000 falls from residents of bavarian

nursing homes," *Journal of the American Medical Directors Association*, vol. 13, no. 2, 187–e1, 2012.

[112] M. W. Rogers, R. A. Creath, V. Gray, J. Abarro, S. McCombe Waller, B. A. Beamer, and J. D. Sorkin, "Comparison of lateral perturbation-induced step training and hip muscle strengthening exercise on balance and falls in community-dwelling older adults: A blinded randomized controlled trial," *The Journals of Gerontology: Series A*, 2021.

[113] T. D. Luna, V. Santamaria, X. Ai, and S. K. Agrawal, "Reactive postural control during sit-to-stand motion," *IEEE Robotics and Automation Letters*, 2022.

[114] A. Hof, M. Gazendam, and W. Sinke, "The condition for dynamic stability," *Journal of biomechanics*, vol. 38, no. 1, pp. 1–8, 2005.

[115] S Morini, A Bassi, C Cerulli, A Marinozzi, and M Ripani, "Hip and knee joints flexibility in young and elderly people: Effect of physical activity in the elderly," *Biology of Sport*, vol. 21, no. 1, pp. 25–38, 2004.

[116] B. E. Maki and W. E. McIlroy, "The role of limb movements in maintaining upright stance: The "change-in-support" strategy," *Physical therapy*, vol. 77, no. 5, pp. 488–507, 1997.